# Studies on Inner Membrane Proteins in E. coli; Characterization of Two Proteins Interacting with RodZ Important for The Cell Shape Maintenance

李, 高馳

(Degree)
博士（学術）

(Date of Degree)
2012-09-25

(Date of Publication)
2013-03-22

(Resource Type)
doctoral thesis

(Report Number)
甲5643

(URL)
https://hdl.handle.net/20.500.14094/D1005643

博士論文

# Studies on Inner Membrane Proteins in *E. coli*; Characterization of Two Proteins Interacting with RodZ Important for The Cell Shape Maintenance

平成 24 年 7 月

神戸大学大学院理学研究科

李高馳

博士論文

# Studies on Inner Membrane Proteins in *E. coli*; Characterization of Two Proteins Interacting with RodZ Important for The Cell Shape Maintenance

# 大腸菌内膜蛋白質の研究：細胞の形態維持に重要な RodZ と相互作用する二つの蛋白質の解析

平成 24 年 7 月

神戸大学大学院理学研究科

李高馳

# CONTENTS


| | |
|---|---|
| **CONTENTS** | I |
| **LIST OF FIGURES AND TABLES** | III |
| **ACKNOWLEDGEMENTS** | V |
| **SUMMARY** | 1 |
| **INTRODUCTION** | 4 |
| *Escherichia coli* | 4 |
| Hypothetical genes (y-genes) | 4 |
| Bacterial cell envelope | 7 |
| Cell division of Rod-type bacteria | 9 |
| Synthetic phenotype analysis | 10 |
| Protein-protein interaction analysis | 11 |
| Objective and outline of this study | 12 |
| **MATERIALS AND METHODS** | 15 |
| I. *E. coli* strains, plasmids and synthetic primers used in this study | 15 |
| I-1 Strains | 15 |
| I-2 Plasmids and synthetic primers | 16 |
| II. Growth media and antibiotics | 22 |
| III. Isolation of sacculi and PG measurement | 23 |
| IV. Transformation of plasmid DNA into competent cells | 23 |
| V. Preparation of plasmid DNA | 24 |
| VI. Lambda InCh integrated chromosomal fusions | 24 |
| VII. Protein localization | 27 |
| VIII. Electron microscopy | 28 |
| IX. BACTH assay | 29 |
| X. β-Galactosidase activity | 29 |
| XI. SDS-PAGE | 31 |
| XII. Western blotting analysis | 33 |

**RESULTS** 35

I. Relations between some y-genes involved in biofilm formation in *E. coli.* 35

I-1. PG of Δ*rodZ* mutant 35

I-2. Characterization of Δ*yhcB* and Δ*yciB* mutant 36

I-2-1. Effects on the cell growth of deletion mutation and over-expression of *yhcB* and *yciB* genes 36

I-2-2. Δ*yhcB*Δ*rodZ* double mutant exhibits a synthetic lethal phenotype. 40

II. Characterization of YhcB protein 40

II-1. Subcellular localization of YhcB 40

II-2. YhcB interacted with RodZ *in vivo* 42

II-3. YhcB interacts with cell shape proteins 50

II-4. The interaction of YhcB with cell-shape proteins is independent on the presence of RodZ. 52

II-5. YhcB interacts with itself. 52

III. Characterization of YciB 55

III-1. Localization of YciB and topology 55

III-2. Interaction between YciB and RodZ in BACTH analysis 61

IV. Genomic organization and transcription expression analysis of *yhcB* and *yciB* 63

**DISCUSSION** 68

I. Role of YhcB 68

II. Why is the Δ*yhcB*Δ*rodZ* double mutant synthetically lethal? 68

III. The interaction domain of YhcB 69

IV. The property of interaction between YhcB and cell shape proteins 70

V. YhcB interacts with itself 73

VI. Characterization of *yciB* 73

VII. Perspective and Future experiments 74

**REFERENCE** 75

# LIST OF FIGURES AND TABLES


Fig. 1 Function assignment of genes in *E. coli* K-12 6

Fig. 2 Types of bacterial cell envelope 8

Fig. 3 Schematic representation of septal ring assembly in *E. coli.* 8

Fig. 4 Synthetic lethality 11

Fig. 5 Principle of BACTH system 13

Fig. 6 Construction of pACYC184-*yhcB* (or *yciB*)-myc. 17

Fig. 7 BACTH plasmid maps 18

Fig. 8 Integration of *araC* $P^{araBAD}$-*yhcB* fusion in chromosome 25

Fig. 9 General methodology to analyze protein-protein interactions with BACTH system 30

Fig. 10 Δ*yciB* mutation causes abnormal cell morphology. 37

Fig. 11 Effects of Δ*yhcB* and Δ*yciB* mutations on cell growth 38

Fig. 12 Effects of YhcB and YciB overproduction on cell growth 39

Fig. 13 Growth of Δ*yhcB*Δ*rodZ* mutants carrying an inducible *yhcB* gene 41

Fig. 14 YhcB is an inner membrane protein 43

Fig. 15 Location of YhcB observed by using immune electron microscopy 44

Fig. 16 Predicted structure of YhcB 45

Fig. 17 YhcB interact with RodZ *in vivo* 47

Fig. 18 Interaction of YhcB deletion derivatives and RodZ 48

Fig. 19 HTH domain of RodZ is not required for the interaction with YhcB 51

Fig. 20 BATCH analysis of YhcB interaction with cell shape proteins and a subunit of cytochrome *bd* oxidase 53

Fig. 21 Interaction of YhcB and shape proteins are RodZ independent. 54

Fig. 22 YhcB interacts with itself. 56

Fig. 23 Prediction of the transmembrane domains of YciB 57

Fig. 24 Model for the topological organization of YciB localized at inner membrane 57

Fig. 25 Membrane topology analysis by Pho-Lac dual fusion system 59

Fig. 26 Topology of YciB 60

Fig. 27 BATCH analysis of YciB interaction with RodZ 62

Fig. 28 Genetic context of *yhcB* and *yciB* 64

Fig. 29 Construction of *lacZ* fusion for expression of *yhcB* gene 65
Fig. 30 Construction of *lacZ* fusion for expression of *yciB* gene 66
Fig. 31 Conventional model of protein folding and proteolysis 71
Fig. 32 Model depicting the interaction of YhcB with bacterial morphogenetic protein and cell wall synthesizing protein 72

Table 1. *E. coli* strains used in this study 15
Table 2. Plasmid constructed using synthetic primers in this study 20
Table 3. Amount of PG in *ΔrodZ* mutant cells 35
Table 4. Growth rates of wild-type and mutant cells carrying plasmids 38
Table 5. β-gal activities of the regions fused on *lacZ* for *yhcB* gene expression 65
Table 6. β-gal activities of the regions fused on *lacZ* for *yciB* gene expression 66

# ACKNOWLEDGEMENTS

I would like to show my deepest gratitude to my supervisor, Prof. Hiroshi Sakamoto for accepting me as his student and for his constant support.

Then, I shall extend my thanks to Dr. Madoka Kitakawa, who has provided me with valuable guidance in every stage of this research and the writing of this thesis. Without her instruction, kindness and patience in performing experiments and in my life of student abroad, I could not have completed my thesis.

I would like to appreciate Dr. Toshinobu Suzaki for guiding me, especially in the research using electron microscope, and for his valuable suggestions. I would also like to thank Prof. Kunio Inoue and Prof. Tetsuro Mimura for their critical reading of this thesis. Acknowledgements are also given to Dr. Chizuko Shichijo, Dr. Xiang Gan, Ms. Atsuko Honjo and the energetic lab members, Kentaro Hamamoto and previous students for their cooperation and encouragement.

Finally I would like to show my love and gratitude to my parents for their unconditional support and encouragement I have received not only during my study but also in my whole life.

## SUMMARY

*Escherichia coli* is a Gram-negative, rod-shaped bacterium that belongs to γ-proteobacteria. For decades since it was identified in 1920, *E. coli* has played an important role in fundamental biological and microbiological studies as well as biotechnology and industry. *E. coli* has been studied extensively as a model organism and probably, the most studied living thing on earth. The complete genome sequence revealed the presence of about 4,400 genes. However, approximately 40% of them are still function unknown or only predicted with no experimental evidence (Riley *et al.*, 2005). They are called y-genes because their tentative names systematically given start with 'y'.

Recently a variety of approaches have been used aiming to elucidate the function of these y-genes. Among them genome-wide investigations of their mutants gave interesting and valuable results. Using a comprehensive deletion mutant library of non-essential genes constructed by Baba *et al* (2006). Several y-genes have been identified as being involved in biofilm formation (Niba *et al.*, 2007). In the present study, I focused on two genes among them, *yhcB* and *yciB*, which were predicted to code for an inner membrane protein from their primary sequences and were found to be involved in biofilm formation.

Transduction analysis mediated by P1 phage indicated that they were functionally related to *yfgA*, another y-gene involved in biofilm formation, because it was unsuccessful to construct mutants of Δ*yfgA*Δ*yhcB* and Δ*yfgA*Δ*yciB*. These findings suggest that these double deletion mutations caused synthetic lethality (Niba *et al.*, 2007). The *yfgA* gene was found to play an important role in maintaining the cell shape and named *rodZ* (shiomi *et al.*, 2008; Bendezu' *et al.*, 2008; Alyahya SA *et al.*, 2009). The analysis of Δ*rodZ* mutant indicated that RodZ was required for the proper synthesis of peptidoglycan (Niba *et al.*, 2009).

In order to characterize *yhcB*, I further examined this synthetic lethal phenotype by constructing strains which harbored Δ*rodZ*Δ*yhcB* double deletion mutation and an inducible *yhcB* gene either on a plasmid or integrated in the chromosome and monitoring the cell growth under *yhcB*-induced or repressed conditions. Results obtained clearly showed that YhcB was required for the growth of Δ*yfgA* mutant. Furthermore, sphere or shorter cell shapes were exhibited by a

suppressor mutant of Δ*yfgA* upon depletion of YhcB, indicating that YhcB might support the function of RodZ in the lateral synthesis of peptidoglycan.

Next, I examined whether YhcB physically interacts with RodZ by bacterial two-hybrid (BACTH) analysis. As a result, YhcB clearly interacted with RodZ in this BACTH system and the most part of YhcB seemed to be required for the interaction or the stability of the protein, because YhcB derivatives with N- or C-terminal deletions showed no detectable or only a weak interaction activity with RodZ.

Because RodZ is important for the rod-type cell determination and interacts with proteins involved in cell morphogenesis, I further examined whether YhcB also interacts with cell shape proteins, MreB, MreC, MreD, RodA and an enzyme in the pathway of peptidoglycan synthesis, MurG. The results obtained indicated that YhcB interacts with MreC, MreD, RodA and MurG, but not with MreB. These results seemed to support the idea that YhcB is also involved in the lateral synthesis of peptidoglycan and the rod-type cell determination. However, YhcB is not equivalent to RodZ, because it seemed not to interact with MreB and instead showed a strong interaction with MurG with which RodZ showed no interaction activity. This observation might indicate that YhcB is functioning to mediate the synthesis of peptidoglycan precursor in the cytoplasm and the elongation of peptidoglycan in the periplasm supporting the role of RodZ.

On the other hand, the gene *yciB* was predicted to encode an IM protein with five TM domains, however the protein product was detected and the expression of this gene seemed to be low in general growth conditions. A deletion mutant Δ*yciB* showed a slow growth phenotype and the overproduction of YciB was very toxic. Some cells of the deletion mutant carrying a cloned *yciB* gene on a multi-copy plasmid exhibited misshapen and gigantic cell morphology, which seemed to indicate that *yciB* is involved in the septum formation and the cell division in *E. coli*, as predicted from the homology to *ispA* gene in *Shigella* (Mac et al, 1996).

I first established the topology of YciB protein using a dual PhoA-LacZ fusion system and confirmed that its N- and C-termini are located in the periplasm and in the cytoplasm, respectively, which is important for the BACTH analysis. Then, similarly to YhcB, I also investigated the interaction of YciB with RodZ. Most probably due to the toxicity of overproduced YciB, the interaction of full-length protein was not

clear unlike the case of YhcB. However, a truncated YciB (amino acid residues 1-120) revealed a strong interaction with RodZ.

From the above findings, I conclude that YhcB and RodZ interact and participate together in a process important for the maintenance of cell envelope and the cell shape determination. On the other hand, YciB might play a new role between the cell elongation and septation, because it also interacts with RodZ but the phenotype of *yciB* mutant suggested its involvement in a cell division process.

# INTRODUCTION

## *Escherichia coli*

*Escherichia coli*, a common inhabitant of the mammalian intestines, has not only been studied as a model in fundamental biological and microbiological studies, but also used as a workhorse in various biotechnological applications, medicine and industry.

*E. coli* belongs to γ- proteobacteria, and its cell is rod-shaped, about 2.5μm long and 0.8μm in diameter, with hemispherical end caps. Recently, the 4.6 Mb genome of *E. coli* was completely sequenced (Blattner *et al.*, 1997) and predicted to encode about 4400 genes and open reading frames (ORFs) (Fig. 1). Since then, significant advances have been made on the systems biology and biotechnology of *E. coli*. The complete genome sequences of *E. coli* K-12 made it possible to perform large-scale proteomics studies on this organism, as well as various omics-studies such as analyses of transcriptome. Several experimental resources have been constructed such as ORF plasmid clone library (ASKA library) (Kitagawa *et al.*, 2005) and a single gene deletion library of predicted ORFs (Keio Collection) (Baba *et al.*, 2006). Many useful tools also have been developed for random transposon insertion, one-step gene disruption, expression analysis and so on. Using these tools enormous amount of data are accumulating and the development of information technology made them easily assessable. However, the function of each gene and the details of genetic system that regulates and co-ordinates gene expression within and across the cellular processes are still far from being complete even in *E. coli*.

## Hypothetical genes (y-genes)

The availability of complete genome sequences of various organisms brought radical changes in life science. If the gene of interest in an organism that is not amenable for various biological analyses was found to be conserved in *E. coli*, analyses of *E. coli* gene might give clues to elucidate the function of the gene or the mechanism in which the gene exert the observed phenotype. Therefore, the advancement in understanding this organism will also give information to research on other organisms. However, even now, about 40% of *E. coli* genes still remain function-unknown (Riley

*et al.*, 2005) (Fig. 1), and these genes are called hypothetical gene or "y-genes", because they were temporarily named after the letter "y".

The research in genetics starts with careful observation of phenotype and then looks for the cause that is in most cases a mutation on its genetic information. On the other hands, molecular biology has developed reverse genetics, which makes it possible to perform the research in reverse direction, i.e. from the cause (gene) to the phenotype (function). Until recently, *E. coli* was thought to be a difficult organism to construct mutant by homologous recombination. This was one of the reasons for *E. coli* to be behind *Saccharomyces cerevisiae* (Giaever *et al.*, 2002) and *Bacillus subtilis* (Kobayashi *et al.*, 2003) in construction of deletion mutants. In 2000, however, an efficient method using lambda RED recombinase had been developed (Datsenko and Wanner, 2000). Then, a comprehensive deletion (replacement with Km resistant gene cassette) mutant library was constructed by this technology. It is a single gene deletion library of predicted ORFs of *E. coli* K-12 except essential genes (Baba *et al.*, 2006), and termed Keio collection. Through the screening of this collection, function of many y-genes have been identified or predicted. A research on biofilm formation in *E. coli* mutants performed in my laboratory also identified several y-genes as biofilm-related (Niba *et al.*, 2007).

Among them, *yfgA*, was found to show various phenotypes upon gene disruption and be important especially in rod-type cell shape maintenance. Hence, it was named *rodZ*, though this name originally came from the phenotype of *yfgA* used to first identify this y-gene (Bendezu´ *et al.*, 2008). They screened transposon mutants that required additional supply of FtsZ for survival or good growth on rich medium, and found that *yfgA* mutant *r*equired an *o*ver*d*ose of Fts*Z* for propagation on LB at or below 30°C. Various researches performed on *rodZ* established this gene as a new player in bacterial cell morphogenesis (shiomi *et al.*, 2008; Bendezu´ *et al.*, 2008; Alyahya SA *et al.*, 2009). Cells lacking the *rodZ* gene were round or otherwise misshapen and exhibited a highly reduced growth rate. Structural analyses showed that RodZ is a remarkable multi-domain protein that, similar to the bacterial actin MreB, assembles and forms helical structures associated with the cell membrane. RodZ has one single trans-membrane domain that divides the protein into a cytosolic and a periplasmic part. Interestingly, RodZ has a helix-turn-helix DNA-binding motif in its N-terminal cytosolic domain. A deletion analysis showed that the HTH motif was required for the

| Function classification | Number |
|---|---|
| Amino Acid Degradation | 142 |
| Cofactor, Prosthetic Groups Biosynthesis | 131 |
| Cell Membrane | 199 |
| Cell Division | 136 |
| Intermediary Metabolism | 164 |
| Energy | 381 |
| Fatty Acid and Lipids Degradation | 59 |
| Nucleosides and Nucleotides Degradation and Recycling | 127 |
| Regulation | 86 |
| DNA Replication | 93 |
| Signal Transduction Pathways | 358 |
| Translation | 151 |
| Transcription | 55 |
| Others | 386 |
| Unknown function (y-gene) | 1964 |
| Total | 4432 |

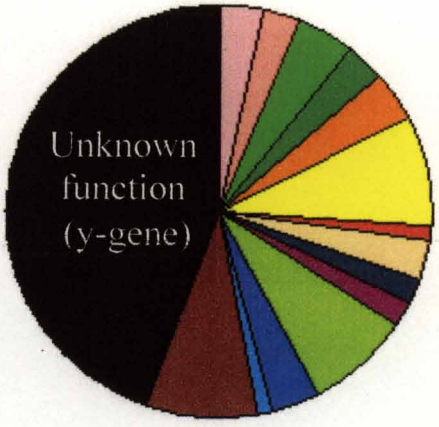


**Fig. 1 Function assignment of genes in *E. coli* K-12**
Genes present in *E. coli* strain MG1655 and W3110 are categorized according to the function assignment of their products. 'y-genes' include genes of computationally predicted function (32%) and completely unknown (15%)
[Adapted from Riley et al. (2005)]

formation of RodZ helices and for full complementation of the defective shape of *rodZ* null mutants. The function of the HTH domain is unknown but bacterial two-hybrid data indicated that it mediates important interactions between RodZ and MreB (van den Ent F *et al.*, 2010).

The screening of Keio collection also identified *yhcB* and *yicB* as genes involved in biofilm formation. Both of them have been predicted to encode inner membrane proteins. In a study of membrane protein complexes, YhcB protein was found together with CydA and CydB, subunits of the cytochrome *bd* ubiquinol oxidase in the inner membrane. Therefore, YhcB was suggested to be a new subunit of the oxidase (Stenberg *et al.*, 2005). However, in a later study on cytochrome *bd*-type ubiquinol oxidase (Mogi *et al.*, 2006), it was found that the cytochrome *bd* oxidase isolated from the Δ*yhcB* cell was completely identical to those from the wild-type strain, suggesting that YhcB was not associated with the CydAB heterodimer and is not required for the assembly or function of the oxidase. In the proteomic analysis of membrane preparations, the molecular mass of YhcB observed by BN-PAGE was significantly larger than that by SDS-PAGE, suggesting that YhcB may form a homo-oligomeric complex. It was also indicated using the C-terminal fusions to an alkaline phosphatase (PhoA) and the green fluorescent protein (GFP), the C-terminus of YhcB was located in the cytoplasm (Maddalo *et al.*, 2011). The other gene *yciB*, whose original name was *ispZ* (Intracellular Septation Protein), encodes a protein homologous to IspA, which is a protein of *Shigella flexneri* with a role in cell division and intracellular spreading (mac *et al.*, 1996). Although *yciB* is not essential for cell survival, both deletion mutation and over-production are harmful to the cell growth.

**Bacterial cell envelope**

Bacterial cell envelope that consists of inner membrane and cell wall is the principal stress-bearing and shape-maintaining element, and its integrity is of critical importance to cell viability. The cell envelopes of most bacteria fall into one of two major groups. Gram-negative bacteria are surrounded by a thin peptidoglycan cell wall, which itself is surrounded by an outer membrane containing lipopolysaccharide. Gram-positive bacteria lack an outer membrane but are surrounded by layers of peptidoglycan many times thicker than is found in the Gram-negatives (Fig. 2).

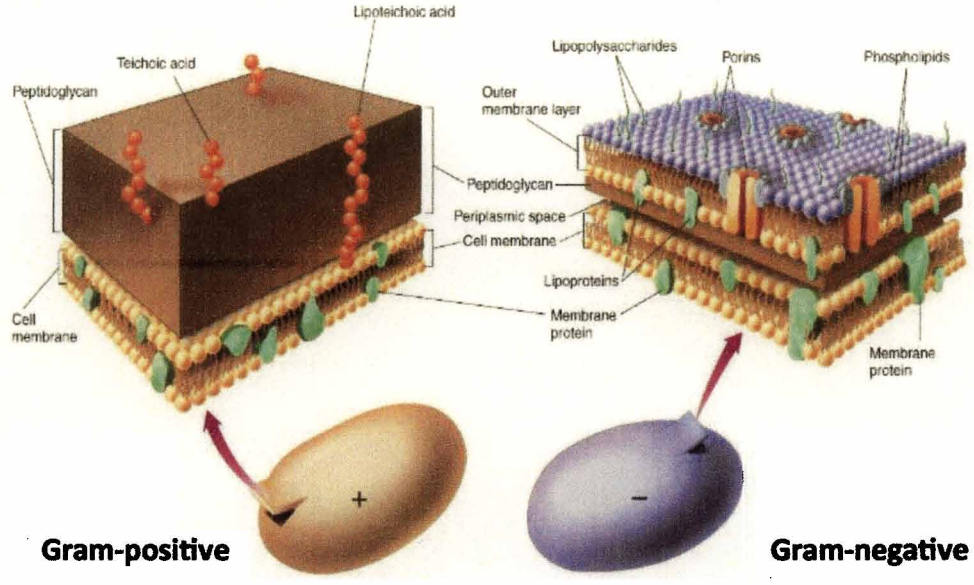


**Fig. 2 Types of bacterial cell envelope**

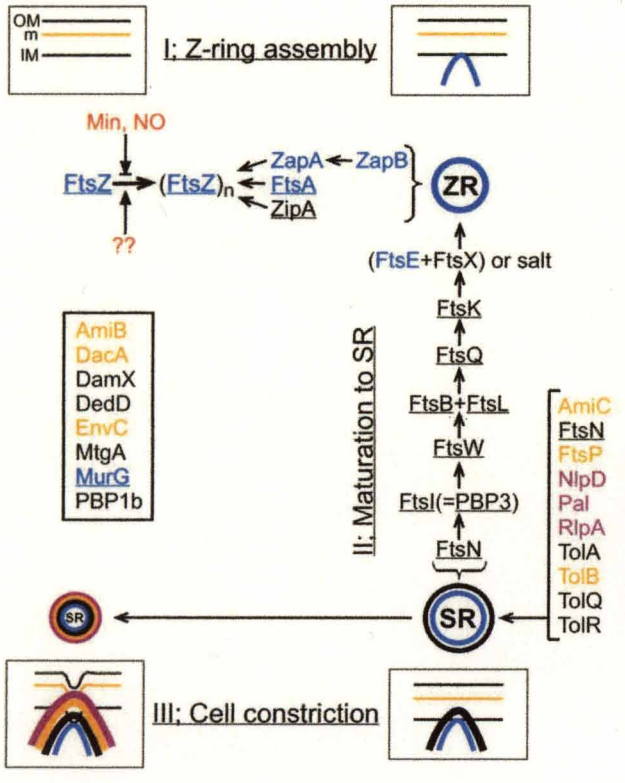


**Fig. 3 Schematic representation of septal ring assembly in *E. coli*.**

Three stages in development of the septal ring are indicated. Proteins that are essential for viability are underlined. Proteins assembling at the cytoplasmic face of the inner membrane are in blue, trans-membrane inner-membrane proteins are in black, periplasmic proteins in orange, and outer-membrane (lipo-) proteins are in purple. Regulators of Z-ring positioning are in red. (de Boer, 2010)

Peptidoglycan of Gram-negative bacteria, such as *E. coli*, is made up of repeating units of the disaccharide N-acetyl glucosamine-N-actyl muramic acid, which are cross-linked by pentapeptide side chains (Vollmer *et al.*, 2008). Because of its rigidity, it determines cell shape. The enterics are rod shaped, but cell shapes can vary. Agents such as enzymes or antibiotics that damage the peptidoglycan cause cell lysis owing to the turgor pressure of the cytoplasm. Lysis can be prevented in media of high osmolarity. However, without the peptidoglycan, cells lose their characteristic shape. The resulting cells are called spheroplasts. With *E. coli*, normal methods of spheroplast production produce nonviable cells, but they can continue metabolism and biosynthesis for hours. However, special methods can be used to produce L forms, which are spherical in shape and can be propagated on high osmolarity media (Joseleau-Petit *et al.*, 2007).

Bacteria lack intracellular organelles, and consequently, all of the membrane-associated functions of the eukaryotic organelles are performed in the inner membrane. Many of the membrane proteins that function in energy production, lipid biosynthesis, protein secretion, and transport are conserved in bacteria. These proteins are located in the inner membrane that is a phospholipid bilayer. In *E. coli* the principal phospholipids are phosphatidyl ethanolamine and phosphatidyl glycerol, but there are lesser amounts of phosphatidyl serine and cardiolipin. Other minor lipids include polyisoprenoid carriers, which function in the translocation of activated sugar intermediates that are required for envelope biogenesis (Raetz and Dowhan, 1990).

**Cell division of Rod-type bacteria**

The characteristic shape of bacterial cells is mainly determined by the cell wall. Rod-shaped bacteria have however different modes of cell wall synthesis, which are involved in cell elongation and cell division, and each seems to employ a different peptidoglycan synthesis complex. For bacterial cell division, detailed researches have recently made significant progress towards elucidating the functional mechanism of the divisome, which was formed by more than ten essential cell division proteins that localize to the Z ring made by the polymerization of FtsZ proteins. In *E. coli*, the first step of divisome assembly begins before constriction, when early cell division proteins, including FtsZ, FtsA and ZipA, localize to the future division site, and ZipA and the actin-like protein FtsA interact with and stabilize the Z ring at the inner membrane.

After a recruitment of the later assembling components (such as FtsK, Q, B, L, W, I, N), Z ring matures to septal ring (SR) to constrict cell into two daughter ones (Fig. 3, de Boer, 2010). Fts family proteins were well known to play critical roles in successful cell division, and temperature-sensitive mutants form filaments when the temperature was shifted to 42 °C.

Although most components of core divisome are widely conserved and essential for the later stages of the bacterial cell cycle, other uncharacterized proteins also seem to be involved in cell division or septation across species. For example, a novel *Shigella flexneri* gene, designated *ispA* (intracellular septation), was found responsible to the failure of cell division within the host epithelial cytoplasm (Mac Síomóin *et al*, 1996). A mutant of this gene has lead to the formation of long filamentous cells lacking septa, which were unable to spread intercellularly. Sequencing of *ispA* locus revealed that it was highly homologous to an uncharacterized *E. coli* gene, *yciB*, located between *trp* and *tonB*, and the ability of *yciB* to complement the *ispA* mutant that is unable to form plaque in cultured cell monolayers indicated they both encode the functionally same protein (enzyme). However, no observation was reported that *yciB* deletion mutation inhibited cell division and formed filamentous cells in *E. coli*. This seems to suggest that the same protein may play different roles in different species. More work is needed to clarify the function of *yciB* and to define the mechanisms of its action.

**Synthetic phenotype analysis**

As described above, still a significant portion of predicted genes remain function-unknown. Many of them seem to be the genes for membrane proteins and involved in the synthesis and maintenance of cell membrane and envelope. One reason for the delay in research of membrane proteins is that they require and associate with the membrane for their proper function and probably also because they are integrated in complex biological systems. Complex biological systems are very robust to genetic and/or environmental changes, because the biological functions in a system can be sustained against single-gene or even multiple-gene mutation possibly by utilizing the redundant pathways (Papp *et al.*, 2004, Reed and Palsson, 2004). Hence, in order to assess the function of these genes, it will be important to investigate the genetic interaction between them and with known genes. For this purpose, seeking synthetic

lethal/sickness phenotypes using double gene-knockout strains (Fig. 4) is one of the appropriate methods. To perform this in genome-wide, however, the construction of another entire set of deletion library and the system to combine two deletions into the same chromosome are required. In *E. coli*, an efficient method to construct such a library was developed (Datsenko and Wanner, 2000) as described above and a few projects of synthetic phenotype analysis are in progress.

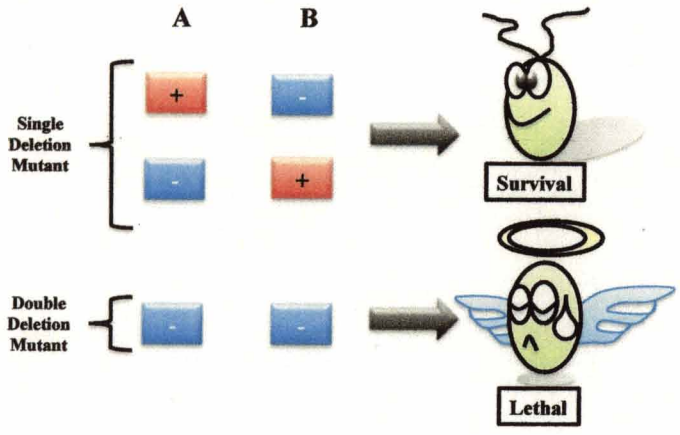


**Fig.4 Synthetic lethality**

A synthetic lethal interaction between two genes is defined when the survival of the combined mutation is less than the product of the survival of the two single mutations.

**Protein-protein interaction analysis**

The protein-protein interaction is also powerful method to indicate and identify the function of y-genes. Several methods have been developed and successfully used not only for the investigation of individual gene (protein) but also to construct a genome wide database (Arifuzzaman *et al.*, 2006). One way of examining the interaction is pull-down assay assisted by 2D gel and mass-spectrometry analysis as well as database of genome sequence. Pull-down assays were generally performed using a plasmid vector which was designed to add a tag to the cloned gene and its protein encoded. In the advance of proteomics, various tags were invented such as 6×His tag (Hochuli E *et al.*, 1988), Glutathione S-transferase (GST) tag (Sheehan D *et al*, 2001; Allocati N *et al.*, 2009) and FLAG tag (Thomas HP *et al.*, 1988). They have been used for western blotting analysis, immunoprecipitation experiments and affinity purification of recombinant proteins expressed, which are indispensable methods for protein-protein interaction analysis. For example, Emili and her group performed a large-scale analysis of protein complexes in *Escherichia coli* using TAP/SPA tagging system (Butland *et al.*, 2005). Through their investigations, an interaction network of protein complexes involved in diverse biological processes was uncovered and validated by sequential rounds of tagging and purification.

The other way is *in vivo* analysis using two-hybrid systems. Two-hybrid system was first developed with yeast *S. cerevisiae* (Young, 1998), in which not only the proteins of yeast itself but of various organisms have been examined by cloning the genes into vector plasmids developed for each TH-system. More recently bacterial TH systems have been reported and successfully used to investigate the interaction of proteins of *E. coli* and other organisms as well. Karimova G *et al.* developed BACTH (Bacterial Two-Hybrid) assay system (Fig. 5), in which two putative interacting proteins are genetically fused to two complementary fragments, T25 and T18, that constitute the catalytic domain of *Bordetella pertussis* adenylate cyclase. Association of the two-hybrid proteins results in functional complementation between T25 and T18 fragments and leads to cAMP synthesis. The produced cAMP then triggers transcriptional activation of catabolic operons, such as lactose or maltose. Using this system, Karimova G *et al.* (2005) screened the interaction network among *E. coli* membrane proteins involved in cell division; Handford JI *et al.* (2009) found that a regulatory complex of proteins, YjeE-YeaZ-YgjD, is essential for the bacterial viability and that these proteins form a link between DNA metabolism and cell division; Bendezú FO *et al.* (2009) confirmed that *E. coli* RodZ and MreB (bacterial actin) are interacting and gave the evidence to support their co-localization.

**Objective and outline of this study**

As described above, three genes, *yfgA* (*rodZ*), *yhcB* and *yciB*, were identified as biofilm related genes through the screening of Keio collection. Furthermore, *rodZ* was found to be important in the cell shape determination and involved in the synthesis of peptidoglycan synthesis. To further investigate the genetic relation and the function of these genes, I analyzed synthetic phenotypes of deletion mutants and performed bacterial two-hybrid analyses. The obtained results revealed a close functional relation between *yhcB* and *rodZ* as well as the interaction of YhcB with cell shape proteins. Maintenance of rod shape in *E. coli* requires the shape proteins MreB, MreC, MreD, MrdB (RodA) and RodZ, which interact mutually and seem to function in the lateral growth of peptidoglycan. Yet, the mechanism of cell morphogenesis remains to be established. My investigations in this study indicated that YhcB is also involved in the cell shape determination and/or the biosynthesis of peptidoglycan cooperating with RodZ. Similarly the relation of YciB and RodZ was examined and a possible interaction

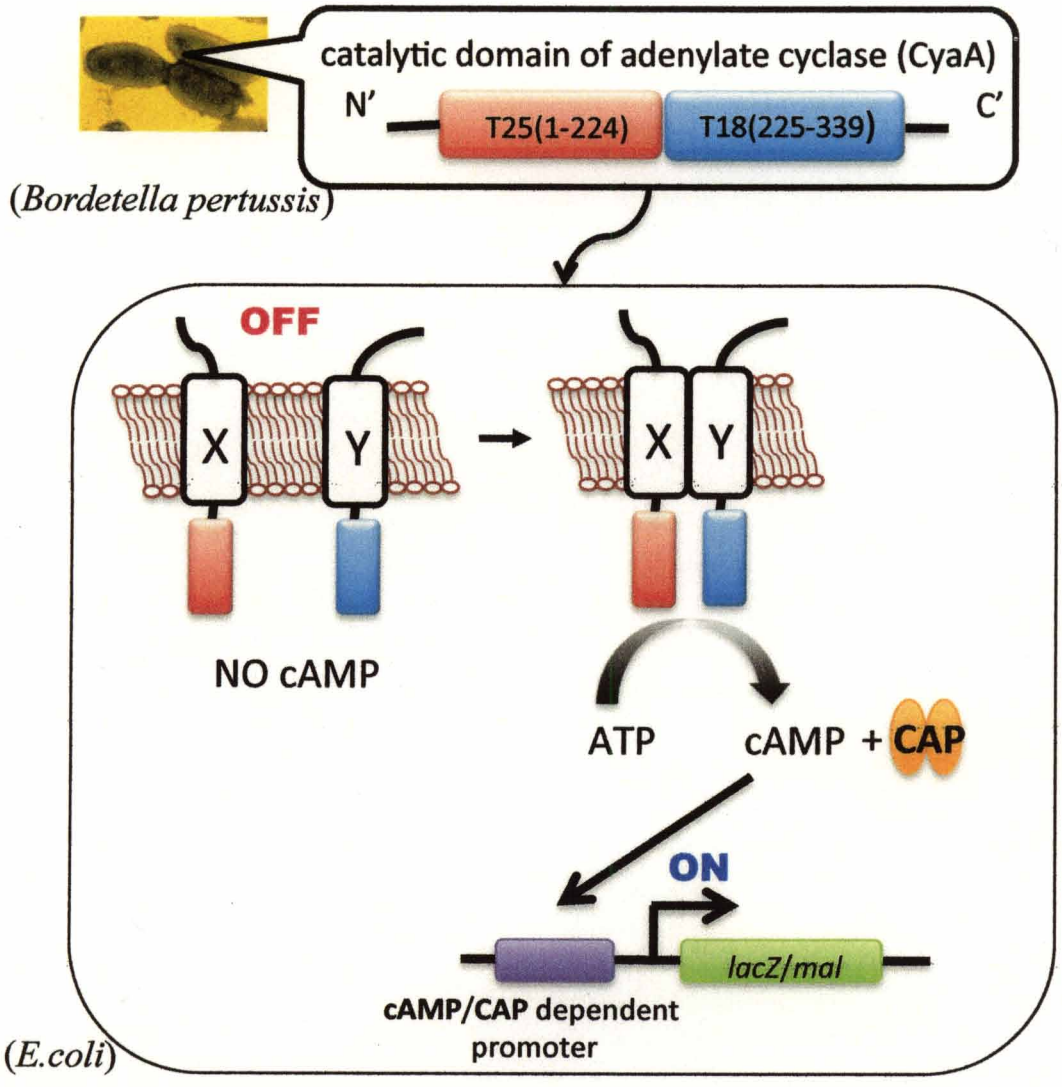


**Fig.5 Principle of BACTH system (Detection of interaction between two membrane proteins)**

Proteins of interest X and Y are genetically fused to the two fragments of the catalytic domain of *B. pertussis* adenylate cyclase and coexpressed in *E. coli cya* mutant cells.

Interaction between the two hybrid proteins results in functional complementation between the T25 and T18 fragments, leading to cAMP synthesis. cAMP, upon binding to the catabolite activator protein (a transcriptional regulator) triggers the expression of *E. coli* catabolic operons, allowing the bacteria to utilize sugars such as lactose and maltose. Efficiencies of complementation can be determined by measuring β-galactosidase activities in the transformed cells. (Karimova G et al., 1998)

between YciB and RodZ was observed. However, the expression level of *yciB* was found to be much lower than *yhcB* and *rodZ*, indicating that *yciB* functions in a different mechanism.

## MATERIALS AND METHODS

### I. *E. coli* strains, plasmids and synthetic primers used in this study

#### I-1 Strains

*E. coli* K12 strains used in this work were listed in Table 1. *E. coli* K12 strain BW25113 (*lacI*$^{q}$ *rrnB*$_{T14}$ *ΔlacZ*$_{WJ16}$ *hsdR514 ΔaraBAD*$_{AH33}$ *ΔrhaBAD*$_{LD78}$) was obtained from Dr. T. Baba (Keio University). Disruptants of each non-essential *E. coli* gene/ORF in Keio collection (http://ecoli.aist-nara.ac.jp/JProject) were obtained from Dr. H. Mori (Nara Institute of Science and Technology). They were constructed by "one-step disruption method" (Datsenko & Wanner, 2000), briefly as follows. Fragments used to construct deletion mutants with kanamycin resistance gene (*kan*) cassette were PCR amplified using primers that were 50nt homologous to the adjacent upstream or downstream flanking region of the target gene followed by the 20nt sequence coming from upstream or downstream region of *kan*. Plasmid pKD13 containing a *kan* cassette was used as template. Cells carrying pKD46, a Red helper plasmid, were transformed with PCR amplified DNA fragments and kanamycin resistant (Km$^{R}$) transformants were selected. The *kan* cassette was designed to ensure the expression of the downstream gene.

**Table 1. *E. coli* strains used in this study**

| Strain | Genotype | source or reference |
|---|---|---|
| XL-1Blue | F$^{-}$ [*proAB+, lacIq, lacZDM15::Tn10 (tetr)*], *hsdR17, supE44, recA1, endA1, gyrA46, thi, relA1, lac* | laboratory stock |
| DH5α | F$^{-}$, *deoR, endA1, gyrA96, hsdR17(rk-mk+), recA1, relA1,supE44, thi-1, Δ(lacZYA- argF)U169, (f80lacZDM15)* | laboratory stock |
| JE8471 | F$^{-}$, *DE(cya)854, trp, his, ilv* | National BioResource Project |
| BW25113 | F$^{-}$, *rph-1, DE(rhaBAD)568, DE(araBAD)567, DElacZ4787, hsdR514, rrnB* | CGSC |
| KR0401 | a derivative of BW25113 | (Niba *et al.*, 2007) |
| KR0411 | KR0401 *ΔyhcB* / pBADs-*yhcB* | This study |
| KR0412 | KR0401 Δ*yhcB*, λ(*araC*, $p_{araBAD}$-*yhcB, bla*) | This study |
| KR0413 | KR0412 Δ*rodZ::kan* | This study |
| KR0422 | KR0401 Δ*rodZ*, λ(*araC*, $p_{araBAD}$-*yhcB, bla*) | This study |
| KR0423 | KR0422 *ΔyhcB::kan* | This study |

Deletion mutations, Δ*rodZ::kan*, Δ*yhcB::kan*, and Δ*yciB::kan* were introduced from mutants of each gene in Keio collection (Baba *et al.*, 2006) by P1kc mediated transduction.

The integration of the inducible *yhcB* gene into chromosome near *attλ*, λ (*araC*, $P_{araBAD}$-*yhcB, bla*), was performed using λInCh as previously described (Niba *et al.*, 2009; Datsenko and Wanner, 2000). λ(*araC ParaBAD-yhcB*) denotes chromosome integration mediated by λInCh.

In order to analyze the interaction of fusion proteins in the absence of RodZ or YhcB, *ΔrodZ::kan* or *ΔyhcB::kan* mutations were introduced into JE8471 from corresponding Keio collection mutants by P1 mediated transduction, then kanamycin resistance gene was eliminated through FLP recombination mediated by pCP20 (Datsenko KA *et al.*, 2000).

**I-2 Plasmids and synthetic primers**

Following plasmids were used in this study.

pACYC184 (Fig. 6)

pACYC184 is an *E.coli* plasmid cloning vector containing the P15A origin of replication. This allows pACYC184 to coexist in cells with plasmids of the ColE1 compatibility group (e.g., pBR322). It is a low copy number vector of about 15 copies per cell.

pKTop (Karimova G *et al.*, 2009)

pKTop was used for the topology determination of inner membrane proteins, encoding the dual reporter $PhoA_{22-472}$/$LacZ_{4-60}$ that are fused in frame with MCS at its downstream. This allows to create an in-frame fusion at the N-terminus of dual reporter. The vector is a derivative of the low copy-number plasmid pACYC184 with a kanamycin resistance selectable marker.

BACTH vector (http://www.euromedex.com) (Fig. 7)

pUT18

pUT18 is a derivative of the high copy number vector pUC19, expressing an ampicillin resistance selectable marker, and encodes the T18 fragment (amino

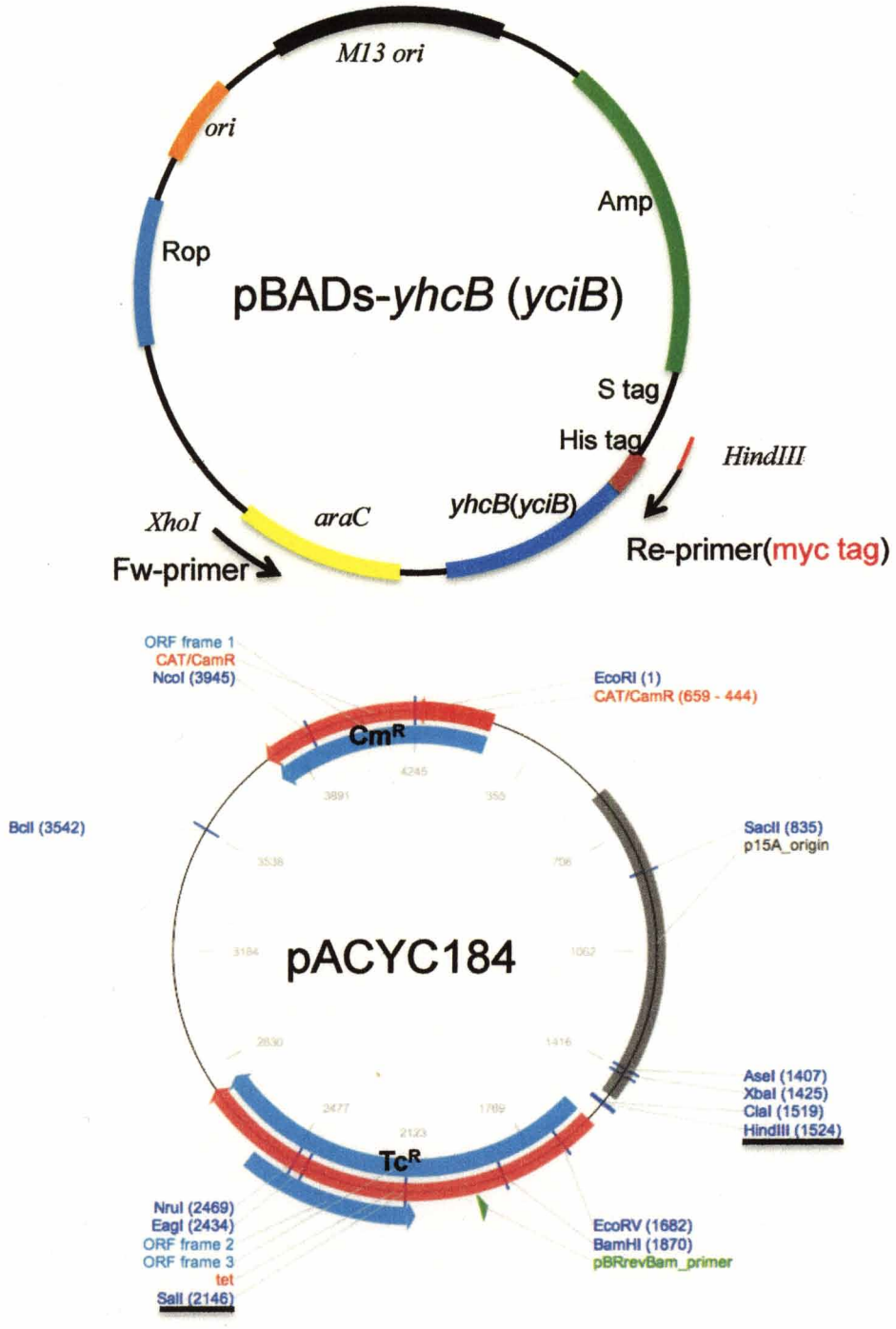


**Fig. 6 Construction of pACYC184-*yhcB* (or *yciB*)-myc.**
The target fragments were amplified from pBADs-*yhcB(or yciB)* as template. The myc-tag carrying sequence was introduced artificially by appending to the reverse primer. The PCR products containing *araC* and *myc* tagged *yhcB(or yciB)* were inserted to pACYC at *SalI* and *HindIII* sites.

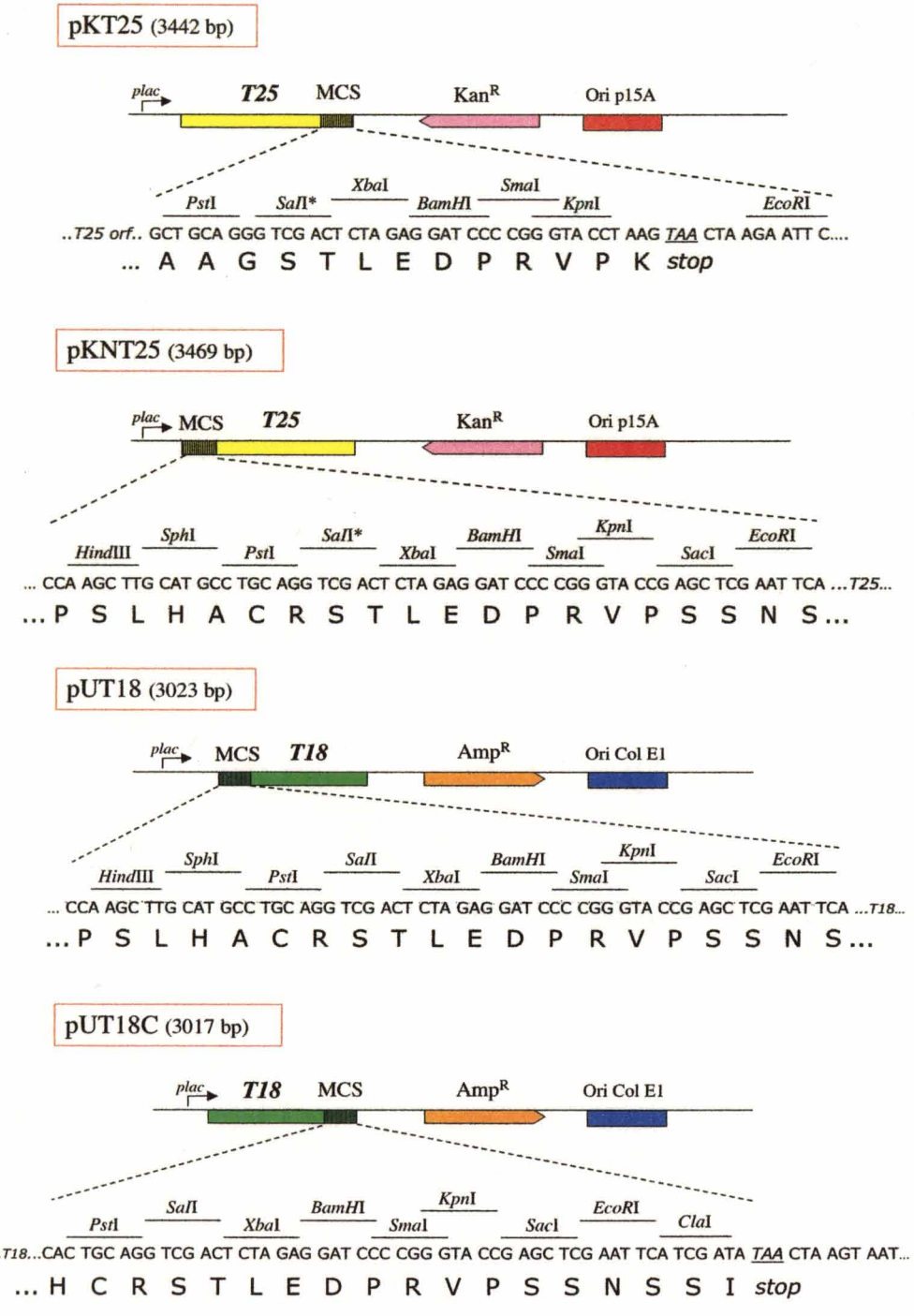


**Fig. 7 BACTH plasmid maps**

acids 225 to 399 of CyaA) that is expressed under the transcriptional control of a lac promoter. The T18 open reading frame lies downstream of a MCS with 9 unique restriction sites. This plasmid is designed to express chimeric proteins in which a heterologous polypeptide is fused to the N-terminal end of T18.

pUT18c

pUT18c differs from pUT18 in that the MCS is located at the 3' end of the T18 open reading frame. This plasmid is designed to create chimeric proteins in which a heterologous polypeptide is fused to the C-terminal end of T18.

pKT25

pKT25 encodes the T25 fragment (corresponding to the first 224 amino acids of CyaA) that is expressed under the transcriptional control of a *lac* promoter. The pKT25 vector is a derivative of the low copy-number plasmid pACYC184, expressing a kanamycin resistance selectable marker. A multi-cloning site sequence (MCS) is inserted at the 3' end of T25 to allow construction of in-frame fusions at the C-terminal end of the T25 polypeptide.

pKnT25

Plasmid pKnT25 was constructed from pKTop (Karimova G *et al.*, 2009) by replacing the region containing PhoA and LacZ fragments of the vector with the fragment coding for T25 using In-Fusion system (ClonTech/Takara Bio). The T25 fragment was amplified by PCR using pKT25 as template and primers, pKTop-T25-5(GATCCCCGGGTACCGAGCTCGAATTCAATGACCATGCAG CAATCGC) and pKTop-T25-3-rv(AGATTGTACTGAGAGTGCACTTATATCGATGGTGCAGC CCGCCGCGTGCG).

pJL30 (Lucht *et al.*, 1994)

pJL30 is a plasmid designed to analyze the transcription and translation activity of cloned gene by measuring the β-galactosidase activity of the *lacZ*-fusion protein.

pBADs-*yhcB* and pBADs-*yciB* (Fig. 6)

Plasmid pBADs-*yhcB* and pBADs-*yciB* containing the S-tagged *yhcB* and *yciB* ORF genes were constructed using pBADs vector (Niba *et al.*, 2007) derived from pBAD322 (Cronan, 2006). The S-tag carrying sequence from pSH-*Leu* (Gan *et al*, 2002) was ligated into the *SphI* and *HindIII* site of the MCS of pBAD322.

The following plasmids were constructed for this study.

Plasmids pACYC-*yhcB* and pACYC-*yciB* containing the *myc*-tagged *yhcB and yciB* genes were constructed using pACYC184 vector. The *myc*-tag carrying sequence was introduced artificially in the reverse primer. The DNA fragments harboring the ORF of *yhcB* and *yciB* genes without the termination codon was PCR amplified from the pBADs-*yhcB* and pBADs-*yciB* plasmids (Lab store) using primers listed in Table 2. Both forward and reverse primers were designed to hybridize with the vector pBADs. The PCR products were ligated into the *SalI* and *HindIII* sites of pACYC184 (Fig. 6).

Plasmids used for BACTH analysis were constructed by amplifying the gene from either chromosomal DNA or from the relevant plasmid by PCR using primers listed in Table 2 and ligating into the indicated vector.

To construct *lacZ* fusions on pJL30 for the expression analysis, fragments with the sequence of interest were PCR-amplified using appropriate primers and cloned into pJL30 *lacZ*-fusion vector (Lucht *et al.*, 1994). Primers used to construct each plasmid are indicated together with restriction enzymes used for cloning (Table 2.). Plasmids *yhcB*#1, *yhcB*#2, and *yhcB*#4 were constructed using pBADs-*yhcB* as template, and plasmids *yciB*#1, *yciB*#3, and *yciB*#4 were from pBADs-*yciB*. Fragment cloned in plasmid *yciB*#5 was amplified using pJL30-*yciB*#2 as template. pJL30-*yhcB*#3 was constructed from pJL30-*yhcB*#1 by digesting with *EcoRI* and self-ligating. Similarly, pJL30-*yciB*#2 was constructed from pJL30-*yciB*#1 by digesting with *ScaI* and *SmaI* and self-ligating.

**Table 2. Plasmid constructed using synthetic primers in this study**

| | Relevant features or primers used to amplify the indicated gene | Restriction site |
|---|---|---|
| pKnT25-*rodA* | ctctagaGACGGATAATCCGAATAAAAAAA | *XbaI* |
| | gcggtaccACGCTTTTCGACAACATTTTCC | *KpnI* |
| pKnT25-*yhcB* | *yhcB* derived from pUT18-*yhcB* | |

| | | |
|---|---|---|
| pKT25-*cydB* | gctctagaGATCGATTATGAAGTATTGCGT | *XbaI* |
| | gcggatccTACAGAGAGTGGGTGTTACGTT | *BamHI* |
| pKT25-*mreB* | gctctagaGTTGAAAAAATTTCGTGGCATG | *XbaI* |
| | cgggatccTCTTCGCTGAACAGGTCGCCG | *BamHI* |
| pKT25-*mreC* | gctctagaGAAGCCAATTTTTAGCCGTGG | *XbaI* |
| | gcggtaccTGCCCTCCCGGCGCACGC | *KpnI* |
| pKT25-*mreD* | gctctagaGGCGAGCTATCGTAGCCAGGGA | *XbaI* |
| | gcggtaccTGCACTGCAAACTGCTGACGGA | *KpnI* |
| pKT25-*murG* | gctctagaGAGTGGTCAAGGAAAGCGATTA | *XbaI* |
| | gcggtaccGCCCGGGCAACCCGGCTCACTT | *KpnI* |
| pKT25-*rodZ* | *rodZ* derived from pUT18c-*rodZ* | |
| pUT18c-*rodZ* | gctctagaGAATACTGAAGCCACGCAC | *XbaI* |
| | ggaattCTGCGCCGGTGATTGTT | *EcoRI* |
| pUT18-*yhcB* | gcctgcagGACCTGGGAATATGCGCTAATT | *PstI* |
| | cgggatccTCGCGCTTCGCGCCAGTA | *BamHI* |
| pUT18-*yhcB*ΔC1 | gcctgcagGACCTGGGAATATGCGCTAATT | *PstI* |
| | cgggatccAGGCTGCTGGAGCTTTTTGC | *BamHI* |
| pUT18-*yhcB*ΔC2 | gcctgcagGACCTGGGAATATGCGCTAATT | *PstI* |
| | cg*ggatcc*ATCTGCACCGGTGCCTGATCGT | *BamHI* |
| pUT18-*yhcB*ΔN | gctctagaGCGTTTTGGTAATCGTAAACTAC | *XbaI* |
| | cgggatccTCGCGCTTCGCGCCAGTA | *BamHI* |
| pKTop-*yciB* | *yciB* derived from pUT18-*yciB* | |
| pKTop-$yciB_{147}$ | cggatccGAAGCAGTTTCTTGATTTTTTAC | *BamHI* |
| | gcggtaccTTGACCCAAATATTTTGCGGC | *KpnI* |
| pKTop-$yciB_{120}$ | CCTCATCCTGTCTCTTGATCAGATC | *BglII* |
| | cgggatccTTCAGCTTCGACCATACCG | *BamHI* |
| pKTop-$yciB_{75}$ | c*ggatcc*GAAGCAGTTTCTTGATTTTTTAC | *BamHI* |
| | gcggtaccCATTTAATAAACTCATCATTGTGGA | *KpnI* |
| pKTop-$yciB_{48}$ | CCTCATCCTGTCTCTTGATCAGATC (in the vector) | *BglII* |
| | cgggatccTTCTCAACCTTACGAAAGCGA | *BamHI* |
| pKTop-$yciB_{42\text{-}179}$ | gctctagaGGTTCGCTTTCGTAAGGTTGA | *XbaI* |
| | cgggatcc TAGGATTTATCTTCCTGCGGC | *BamHI* |

| | | |
|---|---|---|
| pKTop-*yciB*$_{42\text{-}147}$ | gctctagaGGTTCGCTTTCGTAAGGTTGA | *BamHI* |
| | gcggtaccTTGACCCAAATATTTTGCGGC | *KpnI* |
| pUT18-*yciB* | ctctaga GAAGCAGTTTCTTGATTTTTTACC | *XbaI* |
| | cgggatcc AGGATTTATCTTCCTGCGGCAT | *BamHI* |
| pKT25-*yciB* | *yciB* derived from pUT18-*yciB* | |
| pUT18-*yciB*$_{120}$ | *yciB*$_{120}$ derived from pKTop-*yciB*$_{120}$ | |
| pACYC184-*yhcB* | ccgctcgagATCGATGCATAATGTGCCTG | *XhoI=>salI* |
| | cgaagcttTTACAGATCCTCTTCTGAGATGAGTTTTTGTTCC ATACCAGAACCGCGTGG | *HindIII* |
| pACYC184-*yciB* | ccgctcgagATCGATGCATAATGTGCCTG | *XhoI=>salI* |
| | cgaagcttTTACAGATCCTCTTCTGAGATGAGTTTTTGTTCC ATACCAGAACCGCGTGG | *HindIII* |
| pJL30-*yhcB*#1 | cgggatccGGCGCTGTTTCCGCTCTC | *BamHI* |
| | aactgcagCTTCACAAACATGATGGAGGCG | *PstI* |
| pJL30-*yhcB*#2 | cgggatccCGTAATCGTCTGGCAGAGTCTG | *BamHI* |
| | aactgcagCTTCACAAACATGATGGAGGCG | *PstI* |
| pJL30-*yhcB*#4 | cgggatccGGCGCTGTTTCCGCTCTC | *BamHI* |
| | gcaagcttTCCCAGGTCATGAACATCTCCC | *HindIII* |
| pJL30-*yciB*#1 | cggaattcACTTCCTAACGTACCACCAGCA | *EcoRI* |
| | cgggatccCTGAGGGACGTTATGTGTTGTA | *BamHI* |
| pJL30-*yciB*#3 | ggaattcGTGCTTATCTATAGCTGGGTTCG | *EcoRI* |
| | cgggatccCTGAGGGACGTTATGTGTTGTA | *BamHI* |
| pJL30-*yciB*#4 | cggaattcACTTCCTAACGTACCACCAGCA | *EcoRI* |
| | cgggatccCTGCTTCATTTTACGATTCCGT | *BamHI* |
| pJL30-*yciB*#5 | CCCGAAAAGTGCCACCTGACG (in the vector) | *EcoRI* |
| | gcaagcttACCCATTGGCTGACTAACAG | *HindIII* |

## II. Growth media and antibiotics

Cells were cultured in LB medium [1% Bacto-tryptone (Difco, USA), 0.5% Yeast extract (Difco, USA) and 0.5% NaCl (Nacalai Tesque, Japan); solidified by 2% Bacto agar (Wako, Japan) for plates. Ampicillin (100 mg/ml), Kanamycin (30 mg/ml), chloramphenicol (35 mg/ml) and IPTG (1 mM) were added when necessary. LC

medium (1% Bacto-tryptone, 0.5% Yeast extract and 0.25% NaCl; solidified by 1% Bacto agar) and Top agar (1% Bacto-tryptone, 0.5% Yeast extract and 0.05% NaCl; NaOH added at 2mM and solidified by 0.5% Bacto agar (Difco, USA)] were used to propagate P1 phage.

**III. Isolation of sacculi and PG measurement**

PG was isolated essentially as described (Herve *et al.*, 2007). Cells of 200 ml LB cultures grown to $OD_{600}$ of ca. 0.75 were used. After the lysis of cell by hot 4% SDS solution and the overnight incubation at room temperature, a cell wall fraction was obtained by centrifugation at 100,000 g for 1 hour, washed with water and finally suspended in 0.5 ml water. The amount of PG in isolated sacculi was measured by means of a silkworm larvae plasma test using SLP reagent (Wako Pure Chemical Industries Ltd., Osaka) as described previously (Tsuchiya *et al.*, 1996; van Langevelde *et al.*, 1998). The serial dilutions of samples were mixed with an equal volume of SLP reagent reconstituted according to the procedure supplied by company and the OD650 was measured after 40 and 60 min incubation at 30 °C. The amount of PG in the samples was calculated using the standard curve obtained with PG of *Micrococcus luteus* (Wako).

**IV. Transformation of plasmid DNA into competent cells ($CaCl_2$ method)**

5ml of LB medium (containing antibiotics when required) was inoculated with 0.1 ml of overnight culture of cells to be transformed and incubated at 37 °C until the $OD_{600}$ was approximately 0.5. The cells were harvested by centrifuging at 3,000 rpm for 10 min at 4°C, and the supernatant was discarded. Cells were resuspended in 2 ml of ice-cold 50 mM $CaCl_2$/15% glycerol and then collected by centrifugation at 3,000 rpm for 10 min at 4°C. Collected cells were dissolved again, resuspended in 0.05 ml of ice-cold 50 mM $CaCl_2$/15% glycerol and divided equally into two test tubes. 2 μl of the plasmid DNA to be analyzed and the control DNA (vector only) were added in separate tubes and incubated on ice for 30 min. The competent cell mixture was heat shocked at 42°C for 2 min, then mixed with 0.5 ml of LB medium and incubated at 37°C for 60 min. The cells were spread on LB plate containing appropriate antibiotics and incubated at 37°C overnight.

**V. Preparation of plasmid DNA**

Cells from a 1.5 ml overnight culture were collected by centrifugation at 15,000 rpm for 30 sec and the supernatant was discarded. The tube was towel-dried and 200 μl of STET containing lysozyme (0.2 mg/ml) was added. The mixture was vortexed and boiled for 1min. Immediately after that, it was centrifuged at 15,000 rpm for 5 min and the precipitate removed with a toothpick. 8 μl of 5% cetyl trimethyl ammonium bromide (CTAB) was added and again centrifuged at 15,000 rpm for 5 min. 300 μl of 1.2M NaCl was added and then well-mixed before adding 750 μl 100% ethanol. The mixture was centrifuged again at 15,000 rpm for 5 min and the supernatant discarded. 500 μl 70% ethanol was added and the plasmid DNA was collected by centrifugation at 15,000 rpm for 5 min. The ethanol was removed by aspiration or drying at 42 °C, The DNA was dissolved in 30 μl sterilized $H_2O$.

STET buffer:

| | |
|---|---|
| Sucrose | 8 % |
| TritonX-100 | 0.1 % |
| EDTA | 50 mM |
| Tris-HCl (pH 8.0) | 50 mM |

**VI. Lambda InCh integrated chromosomal fusions**

Chromosomal integrations of *araC* $P^{ara}$*BAD-yhcB* were performed via phage λInCh (Fig. 8) as described (Boyd *et al.*, 2000).

Lysate preparation: A single colony of the strain carrying the *araC* $P^{ara}$*BAD-yhcB* fusion plasmid was grown overnight in LB medium containing 2mM $Mg_2SO_4$ and 0.2% maltose with appropriate antibiotics. 0.1ml of ON culture was mixed with 0.01ml of λInCh (prepared from strain JOE59 (SM551), a lysogen of λInCh for pBR derivatives) and incubated at 30 °C for 15min. Then, 1ml LB + MgSO4 (2mM) was added and mixed for an hour at 30 °C. The mixture was spread on plates containing both 0.04mg/ml kanamycin and 0.1mg/ml ampicillin and incubated ON at 30 °C. Several colonies were purified on the same plate and incubated at 30 °C. The culture without lambda infection was used as control to make sure only λInCh-containing strains were selected. Single colonies were picked up, grown in 0.5ml LB at 30 °C for approximately 8 hours to overnight before spotting on normal LB plate and LB plate

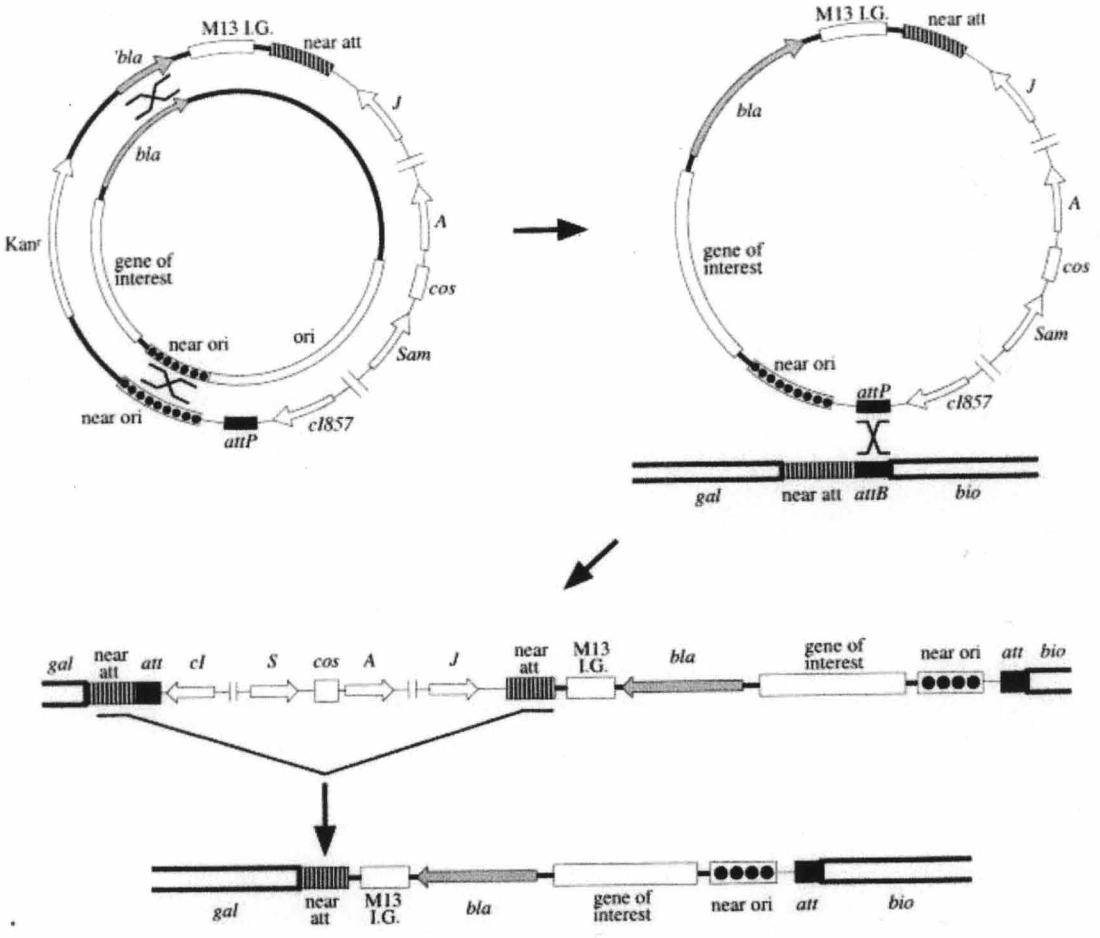


**Fig. 8 Integration of *araC* $P^{araBAD}$*-yhcB* fusion in chromosome**

The three steps involved in transfer of an expression system from a pBR322-derived plasmid to the chromosome in stable single copy. At the upper left, the plasmid and the phage are shown as concentric circles with the phage outside. In the first step, recombination at both the 358-bp *'bla* region and the 409-bp near-ori region results in transfer of the promoter gene expression system and a functional *bla* (Amp$^r$) gene to the phage replacing the Kan$^r$ gene. In the second step a lysogen is formed by site-specific recombination at the *att* site, conferring ampicillin resistance and temperature sensitivity. The orientation at the *att* site is indicated relative to the flanking markers *gal* and *bio*. In the third step, recombination in the 800-bp direct-repeat region, near-att, removes most of the phage DNA conferring temperature independence. The *att* region in the stabilized strain is shown at the bottom.(Boyd *et al.*,2000)

containing both ampicillin and kanamycin, and incubated at 42 °C and 30 °C, respectively. The rest of the above LB culture was left on the desk until required. The culture that was temperature sensitive ($Tm^S$) at 42 °C was selected and 0.2ml portion was inoculated into 5ml of LB containing ampicillin. Cells were grown with good aeration at 30 °C until $OD_{600}$ was approximately 0.5, heated at 42 °C for 15min to induce the propagation of l, then immediately transferred to 37 °C and further cultured for approximately 2~3 h. Next, cells were collected at 3,000 rpm for 10 min and suspended with 0.8 ml SM buffer, lysed by adding 50 ml chloroform and then vortexed. The success of λ propagation was ensured by observing the viscosity and the lysate was stored at 4 °C until needed.

Infection of LE392: A *supF* strain, LE392 was grown in LB medium containing 2mM $Mg_2SO_4$ and 0.2% maltose ON and 0.05 ml was mixed with 0.05 ml of serial dilutions of lysate described above and then incubated at 30 °C for 15min. 0.5ml LB + $Mg_2SO_4$ (2mM) was added and incubated for an hour at 30 °C, then a portion of 0.1ml was spread on plates containing ampicillin and incubated at 30 °C ON. Several colonies were purified on the same plate and incubated at 30 °C ON. Subsequently, single colonies of each $Amp^R$ clone were picked up, grown in 0.5ml LB at 30 °C for approximately 8h to overnight and spotted on LB plate and LB plate containing both ampicillin and kanamycin. The LB plate was incubated at 42 °C and the plate containing both ampicillin and kanamycin was incubated at 30 °C ON. The rest of the above 0.5 ml of LB culture was kept until required. Clones that showed Tm sensitive, kanamycin sensitive and ampicillin resistance phenotype, should be the lysogen of λInCh recombinant that acquired *araC* $P^{ara}$*BAD-yhcB* fusion and $Amp^R$ from the plasmid. A portion of the corresponding culture was inoculated into 1ml LB and cells were grown at 30 °C until the $OD_{600}$ was approximately 0.5, heated at 42 °C for 15min and incubated at 37 °C for approximately 3 h to observe for complete lysis. Two drops of chloroform was added and shaking continued at 37 °C for another 15min. The supernatant was collected at 3,000 rpm for 5min and transferred into a new tube and stored as pure lysate of λInCh recombinant for *araC* $P^{ara}$*BAD-yhcB* fusion.

Transfer of lambda integrated *araC* $P^{ara}$*BAD-yhcB* fusion into the WT strain: The WT strain was grown ON in LB medium containing 2mM $Mg_2SO_4$ and 0.2% maltose. A 0.05ml portion of ON culture was mixed with 0.05ml aliquots of 1/100 dilution of pure lysate and then incubated at 30 °C for 15min. 0.5ml LB + $MgSO_4$

(2mM) was added and mixed for an hour at 30 °C before streaking 0.1ml on plates containing ampicillin. The plates were incubated at 30 °C ON. Colonies were purified on the same plate and single colonies were picked up as above to inoculate in 0.5ml LB medium. Cells were grown at 30 °C streaked on LB plate containing ampicillin and incubated at 42 °C ON. Colonies that appeared ($Tm^R$) should have lost the parts of lambda required for propagation and were purified once more at 42 °C. Resultant clones containing the *araC* $P^{ara}$*BAD-yhcB* fusion on the chromosome were examined for the sensitivity to antibiotics and used for the growth assay.

**VII. Protein localization**

Cell fractionation was performed as described in reference (Gualdi *et al*, 2008)) with some modifications. Cells were grown in 200 ml LB medium with appropriate antibiotics at 37°C until OD600 reached to ~ 0.6, then induced with 0.1% arabinose (final concentration) for 30 min and collected. Centrifugation was carried out at 5,500 rpm for 10 min at 4°C (Beckman J2-MC) and washed with 5 ml of 0.1 M phosphate buffer pH 7.0 (PB). Cells were resuspended in 2 ml of PB with addition of 100 μg of lysozyme/ml and 1 mM EDTA (pH 8.0) and incubated at room temperature for 10 min. Cells were sonicated for 10 sec and repeated 5 times with intervals not to raise the temperature and centrifuged as described above to remove unbroken cells. Supernatant obtained from the low-speed centrifugation was then centrifuged at 38,000 rpm for 1 h at 4°C (Beckman ultracentrifuge, 50Ti Rotor) to separate the cytoplasmic (supernatant) and the membrane fractions (pellet). The pellet was resuspended in 2 ml of 0.1% sarkosyl in phosphate-buffered saline, left for 20 min at room temperature, and centrifuged at 15,000 rpm at 10°C for 18 min (Beckman J2-MC) to remove ribosomes and cytoplasmic proteins that were still associated with the membrane fraction. The pellet was resuspended in 1 ml of 1% sarkosyl, incubated again for 20 min at room temperature, and centrifuged as described above. The supernatant, corresponding to inner membrane fraction, was collected, and the pellet, corresponding to outer membrane fraction, was resuspended in 0.5 ml of $H_2O$. Protein concentrations were determined, and 20 μg of total proteins was loaded onto a 10% sodium dodecyl sulfate-polyacrylamide gel (SDS-PAGE). After separation by SDS-PAGE analysis, S-tag fused proteins were transferred to a PVDF membrane by semi-dry blotter SartorblotII for approximately 1hour according to manufacturer's protocol. Then, S-tag

fused proteins were detected by Western-blotting analysis using S-protein AP-conjugate.

**Solutions:**

1) 0.1M Na Phosphate Buffer (pH 7.0):

| | |
|---|---|
| 1M $Na_2HPO_4$ (pH 7.0) | 5.8ml |
| 1M $NaH_2PO_4$ (pH 7.0) | 4.2ml |

Adjusted to 100 ml with deionized $H_2O$

2) Phosphate Buffered Saline (PBS) pH 7.4

| | |
|---|---|
| PBS tablet (Takara bio, Japan) | 1 tablet |
| Deionized $H_2O$ | 100ml |
| measure pH | |

3) 2% Sarcosyl/PBS

| | |
|---|---|
| Sarcosyl sodium salt | 2.0g |
| PBS | 100ml |

4) 1% Sarcosyl /PBS

| | |
|---|---|
| Sarcosyl sodium salt | 1.0g |
| PBS | 100ml |

5) 0.1% sarcosyl/PBS:

| | |
|---|---|
| 2% sarcosyl/PBS | 100ml |
| PBS | 2ml |

*All solutions were autoclaved before use

**VIII. Electron microscopy**

From overnight culture, cell was diluted and grown to mid logarithmic phase. Formvar-carbon coated copper grids were floated for 3 min onto a drop of the culture to mount cells, washed in drops of 0.9 % NaCl and distilled water, then stained with 1 % uranyl acetate five times. The fixed cells were dehydrated through a graded ethanol series (50%, 70%, 90%, 95%, 99% and 100%) and embedded in LR white embedding

resin (Electron Microscopy Sciences) according to the instruction of manufacturer. Ultra-thin sections (80-100 nm) were mounted on a coated nickel grid. The *myc*-tagged proteins were detected by soaking in PBST/2%BSA solution containing anti-*myc* (1/120 dilution, NEOMARKERS, Clone 9E10.3) for 1-2 hr at room temperature, washed with PBST, then next incubating in PBST/2%BSA solution containing anti-mouse IgG conjugated with gold particles (10nm) (1/120 dilution; BBINTERNATIONAL, Product code: EM.GAM10). Images were obtained by transmission electron microscope (H-7100, Hitachi, Tokyo, Japan) at an acceleration voltage of 80 kV.

**IX. BACTH assay**

Bacterial two hybrid analysis was performed essentially as described (Karimova *et al.*, 1998) (Fig. 9). The genes encoding the two proteins of interest (X or Y) were amplified by PCR using appropriate primers (Table. 2) and sub-cloned into pKT25 (or pKNT25) and pUT18 (or pUT18C) vectors in frame with the T25 and T18 fragment open reading frames by using standard molecular biology techniques. The two recombinant plasmids encoding the T25-X (or X-T25) and T18-Y (or Y-T18) hybrid proteins were transformed into indicator strain JE8471. The resultant transformants were streaked on the LB medium containing antibiotics, IPTG (0.5 mM) and X-gal (40μg/ml) and incubated at 30 °C.

**X. β-Galactosidase activity**

β-Galactosidase activity was measured essentially as described (Miller, 1972). From overnight culture, 0.1ml cell was sub-culture into 5ml LB medium and grown at 37 °C to an $OD_{600}$ of approximately 0.4 to 0.6. An aliquote of the culture was taken and the $OD_{600}$ used for calculation of β-galactosidase activity was measured and kept at -20 °C. The frozen sample was thawed and up to 0.3 ml of the culture depending on its activity was added into 350 μl of Z buffer containing 0.2% of sarkosyl. The final volume was adjusted to be 0.3 ml by adding extra medium for the sample with less volume.

For time course experiments, the $OD_{600}$ of over-night culture was measured and then cells were inoculated to make a final $OD_{600}$ of 0.05 into 20 ml LB medium with appropriate antibiotics. About 1 ml of culture was taken at appropriate intervals and kept frozen at -20 °C until subjected to the measurement of β-galactosidase activity.

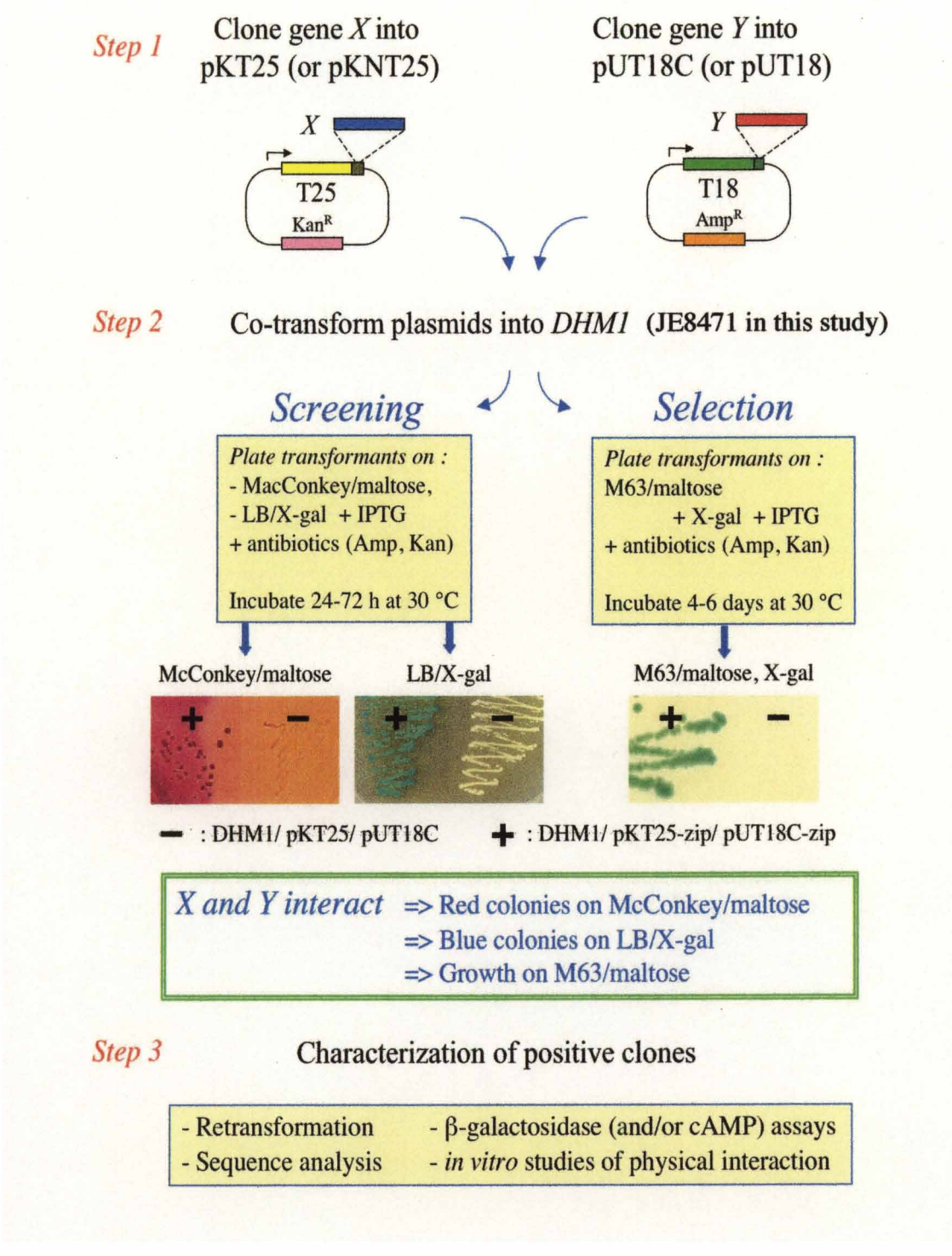


**Fig. 9 General methodology to analyze protein-protein interactions with BACTH system (from EUROMEX Cat N⁰:EUK001)**

The mixture of the sample and Z-buffer was incubated at 30 °C for 30 min before 150 µl of ONPG (O-nitrophenyl galactopyranase) solution was added and incubation was continued until a yellow color developed. The reaction time was measured and the reaction was stopped by adding 375 µl of 1M $Na_2CO_3$ when sufficient color was observed.

Z-Buffer (200ml) contains:

| | |
|---|---|
| 60mM $Na_2HPO_4.12H_2O$ | 4.3g |
| 40mM $NaH_2PO_4.2H_2O$ | 1.24g |
| 10mM KCl | 0.15g |
| 1mM $Mg_2SO_4.7H_2O$ | 0.05g |

After autoclave,

Add 270µl β-Mercaptoethanol (50mM)

For the lysis of cells, add 0.4g Sodium Lauryl Sarkosyl salt (final= 0.2%)

ONPG: 4mg/ml (10ml solution)

| | |
|---|---|
| 40mg | ONPG |
| 10ml | Z-Buffer (without Sarkosyl) |

1M $Na_2CO_3$ (100ml):

| | |
|---|---|
| 10.5g | $Na_2CO_3$ |
| 100ml | Deionized $H_2O$ |

The sample was centrifuged at 3,000 rpm for 5min and the $OD_{420}$ and $OD_{550}$ was measured. The activity was calculated using the formula;

$$\text{Activity (Miller Units)} = \frac{1000 \times (OD_{420} - 1.75 \times OD_{550})}{OD_{600} \times \text{Time (min)} \times \text{Volume (ml)}}$$

**XI. SDS-PAGE**

Cells were cultured in 2ml LB medium overnight at 37 °C with the appropriate antibiotics. The cells were collected at 15,000rpm for 1 min in microfuge and resuspended by Bugbuster Protein Extraction Reagent (Novagen). The cell extract was mixed with an equal volume of 2×SDS loading buffer. The mixture was heated and then loaded on to a 12.5% SDS-PAGE.

**Solutions used are as follows:**

2× SDS loading buffer

| | |
|---|---|
| 0.25 M Tris/HCl (PH 6.8) | 25ml |
| β-mercaptoethanol | 5ml |
| SDS | 2g |
| Sucrose | 5g |
| Bromophenol blue | 2mg |
| | $H_2O$ to 50ml |

12.5% SDS-Gel:

| Separating Gel | | Stacking Gel | |
|---|---|---|---|
| Solution A | 3ml | Solution A | 0.35 ml |
| Solution B | 1.8ml | Solution C | 0.6 ml |
| TEMED | 7.5 ml | TEMED | 2.5 ml |
| 10% APS | 75 ml | 10% APS | 25 ml |
| $H_2O$ | 2.4ml | $H_2O$ | 1.45 ml |

Solution A (30% Acrylamide ):

| | |
|---|---|
| Acrylamide | 29.2 g |
| N,N'-methylenebisacrylamide | 0.8 g |
| Make up to 100 ml with water. | |

Solution B (1.5M Tris-HCl buffer, pH 8.8)

| | |
|---|---|
| Tris | 18.2g |
| SDS | 0.4g |
| HCl | 2ml |
| Make up to 10oml with water | |

Solution C (0.5M Tris-HCl buffer, pH 6.8):

| | |
|---|---|
| Tris | 6.1 g |
| SDS | 0.4g |
| HCl | 4.2 ml |
| Make up to 100 ml with water. | |

SDS running buffer (pH ~8.5):

| | |
|---|---|
| Glycine | 57.6 g |
| Tris | 12 g |
| SDS | 4 g |
| Make up to 4l with water. | |

Electrophoresis was performed at room temperature under the constant current of 25 mA using Mini-gel electrophoresis apparatus (ATTO, Japan).

**XII. Western blotting analysis**

After separation by SDS-PAGE analysis, tag fused proteins were transferred to a PVDF membrane by semi-dry blotter SartorblotII for approximately 1hour according to manufacturer's protocol. Then, the blotted membrane was soaked into TBST-BSA (Wako) (0.3%) buffer containing properly diluted primary antibody and incubated for 30 minutes at room temperature. Antibody anti-CyaA (3D1) (Santa cruz biotechnology) was used at the concentration of 1~2 mg/ml.

The membrane was washed four times with TBST buffer, and soaked into TBST-BSA (0.3%) buffer containing labeled secondary antibody and incubated for 30 minutes at room temperature. Anti-mouse IgG AP conjugate (promega, USA) was used at 8,000-fold dilution. The membrane was washed four times with TBST buffer and used in immune-detection of protein by the method appropriate to the secondary antibody. For detection using alkaline phosphatase (AP) conjugated secondary antibody. The washed membrane was soaked in the NBT/BCIP solution.

In case of S-tagged proteins, the blotted membrane was soaked into TBST containing gelatin (1%) for 1hour and then into the solution of TBST containing S-protein AP conjugate (Novagen) (0.5 micro litter/5 ml) for 30 min. The membrane was washed with TBST four times and the tagged proteins were detected by reaction with NBT/BCIP in the following solution.

NBT/BCIP solution

| | |
|---|---|
| Nitro Blue Terazolium (NBT) | 0.033% (w/v) |
| BromoChloroIndoly Phosphate (BCIP) | 0.0165% (w/v) |
| Tris/HCl (pH 9.5) | 0.1M |
| NaCl | 0.1M |
| $MgCl_2$ | 5mM |

The membrane was incubated for a while at room temperature until the bands of the target protein were detected. The reaction was stopped by wash the membrane

with deionized water.

| TBST | |
|---|---|
| 1M Tris-Cl (pH8) | 5ml |
| NaCl | 4.5g |
| $H_2O$ | to 500ml |
| Add Tween 20 | 0.5ml |

## RESULTS

### I. Relations between some y-genes involved in biofilm formation in *E. coli.*

#### I-1. PG of Δ*rodZ* mutant

As described in INTRODUCTION part, Δ*rodZ* mutant is non-motile, slow growth and sphere. A possible reason causing this phenotype is that *rodZ* mutant is defective in peptidoglycan synthesis. Therefore, I purified and examined the PG (peptidoglycan) in mutant cells. The results obtained (Table. 3) showed the amount of PG of Δ*rodZ* mutant was indeed reduced when cells were exponentially growing although at a later growth stage mutant cells acquired the PG similar to wild type cells.

**Table 3. Amount of PG in *ΔrodZ* mutant cells**

| | av | sd | % |
|---|---|---|---|
| KR0401 (WT) | 1891 | 695 | - |
| KR0401Δ*rodZ* | 336 | 197 | 18 |
| KR0401Δ*rodZ*-mot$^+$ | 1637 | 675 | 87 |

The amount of PG in isolated sacculi (μg) was normalized by the $OD_{600}$ of culture. The averages (av) and standard deviations (sd) are from four independent analyses.

However, this phenotype was not stable and often the PG comparable to the wild type cell was observed even in earlier growth stages. A possible reason for this could be: Δ*rodZ* mutant easily acquires a suppressor(s) mutation that gives a faster growth-rate, motility and near rod-type cell shape (Niba *et al.*, 2010). However it could also be; the amount of PG in Δ*rodZ* mutant significantly fluctuated depending on the subtle difference in culture conditions or the time of harvesting cells. Therefore, I speculated that the reduced PG of mutant is not due to the defect in PG synthesis itself but due to abnormality in transport, assembly, regulation or cooperation with other molecules required in the proper synthesis of PG.

Because previous investigation in our laboratory a few y-genes that were identified as being involved in biofilm formation were indicated to confer synthetic lethal phenotype with *rodZ* (*yfgA*) upon disruption of the gene. Among them I focused on two genes, *yhcB* and *yciB*, and performed various investigations to clarify their

function and relation to *rodZ*.

## I-2. Characterization of Δ*yhcB* and Δ*yciB* mutant

### I-2-1. Effects on the cell growth of deletion mutation and over-expression of *yhcB* and *yciB* genes

YhcB and YciB are described as putative conserved and non-essential proteins (Pec (Profiling of *E. coli* Chromosome) Ver.4). Indeed, a deletion mutant of *yhcB* (Δ*yhcB*) did not show any growth defect nor the reduced growth rate even at different temperatures (data not shown). On the other hand Δ*yciB* mutant showed a slower growth rate compared to the wild type parental strain and significant portion of cells appeared in irregular and/or gigantic cell shape under TEM observation (Fig. 10). This abnormal cell morphology was more frequently observed when the *yciB* gene was over-expressed from the multi-copy plasmid. Furthermore, many cells appeared to be dead and only the cell envelope seemed to be left.

It has also been reported that over-production of YciB is toxic to the cell, while that of YhcB presents no effect to the cell growth (GenoBase). However, no detail of these results is available. Therefore, I first examined if the similar phenotypes are observable with our strains. For this analysis, I first constructed plasmid pACYC-*yhcB* and pACYC-*yciB* as described in MATERIALS AND METHODS and transformed into deletion mutants and wild type (WT) strain KR0401. The resultant transformants were first grown overnight in LB medium containing the antibiotic to sustain the plasmid, and then sub-cultured in LB medium with or without L-arabinose (0.1%). Growth was monitored at hourly intervals by measuring OD600 of the culture. As shown in Fig. 11 and Table 4, the growth rate of Δ*yhcB* mutant was almost the same as WT, while Δ*yciB* showed a moderate reduction and which was complemented by pACYC-*yciB* under non-inducible condition (in the absence of L-arabinose). In contrast, both pACYC-*yhcB* and pACYC-*yciB* inhibited the cell growth in the presence of L-arabinose (Fig. 12). Interestingly, however, the growth of cells carrying plasmid pACYC-*yhcB* didn't stop immediately but increased to some extent (OD≈0.9) after induction. These results seem to indicate that the functions of *yhcB* and *yciB* are rather different, although both genes showed synthetic lethal phenotype with *rodZ* upon gene disruption and are predicted to encode IM proteins. Recently it was reported that most of membrane proteins somehow

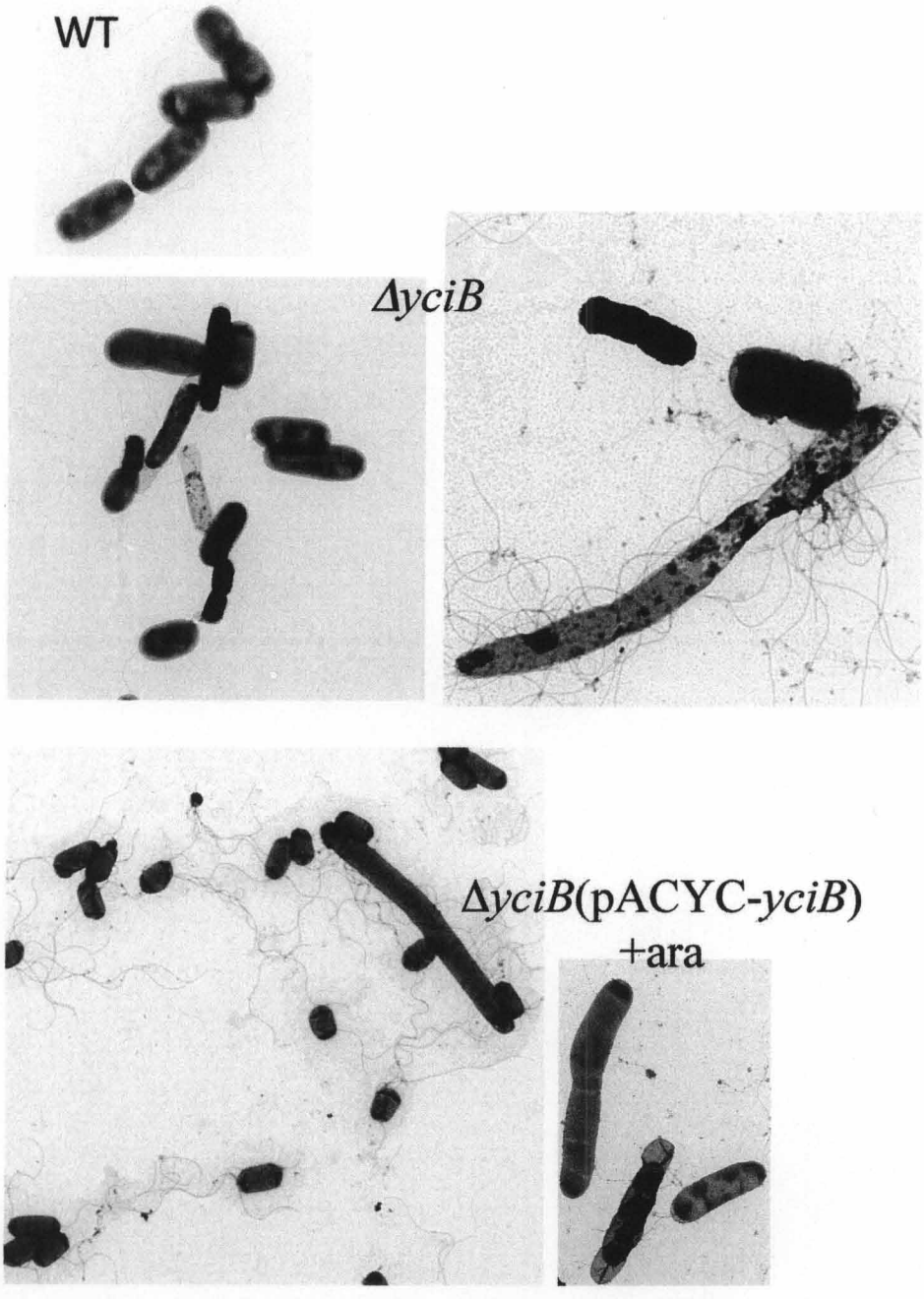


**Fig. 10 Δ*yciB* mutation causes abnormal cell morphology.**
Wild-type and Δ*yciB* cells were cultured in LB medium. Δ*yciB* carrying a multi-copy plasmid with *yciB* (pACYC-*yciB*) were grown in LB containing chloramphenicol and L-arabinose (0.1%) was added to induce the *yciB* gene. Cells were stained with 0.1% uranyl-acetate and observed by TEM.

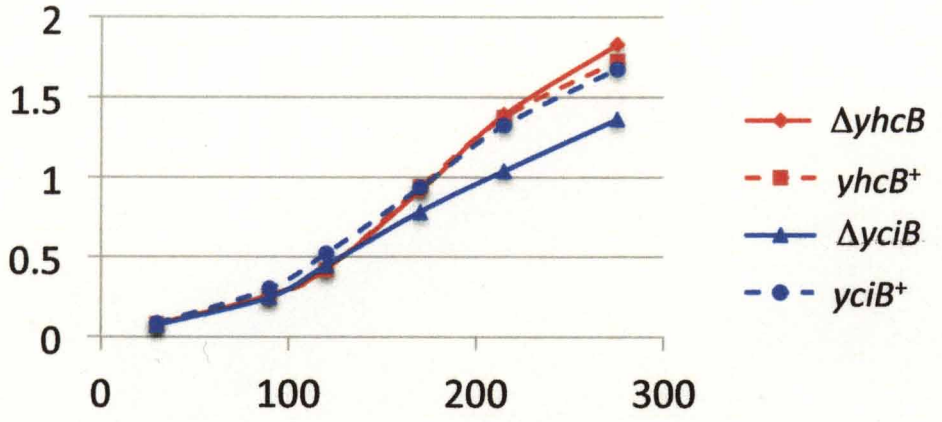


**Fig. 11 Effects of Δ*yhcB* and Δ*yciB* mutations on cell growth**
Cell growth of deletion mutants carrying the vector plasmid (*ΔyhcB, ΔyciB*) or the plasmids with cloned *yhcB (yhcB+)* and *yciB (yciB+)* were measured by $OD_{600}$.

**Table 4. Growth rates of wild-type and mutant cells carrying plasmids.**

| | | doubling time (min) | |
|---|---|---|---|
| strain | gene on plasmid | not induced | induced |
| WT | vector only | 68 | 74 |
| *ΔyciB* | vector only | 78 | 112 |
| *ΔyhcB* | vector only | 65 | 84 |
| WT | *yciB* | 77 | << |
| *ΔyciB* | *yciB* | 76 | << |
| WT | *yhcB* | 70 | 151 |
| *ΔyhcB* | *yhcB* | 66 | 187 |

Wild type, Δ*yhcB* and Δ*yciB* cells carrying indicated plasmids were grown in LB medium containing antibiotics. The cloned gene was induced by adding 0.1% arabinose. Growth rates were calculated from the increase of $OD_{600}$ for each culture.

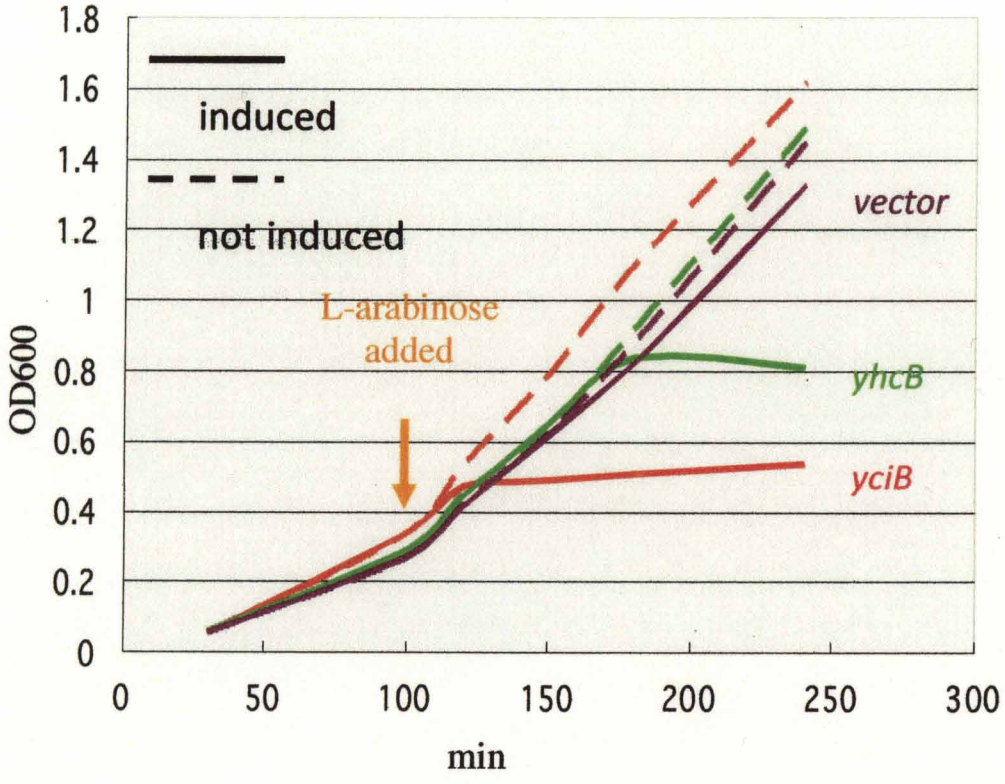


**Fig.12 Effects of YhcB and YciB overproduction on cell growth**
Wild type cells carrying vector plasmid (vector), with cloned *yhcB* (*yhcB*) or *yciB* (*yciB*) gene were grown in LB medium containing chloramphenicol. At indicated time L-arabinose was added in a portion of the culture.

inhibit the cell growth when over produced even though they are not toxic themselves, because overproduced membrane proteins would inhibit the transport of other membrane proteins and proper localization (Wagner *et al.*, 2007). This might be a reason of the delayed growth inhibition by the induction of *yhcB* on the plasmid.

### I-2-2. Δ*yhcB*Δ*rodZ* double mutant exhibits a synthetic lethal phenotype.

I further examined this synthetic lethal phenotype by constructing strains which harbor Δ*rodZ*Δ*yhcB* double deletion mutation and an inducible *yhcB* gene integrated in the chromosome, and monitoring the cell growth under *yhcB*-induced or repressed conditions. As shown in Fig. 13A, the growth of strain KR0413 (*ΔyhcB ΔrodZ::kan* $\lambda P_{araBAD}$-*yhcB*) was retarded when the cell density was about $OD_{600}$ of 0.5 after 3.8 generations in a medium containing 0.2% glucose, whereas it continued beyond $OD_{600}$ of 1.2 in the presence of 0.1% L-arabinose. The growth inhibition in the presence of glucose was also observed on the agar plate (Fig. 13B). In case of strain KR0411 (Δ*yhcB* Δ*rodZ::kan*) that carried $P_{araBAD}$-*yhcB* gene on multi-copy plasmid, cells continued to grow more than 5 generations under the repressed condition and the cell density reached over 1 $OD_{600}$. This might indicate that KR0411 probably contained more YhcB molecules than KR0413 and it took more generations under the repressing condition until the amount of YhcB in cell dropped to a critical level for the cell growth.

I tried to construct strains similar to KR0413 that harbor double deletion mutation, Δ*yciB*Δ*rodZ* and carry an inducible *yciB* gene. However, it was unsuccessful. The reason for this was not clear, but one problem was the phenotypes of both *yciB* and *rodZ* deletion mutations were very unstable. Spontaneous suppressor mutations seemed easily to occur and faster-growing cells emerged. Therefore, in case of *yciB* gene I could not proceed further to confirm the synthetic lethality with *rodZ* upon gene disruption.

Aiming to elucidate the function of *yhcB* and *yciB* in the cell, next I investigated their protein products, the localization and the interaction with other proteins in the cell, and the expression and genetic organization of these genes.

## II. Characterization of YhcB protein

### II-1. Subcellular localization of YhcB

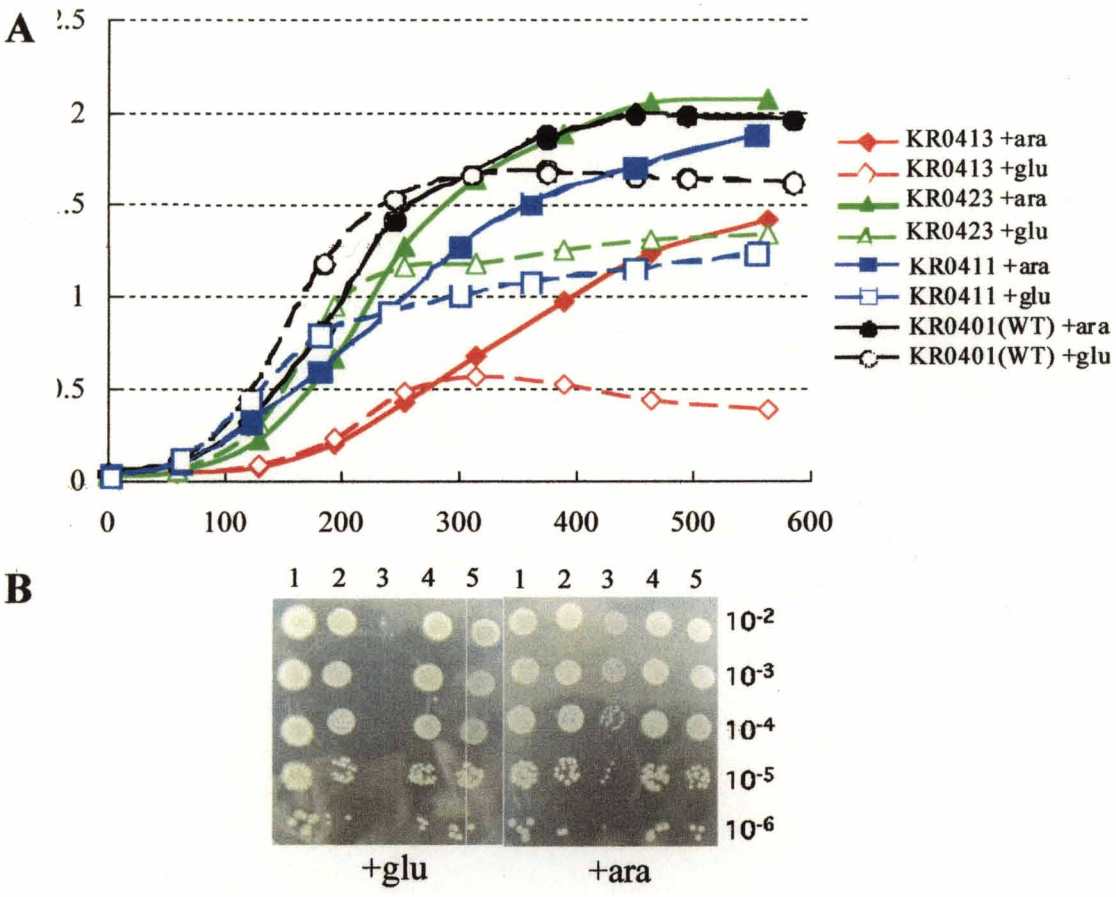


**Fig. 13 Growth of Δ*yhcB*Δ*rodZ* mutants carrying an inducible *yhcB* gene.**

**A.** Cells of indicated strains grown overnight in LB medium containing 0.1% arabinose were inoculated to give an OD600 of 0.025 into LB medium containing either 0.1% arabinose or 0.2% glucose. Ampicillin was also added at 100 μg/ml to the culture of Strain KR0411. Aliquots of culture were taken and OD600 were measured at indicated time intervals. KR0413 (*ΔyhcB ΔrodZ::kan* λ(*araC*, $p^{araBAD}$-*yhcB, bla)*:diamond (red); KR0423 (*ΔrodZ ΔyhcB::kan* λ(*araC*, $p^{araBAD}$-*yhcB, bla)*:triangle (green); KR0411 (*ΔyhcB ΔrodZ::kan*/pBADs-*yhcB*):square (blue); KR0401 (WT):circle (black). Solid (——) and dotted (…) lines indicate the culture with arabinose and glucose, respectively.

**B.** Strains KR0412 (*ΔyhcB* λ(*araC*, $p^{araBAD}$-*yhcB, bla)*; lane 1), KR0422 (*ΔrodZ* λ (*araC*, $p^{araBAD}$-*yhcB, bla)*;lane 2), KR0413 (*ΔyhcB ΔrodZ::kan* λ(*araC*, $p^{araBAD}$-*yhcB, bla)*; lane 3), KR0423 (*ΔrodZ ΔyhcB::kan* λ(*araC*, $p^{araBAD}$-*yhcB, bla)*; lane 4) and KR0411 (*ΔyhcB ΔrodZ::kan* / pBADs-*yhcB*; lane 5) were cultured in LB medium containing 0.1 % arabinose. Ten fold serial dilutions were made and 5 μl of each were spotted on LB agar plate containing either 0.1% arabinose or 0.2% glucose as indicated, and plates were incubated overnight at 37°C.

The primary structure of YhcB deduced from nucleotide sequence of the gene predicted that YhcB is an inner membrane protein of 132 amino acids and calculated molecular weight of 15kDa. In order to experimentally confirm its IM localization, I extracted and fractionated proteins in the cell of Δ*yhcB* mutant carrying pBADs-*yhcB* as described in MATERIALS AND METHODS Fig. 14A. The examination of cytoplasmic, inner and outer membrane fractions by SDS-PAGE followed by Western blotting analysis using S-protein AP conjugate as probe, detected the tagged protein of about 20kDa mainly in the inner membrane fraction Fig. 14B. This result strongly indicated that YhcB is indeed an inner membrane protein. The IM localization of YhcB was further supported by immunoelectron microscopy. Analysis was performed using cells of Δ*yhcB* carrying pACYC-*yhcB*. This plasmid was constructed to produce YhcB tagged with Myc. Therefore, the cellular location of YhcB-Myc was examined using anti-Myc antibody labeled with gold. The results obtained indicated that YhcB was distributed along the membrane and no localization either at the pole or the middle of the cell (Fig. 15), though further investigation and refining of the analysis are still necessary.

**II-2. YhcB interacted with RodZ *in vivo***

It was predicted that RodZ contains a helix-turn-helix domain in its N-terminus which is located at the cytoplasmic side of the inner membrane. Recent study has indicated that with this domain RodZ interacts with MreB, the bacterial actin, and assembles in complex (van den Ent *et al*, 2010). YhcB was likewise predicted, based on the information obtained from its primary structure, to possesses a potential PPI (protein-protein interaction) motif of coiled-coil structure at the cytoplasmic side (Fig. 16). In addition, synthetic phenotype described above indicated a functional interaction between YhcB and RodZ. Therefore, I next investigated whether they associated *in vivo* using a BACTH system (Karimova *et al.*, 1998).

In this system, two complementary fragments T18 and T25 derived from the adenylate cyclase of *Bordetella pertussis* are fused with proteins of interest, expressed in a *cyaA* mutant strain and the activity of *lacZ* is examined. I first constructed YhcB-T18 and T25-RodZ fusions using plasmid pUT18 and pKT25, respectively, because it was predicted that both proteins have a single trans-membrane domain and C-terminus of YhcB (Maddalo G, 2011) and N-terminus of RodZ (Newitt, 1999,

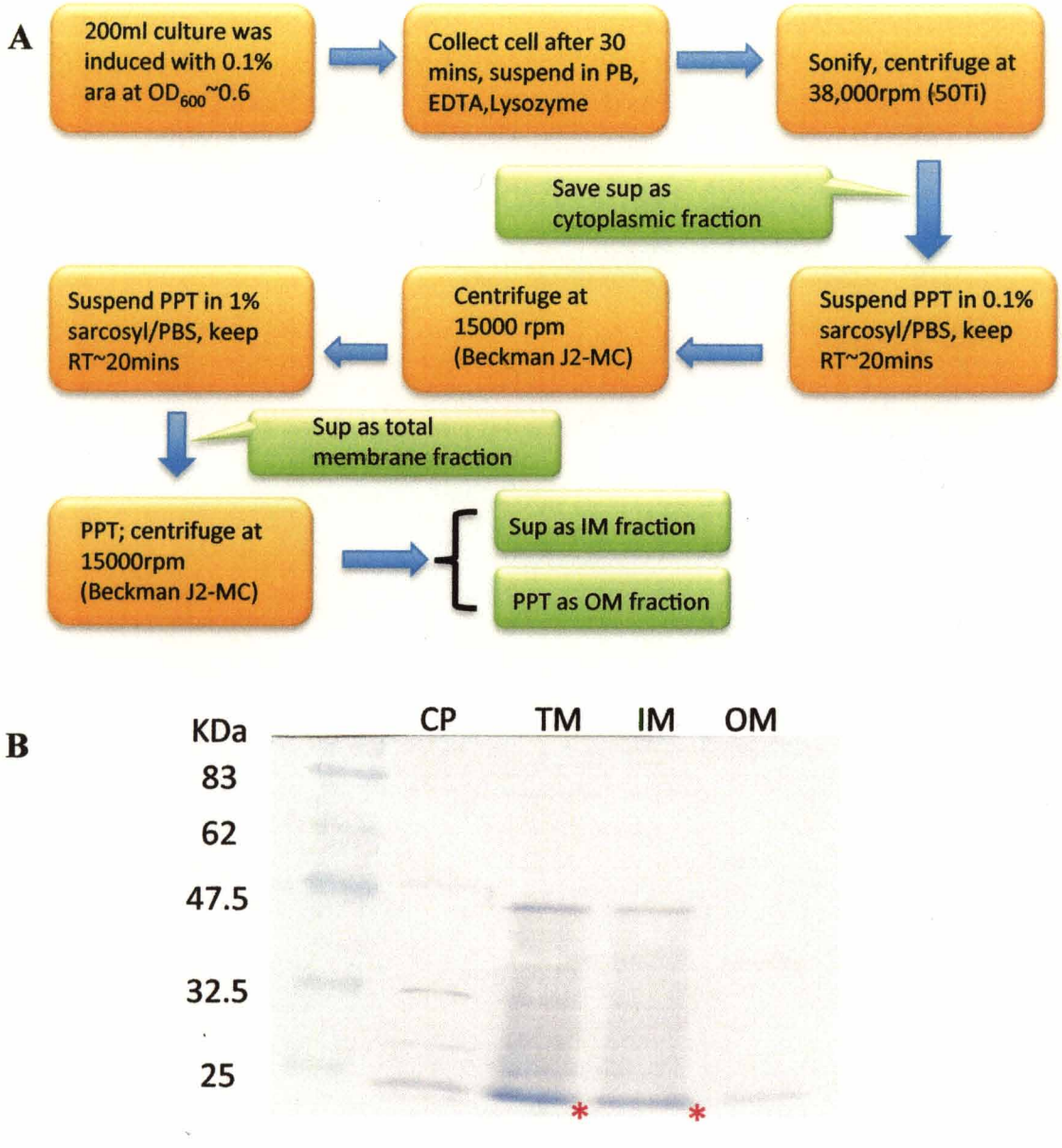


**Fig.14 YhcB is an inner membrane protein**

**A.** The procedure of cell fractionation (see Materials and Methods)

**B.** Cells (Δ*yhcB*) expressing S-tagged YhcB (mw=15kDa) from plasmid pBADs-*yhcB* were fractionated and subjected to Western blotting analysis using AP conjugated S-protein. Tagged protein of about 20kDa was mainly observed in IM fraction. (CP:cytoplasm, TM:total membrane, IM: inner membrane, OM: outer membrane)

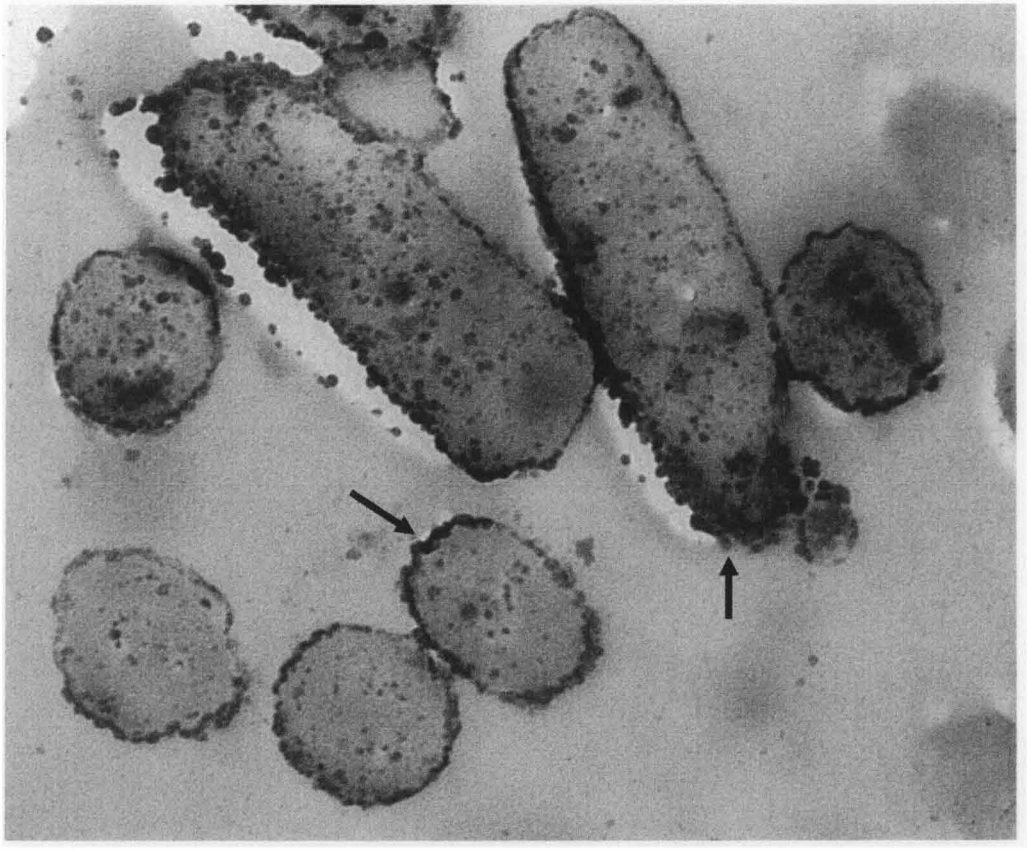

**Fig. 15 Location of YhcB observed by using immune electron microscopy**
Immunogold electron micrograph of thin sections of *cells* (Δ*yhcB*) expressing YhcB-Myc from plasmid pACYC*myc*-yhcB. Plasmid pACYC*myc* is a derivative of pACYC184, cloned gene on which is Myc tagged and inducible by L-arabinose.

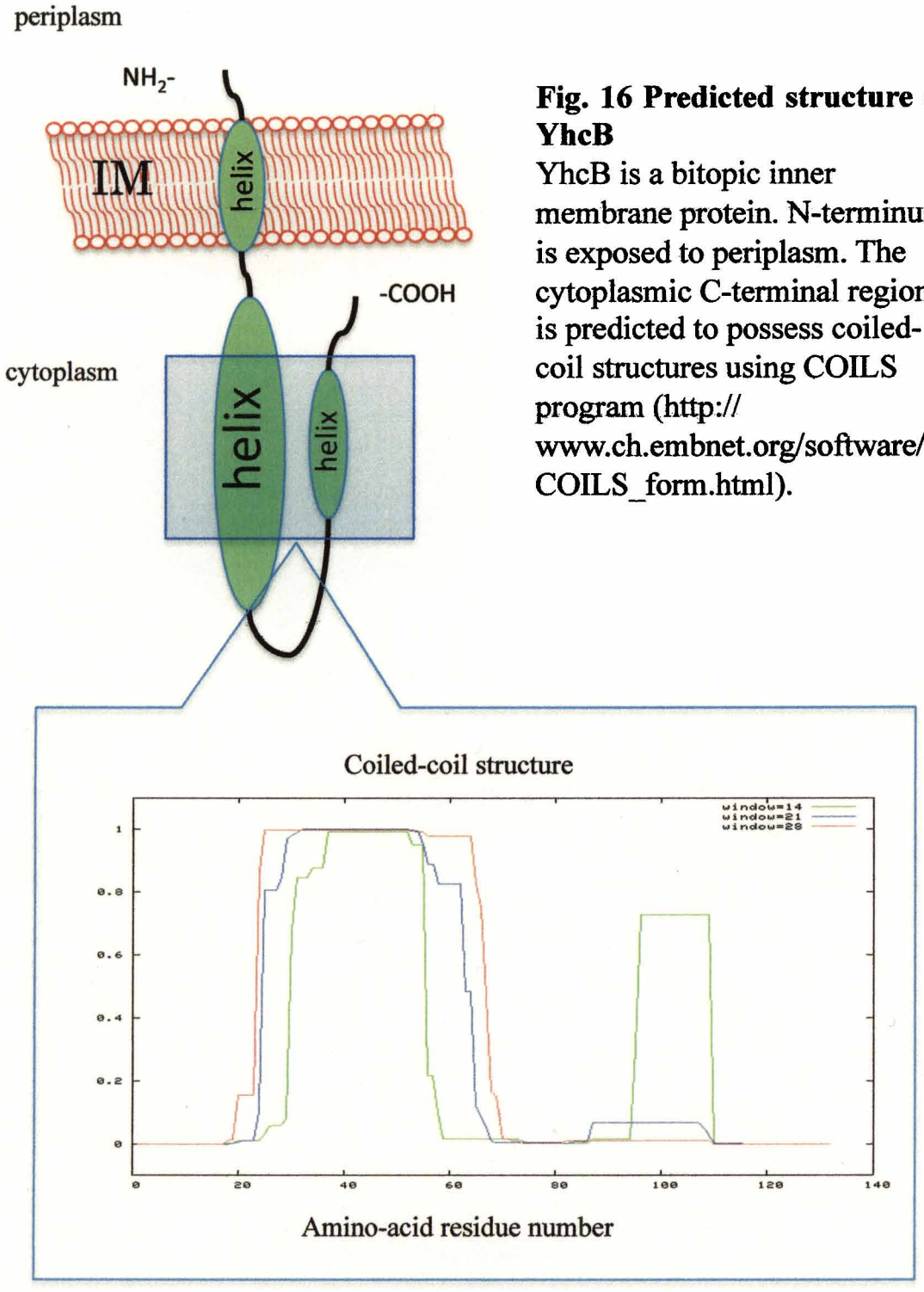


**Fig. 16 Predicted structure of YhcB**

YhcB is a bitopic inner membrane protein. N-terminus is exposed to periplasm. The cytoplasmic C-terminal region is predicted to possess coiled-coil structures using COILS program (http://www.ch.embnet.org/software/COILS_form.html).

Shiomi, 2008) are located in the cytoplasm. The transformants carrying YhcB-T18 and T25-RodZ formed blue colonies on LB medium containing X-Gal (Fig. 17A) and exhibited a high β-galactosidase activity (Fig. 17B), showing that indeed YhcB physically interacted with RodZ. YhcB and RodZ were also cloned into pKnT25 and pUT18c and co-transformed to JE8471, because the copy number of plasmid pKT25 (pKnT25) and pUT18 (pUT18c) is different and this could affect to the observed interaction as previously reported (Karimova *et al.*, 2009). The result obtained further confirmed the strong interaction between these proteins.

Next, we investigated which part of YhcB is required for the interaction using deletion mutants of *yhcB*. YhcB is predicted to contain two specific domains, a TM (trans-membrane) domain which extends from residue 4 to 25 (Maddalo G, 2011) and a large putative coiled-coil structure at amino acid residues 28 to 99 (COILS - Prediction of Coiled Coil Regions in Proteins). As shown in Fig. 18A, YhcBΔN (amino acid residues 22-132) and YhcBΔC1 (1-84), a half of the coiled-coil structure from the C-terminus deleted, gave white colonies upon co-transformation with pKT25-rodZ indicating that they did not interact apparently with RodZ. On the other hand YhcBΔC2 (1-113), which retained the coiled-coil structure, gave pale blue colonies indicating a week interaction (Fig. 18B). The extent of interactions was quantitatively assessed by assaying β-galactosidase activity, and results obtained were consistent with the color assay (Fig. 18C). These results indicated that the TM and the cytoplasmic helical structures are required for interaction with RodZ and the very C-terminal region predicted to have no secondary structure (Rost B *et al*, 2004) is also important. These last 20 amino acid residues might influence on the correct spatial folding of YhcB.

However, it could be the reason for these week or undetectable interactions that deletion mutants of YhcB-T18 fusion were not produced in the cell by some reason. Therefore, next I examined the expression of YhcB and its variants by Western blotting analysis. Total extracts of cells grown at 30℃ without or with IPTG induction were separated by SDS-PAGE and fusion proteins were detected using antibody to T18 as described in MATERIALS AND METHODS. As shown in Fig. 18D, regardless whether induced or not by IPTG, YhcB-T18 fusion protein was well expressed. The molecular mass of detected protein (approximately 30 kDa) is as expected for the fusion protein, that is 15 kD of YhcB and 17kD of the T18 tag. On the other hand, the amount of detected YhcB deletion mutants were drastically reduced. The large C-terminal

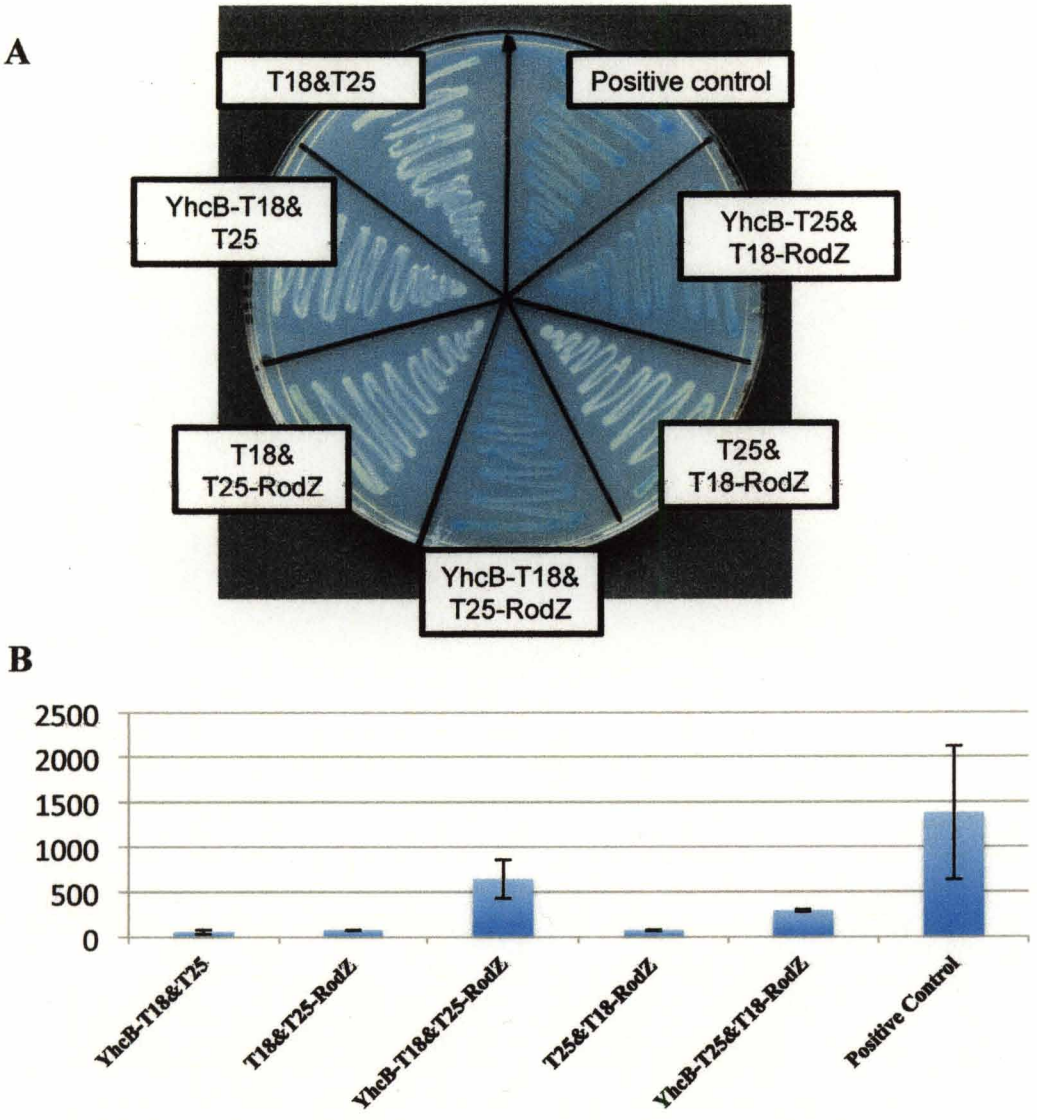


**Fig. 17 YhcB interact with RodZ *in vivo***

**A.** YhcB-RodZ interaction was monitored by BACTH system. T18 and T25 are complementary fragments derived from the adenylate cyclase of *Bordetella pertussis*. Transformants expressing indicated fragments or fusion proteins were streaked on a LB indicator plate containing X-gal (40 μg/ml) and IPTG (0.5 mM), and incubated at 30 °C for one day. Blue color indicates a positive interaction between each fusion protein. Positive control is the interaction of Leucine Zipper Motif.

**B.** Single colonies were picked up from each transformation and cultured in LB medium supplemented with appropriate antibiotics, and β-galactosidase assays were carried out according to Miller (1972). Average and standard deviation calculated from the measured activities of independent three analyses are shown.

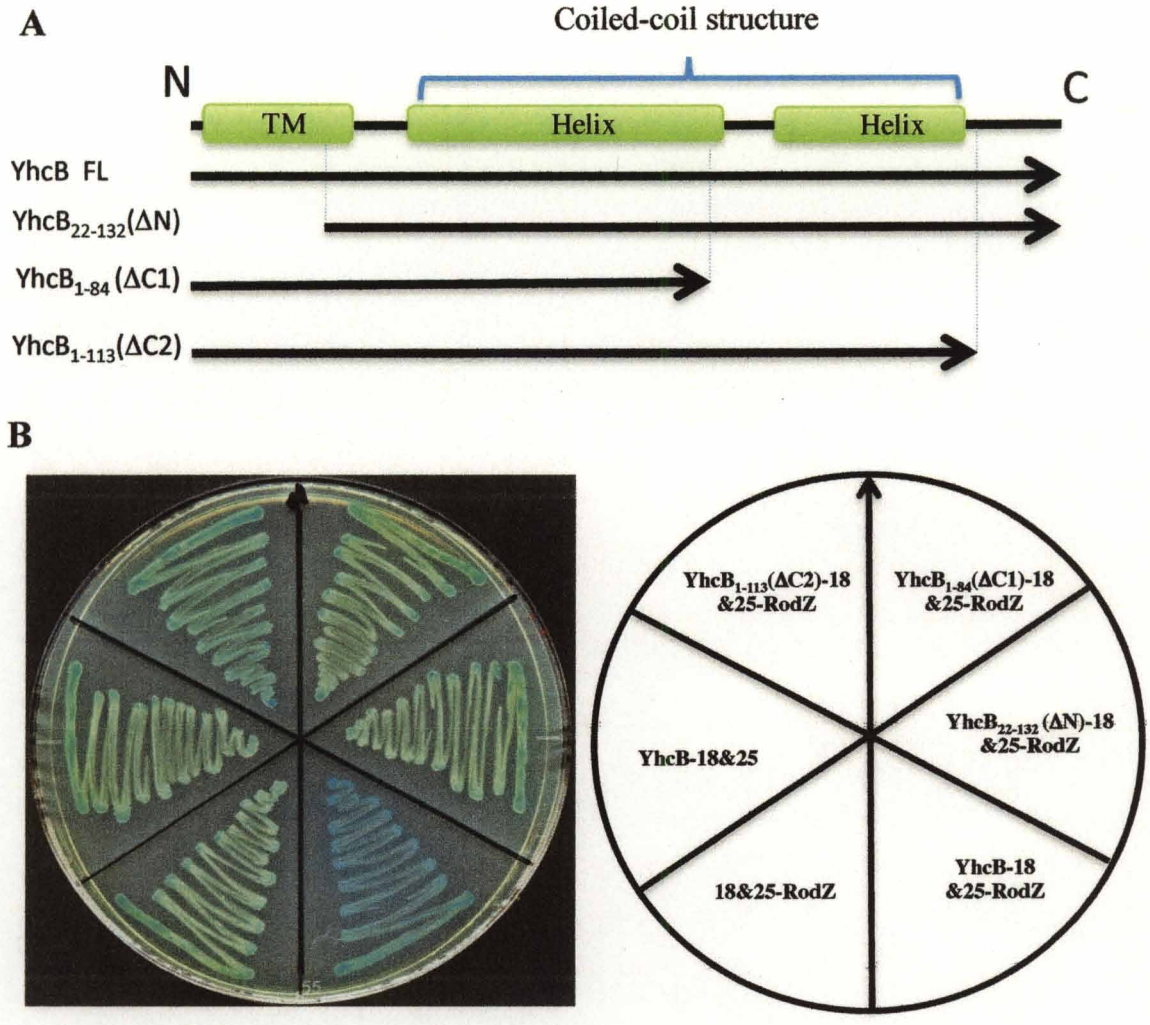


**Fig. 18 Interaction of YhcB deletion derivatives and RodZ**

**A.** Schematic representation of YhcB and its truncated derivatives. Predicted transmembrane domain (TM) and cytoplasmic helical structures (helix) are indicated. Thick lines show regions cloned into pUT18.

**B.** Transformants of JE8471 with indicated plasmids were streaked on a LB indicator plate containing X-gal (40μg/ml) and IPTG (0.5 mM), and incubated at 30℃ for 48hrs. Blue darkness indicates the strength of interaction between each fusion protein with T25-RodZ.

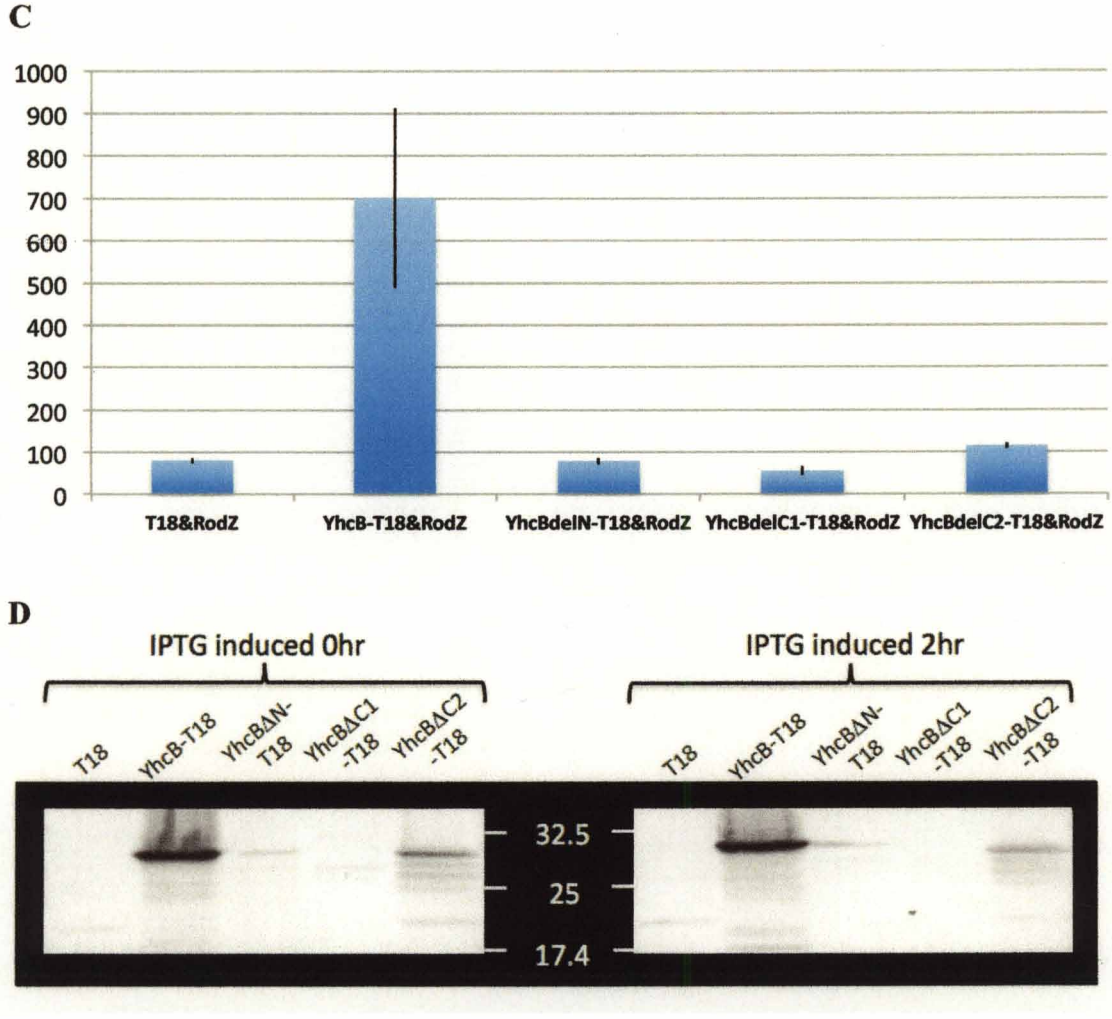


**Fig. 18 Interaction of YhcB deletion derivatives and RodZ. (continued)**
**C.** Interaction in each co-transformants was also examined quantitatively β-galactosidase assay as described in Materials and Methods.
**D.** Cells of each indicated co-transformants were cultured in LB medium containing appropriate antibiotics at 30℃, and subsequently induced by IPTG (0.5 mM) at around $OD_{600}$ of 0.6 when indicated. Total cell lysates were prepared, separated on SDS-PAGE and then probed with anti-CyaA (T18) antibody as described in Materials and Methods.

deletion protein (YhcB$\Delta_{1\text{-}84}$) was not visible after 2 hours of induction with IPTG, although it could slightly be detected before induction. The protein with a very C-terminal deletion (YhcB$\Delta_{1\text{-}112}$) seemed to be subject to the proteolysis, because various shorter bands were observed. These results indicated that truncated YhcB-T18 fusion proteins were unstable and this could be the reason of the observed week or non-detectable interactions and the low β-galactosidase activity. Alternatively, the absence of interaction might have led to the degradation of unincorporated proteins. In deed, it was reported that a hybrid protein was unstable in the absence of its interacting partner (Robichon C, 2011). In any event, the C-terminal region of YhcB seemed to be important for its interaction with RodZ. On the other hand, the helix-turn-helix domain (amino acid residues 30-49) of RodZ that was required for proper function of RodZ (Niba *et al.*, 2009) was dispensable for the interaction (Fig. 19).

**II-3. YhcB interacts with cell shape proteins**

RodZ is important for rod-type cell determination (Shiomi *et al.*, 2008; Bendezu′ *et al.*, 2008; Alyahya SA *et al.*, 2009). In *E. coli* RodZ was shown to interact *in vivo* with other cell shape proteins, MreB and MreC (Bendezú FO, 2009). The RodZ in *Caulobacter crescentus*, another Gram-negative, rod-type bacterium, was reported to interact with other cell shape proteins MreD and RodA as well as MreB (White CL, 2010). Therefore, I next examined whether YhcB also interacts with these proteins and MurG, N-acetylglucosaminyl transferase, which catalyses the final step of peptidoglycan precursor synthesis. MreB is localized in the cytoplasm and the other three shape proteins are inner membrane proteins. MreC has a TM domain and is bitopic with a large C-terminal end at the periplamic side (lee JC etc al., 2002). The other two, MreD and RodA, are multi-pass membrane proteins. The C-terminal end of MreD is located at the cytoplasmic face, while RodA's C-terminus is exposed to the periplasm (Uniprot database). MurG was predicted to be a cytoplasmic protein adhered to the cytoplasmic face of IM.

According to the topologic information, DNA fragments encoding MreB, C, D and MurG were cloned into pKT25 vectors to generate recombinant plasmids expressing hybrid proteins fused at the C terminus of the T25 fragment of CyaA (adenylate cyclase). The *rodA* gene was cloned into a different vector, pKNT25, to express a hybrid RodA protein fused to the N terminus of T25. These plasmids were

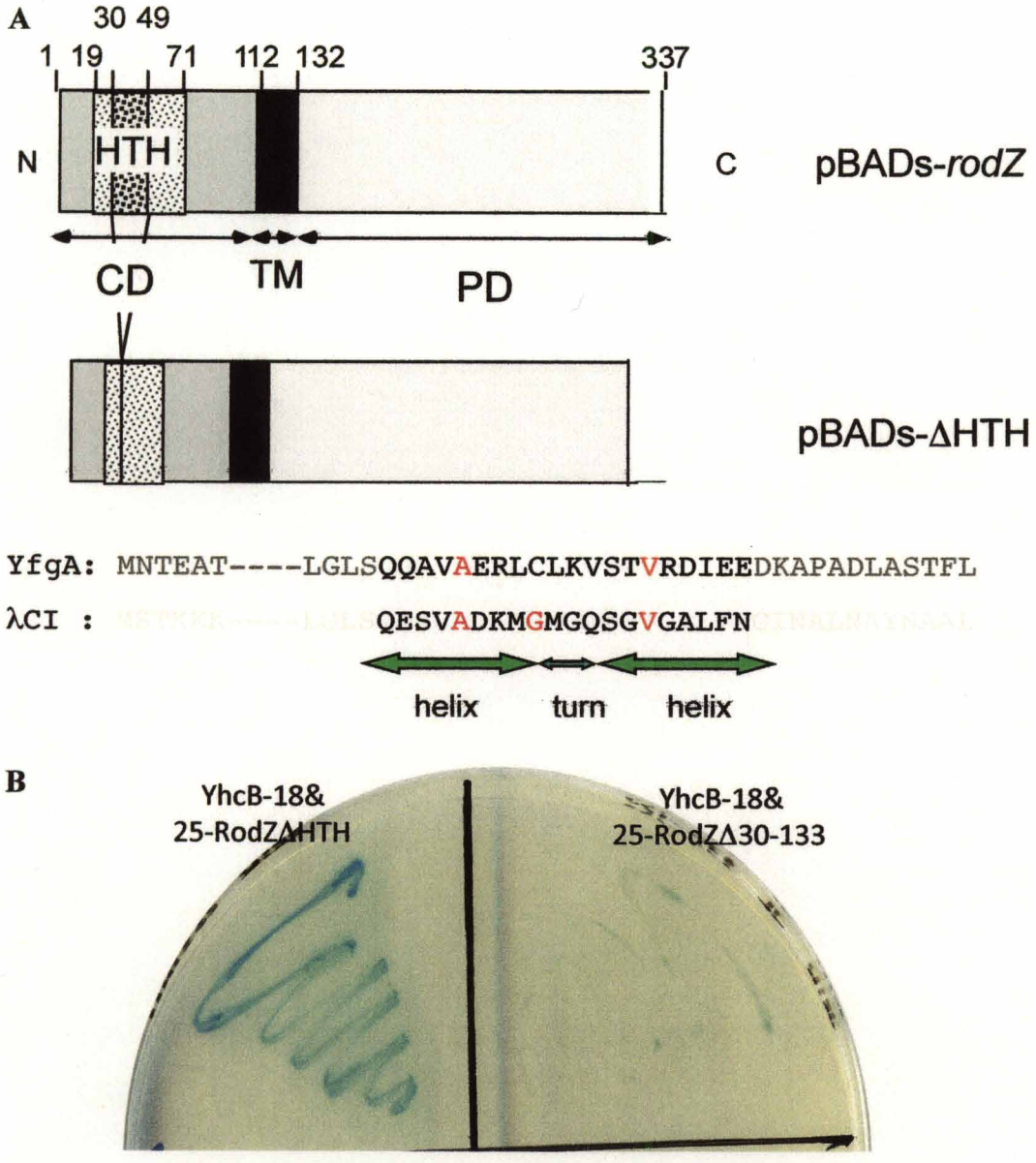


**Fig. 19 HTH domain of RodZ is not required for the interaction with YhcB**
**A.** Structures of RodZ and ΔHTH derivative are depicted. CD, TM and PD indicate cytoplasmic domain, transmembrane domain and periplasmic domain, respectively. The amino acid sequence of HTH domain was aligned with that of λcI. Highly conserved residues are colored (red).
**B.** Transformants of JE8471 with indicated plasmids were streaked on a LB indicator plate containing X-gal (40μg/ml) and IPTG (0.5 mM), and incubated at 30℃ for 48hrs.

co-transformed with pUT18-*yhcB* into JE8471 and the interactions were examined. MreC, MreD, RodA and MurG fusions gave dark blue colonies on LB agar plates containing X-gal (Fig. 20A). Also, the β-galactosidase activities of their interactions were high, 476, 254, 379 and 270 of Miller units (average), respectively (Fig. 20B). In contrast, no significant interaction of MreB with RodZ was detected using this system. Thus, I concluded that YhcB interacted with shape proteins MreC, MreD, RodA, RodZ and an enzyme for PG synthesis MurG *in vivo*, but not with the cytoskeleton MreB. Here it is notable that no interaction between RodZ and MurG was observed (White CL, 2010), while RodZ seemed to interact with MreB (Bendezú FO, 2009). This might suggest that YhcB connects the function of RodZ and MurG, because PG of *rodZ* mutant seems to be reduced as described above.

**II-4. The interaction of YhcB with cell-shape proteins is independent on the presence of RodZ**

Next, I also investigated whether YhcB directly associated with cell shape proteins or the interactions were mediated by RodZ. For this purpose, I performed the BACTH analysis in the absence of RodZ using JE8471Δ*rodZ* as indicator strain. The results of interactions with MreC, MreD and RodA are shown in Fig. 21. In case of MreC and MreD, co-transformants of JE8471Δ*rodZ* gave dark green colonies similarly to JE8471(WT), showing that the interactions of YhcB with MreC and MreD are independent on RodZ. On the other hand, RodA-T25 seemed to give colorless colonies in JE8471Δ*rodZ* carrying pUT18-yhcB, indicating that RodZ is required for the YhcB-RodA interaction. However, the interaction with RodA in the absence of RodZ was not clear, because about 20% of transformants were blue as in the presence of RodZ. A possible explanation for this observation is that the overproduction of RodA-T25 fusion protein in Δ*rodZ* mutant could be deleterious to the cell and RodA-T25 fusion protein was not produced in colorless transformants, because significant number of transformants could not grow upon single-colony purification.

**II-5. YhcB interacts with itself.**

In a recent study on cell envelop complex in *E. coli*, it was reported that the molecular mass of YhcB detected in a native PAGE system was approximately 5-12 times larger than the one estimated from the nucleotide length of *yhcB* gene (Maddalo,

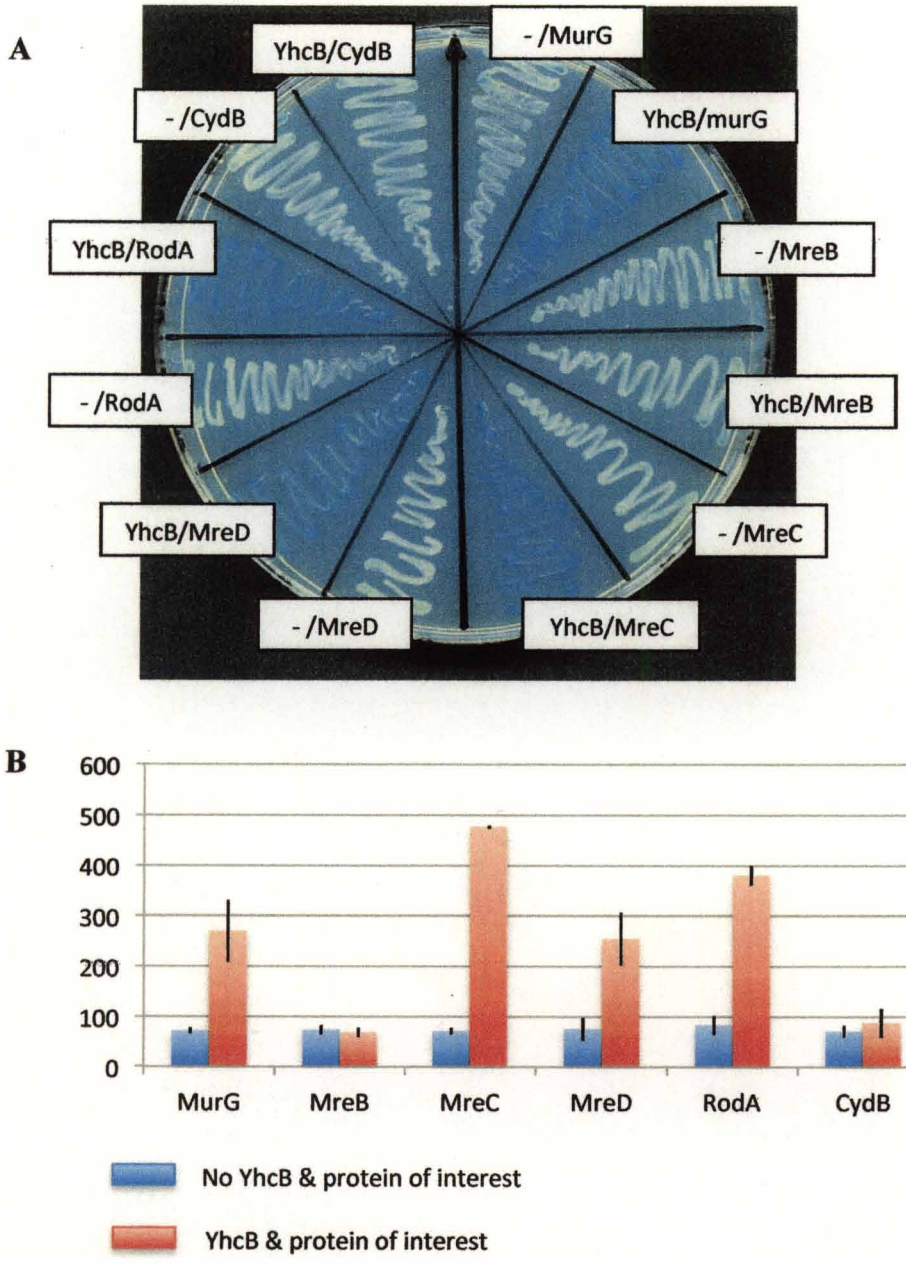


**Fig. 20 BATCH analysis of YhcB interaction with cell shape proteins and a subunit of cytochrome *bd* oxidase**

**A.** Transformants of JE8471 (Δ*cya*) with plasmids containing the indicated gene-fusions were streaked on an indicator plate containing 0.5 mM IPTG and 40μg/ml X-gal. '-'indicates vector only. The plate was incubated at 30℃ for 24hrs. Blue color indicates the positive interaction.

**B.** Interaction between YhcB and indicated proteins were quantified by measuring β-galactosidase activities of transformants harboring the corresponding plasmids.

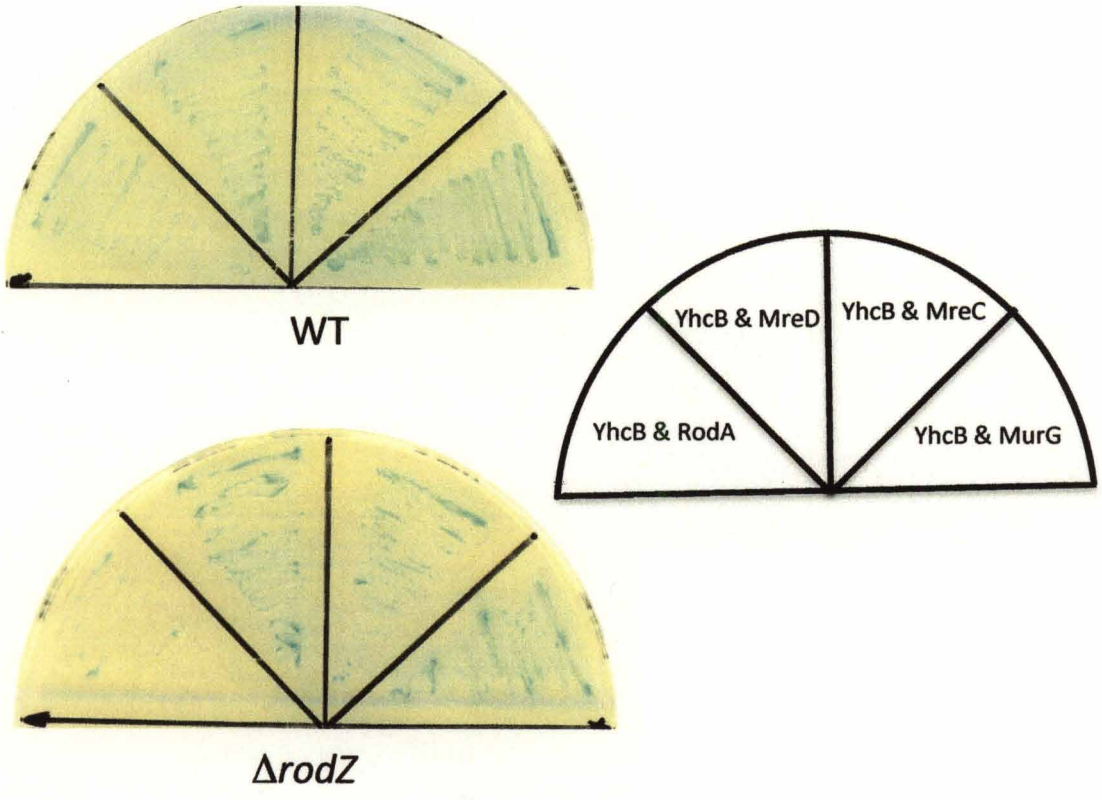


**Fig. 21 Interaction of YhcB and shape proteins are RodZ independent.** Plasmids containing the T25-fusion of indicated gene and pUT18-yhcB were co-transformed into JE8471 (upper) or JE8471Δ*rodZ* (lower) and interactions were examined on an indicator plate.

2011). It seems to indicate that YhcB monomers form a homo-oligomeric complex in inner membrane. To examine whether YhcB indeed interacts with itself, I performed BACTH analysis. As described above, the C-terminus of YhcB is localized in the cytoplasm. Therefore, pKnT25-*yhcB* was constructed and co-transformed with pUT18-*yhcB* into JE8471 cells. The dark blue colony color and the β-galactosidase activity of about 1,500 Miller units clearly showed that YhcB interacted with itself (Fig. 22). These results seem to indicate that YhcB indeed resides in IM forming a homo-oligomeric complex as suggested by Maddalo *et al.* (2011). In addition, I noticed that the cells carrying both pKnT25-yhcB and pUT18-*yhcB* grew significantly slower than those harboring either only pKnT25-*yhcB* or pUT18-*yhcB*. The reason for this could be that the excessive YhcB produced from both plasmids is harmful to the cell as in the case observed with pACYC-*yhcB* (Fig. 12, See Section I-2-1).

Finally I also investigated whether YhcB interacts with CydB, because the recent study of membrane protein complexes by Stenberg *et al.* (2005) reported that the YhcB protein was found together with CydA and CydB in the inner membrane and suggested that YhcB could be a new subunit of the cytochrome *bd* ubiquinol oxidase. On the other hand, the more recent study by Mogi *et al.* (2006) has shown that YhcB was not required for the assembly and function of the cytochrome *bd* complex (Mogi *et al.*, 2006). However, there is no strong evidence to deny the existence of YhcB in the CydAB complex. The results obtained (Fig. 20) showed no significant interaction between them, which seems to support the latter observation and indicate that YhcB is not a subunit of the cytochrome *bd* oxidase.

## III. Characterization of YciB

### III-1. Localization of YciB and topology

YciB was predicted to be an IM protein of 179 amino acids. However, the identification of YciB protein by Western blotting analysis is so far unsuccessful. The cells which carry plasmids containing a tagged *yciB* did not give any detectable protein, which is probably due to a low level of expression of *yciB* as described below.

Recently several methods to predict the topology of multi-pass membrane proteins were developed and YciB was predicted to contain five TM domains from its primary structure (Fig. 23 & Fig. 24) (TMpred, Hofmann & W. Stoffel, 1993). These *in*

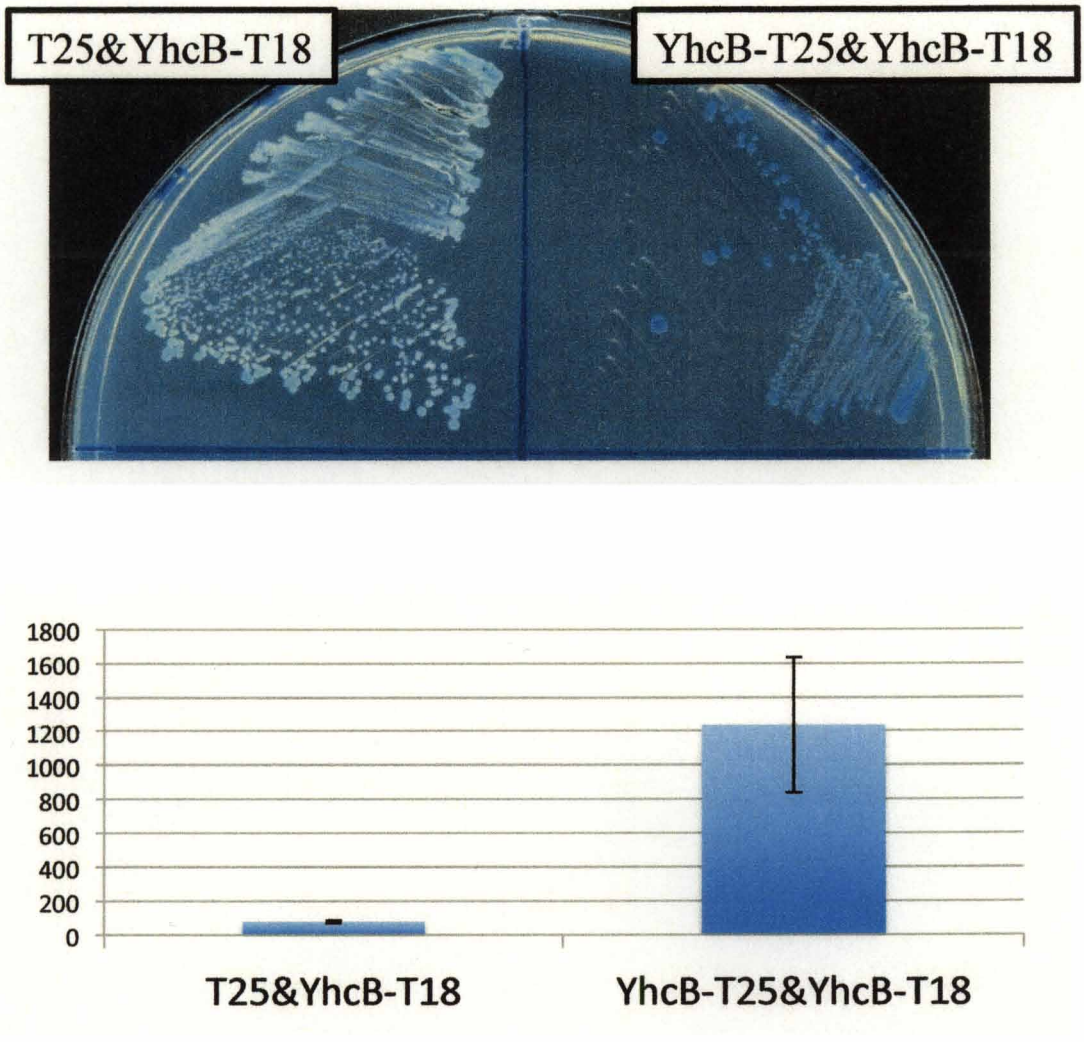


**Fig. 22 YhcB interacts with itself.**
The *yhcB* was cloned into pKnT25 as well as pUT18 and self-interaction was examined on the indicator plate (upper) and by the assay of β-galactosidase activity (lower).

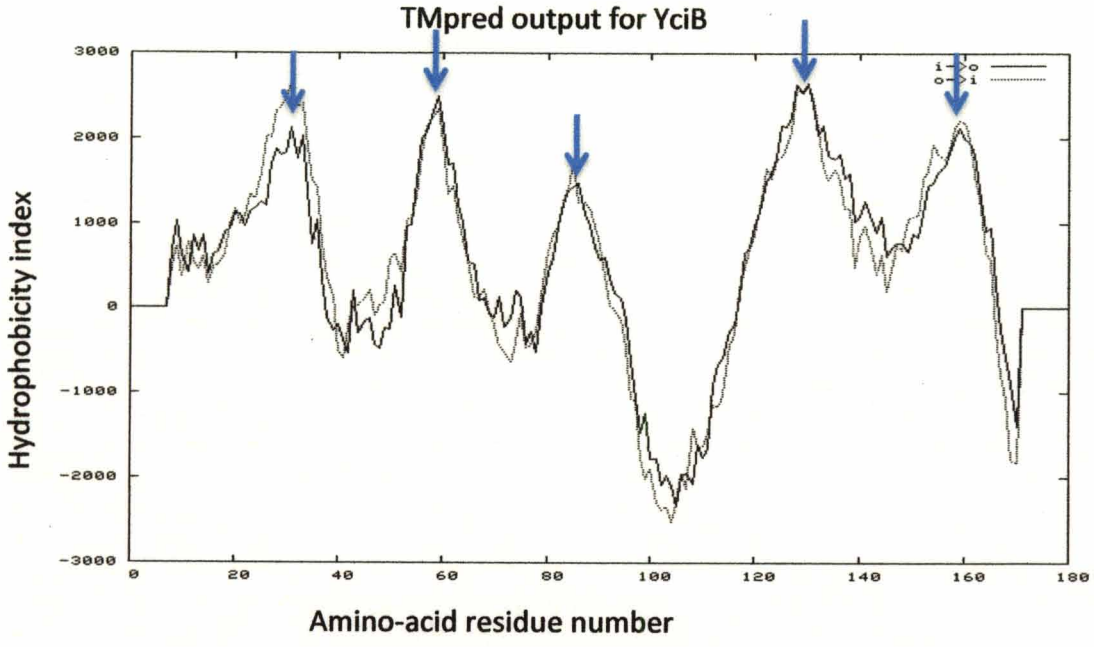


**Fig. 23 Prediction of the transmembrane domains of YciB**
Hydrophobicity plot of YciB was generated using TMpred program (http://www.ch.embnet.org/software/TMPRED_form.html). Possible TM domains are marked by arrows.

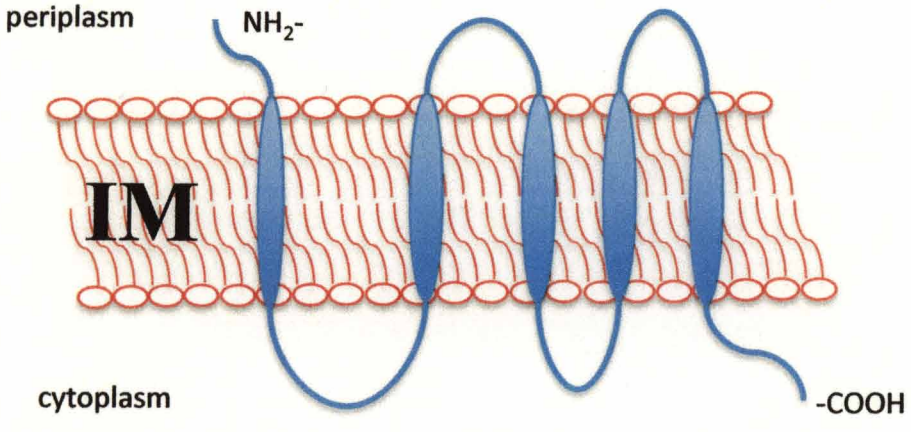


**Fig. 24 Model for the topological organization of YciB localized at inner membrane.**

*silico* analyses play important roles in structural biology, because the structure determination of multi-pass membrane proteins is extremely difficult by the common biophysical, biochemical and molecular biological methods. Furthermore, Karimova *et al.* (2009) developed a method that experimentally determines the topology of IM proteins. They constructed a plasmid pKTop that contains a dual reporter $PhoA_{22\text{-}472}/LacZ_{4\text{-}60}$, which consists of the *E. coli* alkaline phosphatase fragment and the α-peptide of *E. coli* β-galactosidase fused in frame (Gouzel Karimova *et al.*, 2009). The $PhoA_{22\text{-}472}$ lacks the signal peptide ($PhoA_{1\text{-}21}$) and has no ability of inner membrane insertion. Therefore, in this system, if the gene cloned on pKTop produces a fusion protein that can translocate the dual reporter across the inner membrane into the periplasm, PhoA is active and detected by the color blueness using BCIP, a chromogenic substrate of alkaline phosphatase. The cytoplasmic location determination relies on the principle of α-complementation of the β-galactosidase, where a fragment of the *lacZ* gene (*lacZ*α) in the plasmid can complement another mutant *lacZ* gene (*lacZ* ΔM15) in the cell. Thus, if the fusion protein expressed from the gene cloned on pKTop locates the dual reporter in the cytoplasm and exhibits β-galactosidase activity, colonies are colored red by Red-gal added in the medium (Fig. 25). This dual reporter system seemed to be useful for the analysis of YciB, because the methods of detecting both PhoA and β-galactosidase activity are very sensitive.

According to the structure and topology of YciB predicted by TMpred, serial deletion mutants deleted from the C-terminus were designed as shown in Fig. 26A, and each fragment was cloned into pKTop. The resultant pKTop clones containing these fusions were introduced into *E. coli* DH5α (*phoA*$^-$, *lacZ* ΔM15) and the expression and topology of the fusion protein were analyzed by BCIP and Red-gal. $YciB_{147}$ (1-443nt) and $YciB_{75}$ (1-227nt) fusion proteins exhibited strong phosphatase activity but low β-galactosidase activity indicating that the C-termini of these positions were localized at the periplasmic side of the inner membrane. In contrast, the full length of YciB, $YciB_{120}$ (1-359nt), $YciB_{48}$ (1-146nt) fusion protein showed high β-galactosidase activity but low phosphatase activity, showing that the C-termini of these proteins are positioned in the cytoplasm (Fig. 26B).

I also constructed a pKTop recombinant containing an N-terminal deletion mutant (123-537nt, 42-179aa) that lacks N-terminal region predicted to be periplasmic and the first TM domain. The C-terminus of this mutant was indicated to be

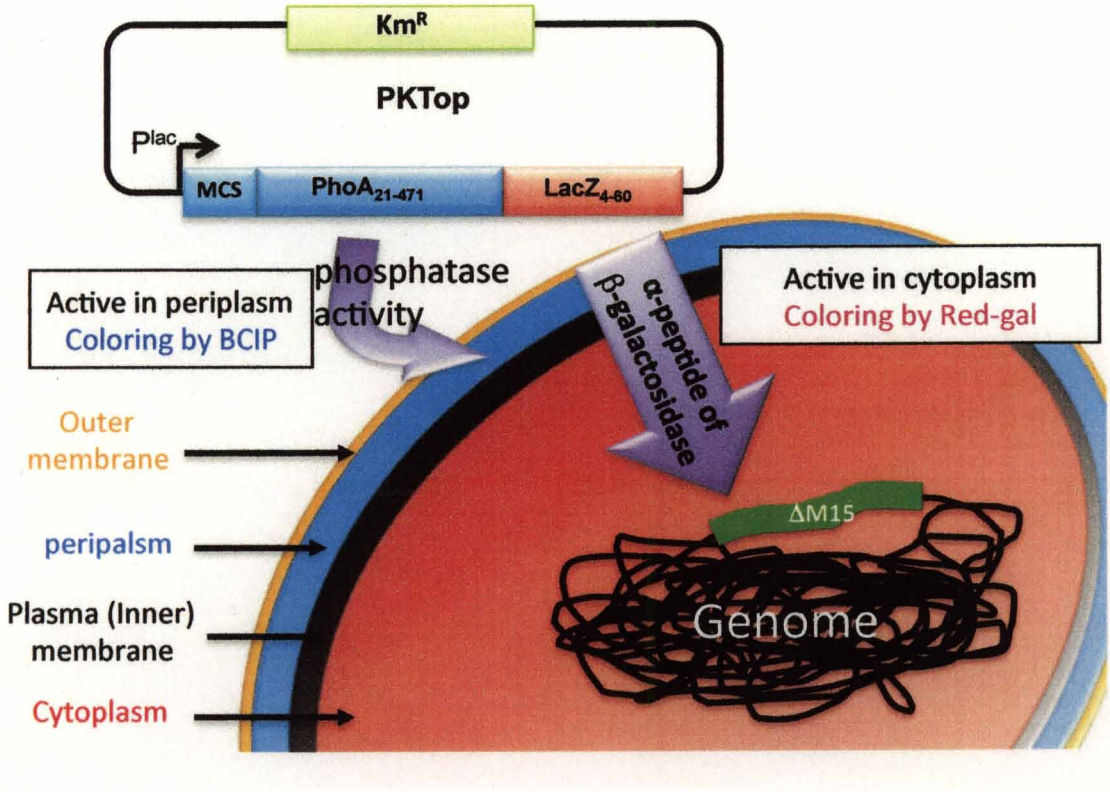


**Fig. 25 Membrane topology analysis by Pho-Lac dual fusion system.**
Plasmid pKTop contains a dual reporter $PhoA_{22-472}/LacZ_{4-60}$, which consists of the *E. coli* alkaline phosphatase fragment and the α-peptide of *E. coli* β-galactosidase fused in frame. Fusion protein localized at periplasm exhibites alkaline phosphatase (PhoA) activity; fusion protein localized at cytoplasm exhibites β-galactosidase (lacZ) activity.

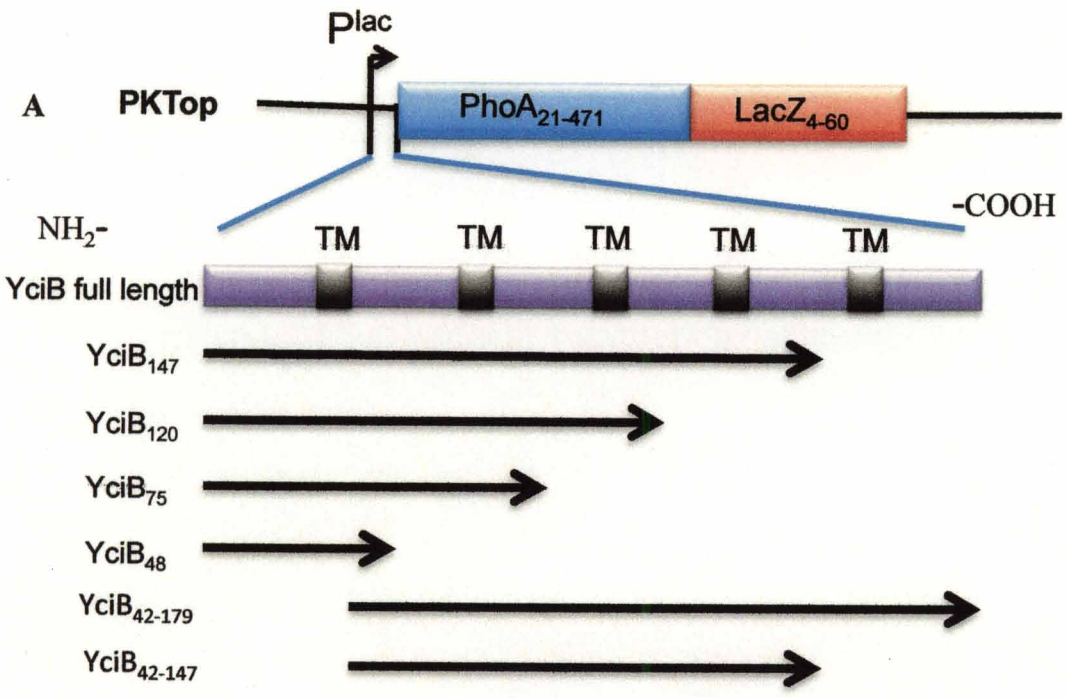


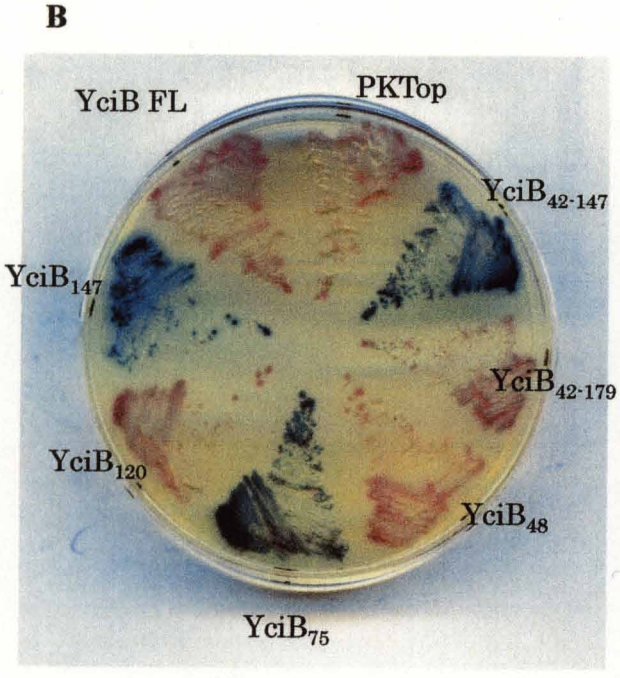


**Fig. 26 Topology of YciB**
**A.** Schematic representation of YciB and its truncated derivatives
**B.** *E.coli* DH5α cells expressing the different length YciB-Pho-Lac fusions were plated on indicator medium with two chromogenic substrates, BCIP (for phosphatase activity) and Red-Gal (for β-galactosidase activity). Blue coloration of colonies (high phosphatase activity) indicates periplasmic location of the fusion point. Red coloration of the colonies (high β-galactosidase activity) indicates cytosolic location of the fusion point.

cytoplasmic same as YciB-FL clone. Similarly, a mutant *yciB*$_{42\text{-}147}$ that is deleted both at N- and C-termini gave the same topological result (blue color) as the clone YciB (1-443nt, 1-147aa). These results seem to indicate that neither N-terminal nor C-terminal region is required for the membrane localization of YciB and the determination of membrane topology as well. Alternatively, the first 41aa region of YciB predicted to be periplasmic and TM domain might not function as signal peptide of cell membrane translocation and localized in the cytoplasm.

As summary, YciB is indeed a multi-pass IM protein and its C-terminus is located at the cytoplasmic side. N-terminus is most probably in the periplasm but further examinations are necessary to confirm it.

**III-2. Interaction between YciB and RodZ in BACTH analysis**

As in the case of YhcB and RodZ, the synthetic lethality of Δ*yciB*Δ*rodZ* was indicated from the genetic analysis by P1 transduction (Niba *et al.*, 2007), which could not be further confirmed though, as described above. Nevertheless, it is conceivable that YciB and RodZ interact or form a complex and play a role required for the cell growth. Thus, according to the topology information described above, I performed BACTH analysis to investigate the interaction between YciB and RodZ. YciB was C-terminally fused to T18 fragment of adenylcyclase (*cya*) (YciB-T18) and the interaction with T25-RodZ was examined. However, no significant interaction was observed (Fig. 27A) On the other hand, the C-terminal deletion clone YciB$_{1\text{-}120}$-T18 formed blue colonies when transformed into the host strain JE8471 carrying pKT25-*rodZ*, indicating that this truncated protein interacted with RodZ. More interestingly, when the T25 fragment of *cya* was fused to the N-terminus of YciB, which was predicted to be localized in the periplasm (T25-YciB), an interaction with T18-RodZ was detected (blue colony), though the β-galactosidase activity measured was much lower compared to the interaction of YciB$_{1\text{-}120}$-T18. I suspected that these unexpected results could be due to the differential expression of *yciB* derivatives in cells, because it was shown that overproduction of YciB was deleterious to the cell. Next, therefore, the proteins extracted from cells carrying these plasmids were examined by SDS-PAGE followed by Western blotting analysis. As shown in Fig. 27B, no full length YciB protein was detected but, in contrast, the band of 30 kDa expected for YciB$_{120}$-T18 was well detected. These results strongly indicated that the reason for no-interaction between

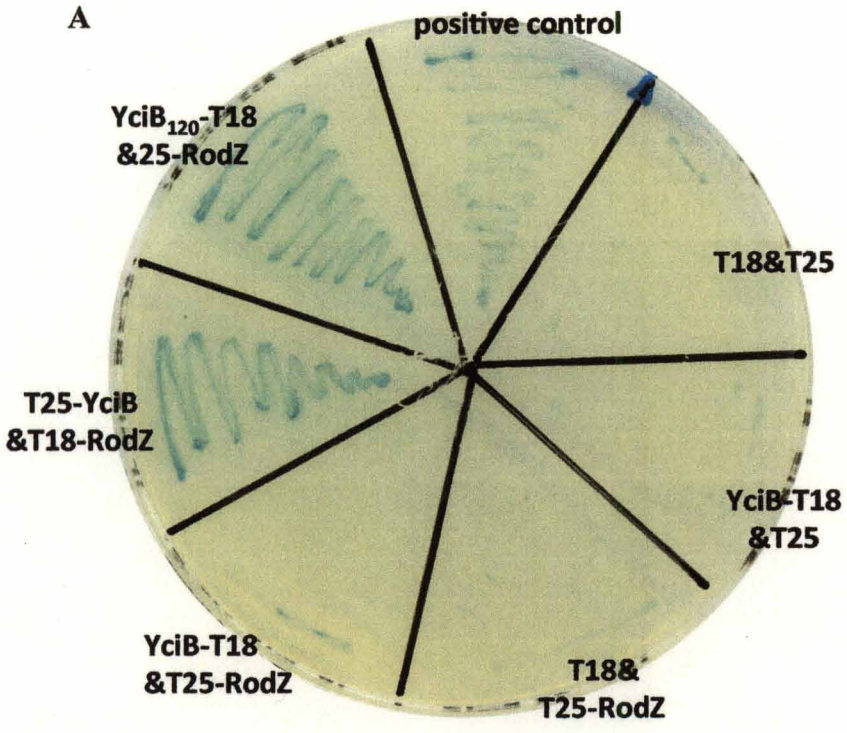


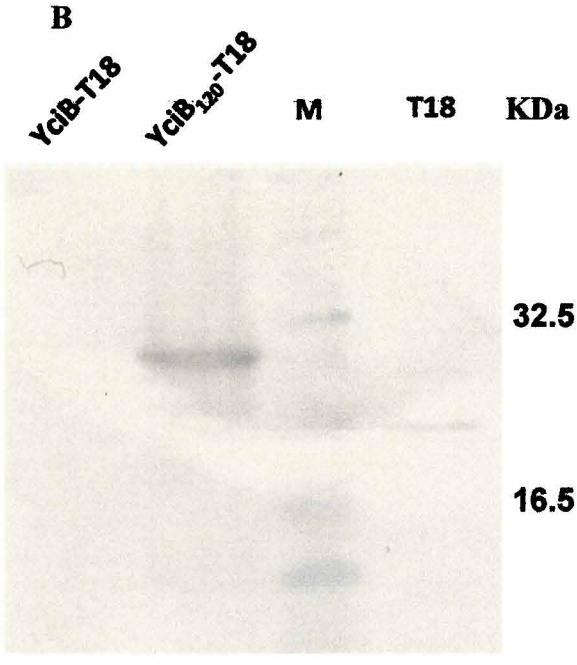


**Fig. 27 BATCH analysis of YciB interaction with RodZ**

**A.** BACTH analysis was carried out using plasmids containing the indicated fusions, and plated on indicator plate containing 0.5 mM IPTG and 40μg/ml X-gal. Blue color indicates a positive interaction between each fusion protein.

**B.** Cells of each indicated co-transformants were cultured in LB medium containing appropriate antibiotics and subsequently induced at 30℃ by IPTG (0.5 mM), at around $OD_{600}$ of 0.6 when indicated. Total cell lysates were prepared, separated on SDS-PAGE and then probed with anti-CyaA (T18) antibody as described in MATERIALS AND METHODS.

YciB and RodZ detected the low expression of full length YciB protein and/or the rapid degradation. On the contrary, probably the $YciB_{120}$-T18 that is about two third of intact YciB is not harmful when over expressed and still retained the ability to interact with RodZ. The reason why blue colonies and a low β-galactosidase activity was detected in the cell that should express T25-YciB might be explained if the fusion protein attached with T25 at the N-terminus could not be well inserted into the cell membrane and therefore T25 remained in the cytoplasm, which would have given a chance to interact with T18-RodZ in the cytoplasm. The fusion protein unable in IM insertion might be also less harmful compared to wild type YciB and expressed more in the cell, though I could not examine this possibility because the antibody against T25 was not available.

**IV. Genomic organization and transcription expression analysis of *yhcB* and *yciB***

The genomic context can often reveal clues to the function of genes, since genes coding for proteins with related cellular function often cluster together to allow co-regulation. With this concept in mind I searched for operon arrangements of *yhcB* and *yciB* gene in organisms that are related to *E. coli* (Fig. 28). The *yhcB* exists only in γ-proteobacteria, and it is conservatively arranged with downstream *degQ* and *degS* in chromosomal genome. To assess whether *yhcB* is co-transcribed with *degQ* and *degS*, DNA fragments containing indicated regions (Fig. 29) were cloned and fused with *lacZ* as described in MATERIALS AND METHODS. The expression of *yhcB* was found to be much higher than that of *degS*, indicating that *yhcB* is transcribed separately from *degQ* and *degS*. Although *degQS* was reported as an operon (Mendoza *et al.*, 2009), the β-galactosidase activities of #1, #2 and #3 clones were similar suggesting the presence of a weak promoter for the expression of *degS* downstream from the promoter of *degQ* (Table 5.). However, more examinations are necessary to clarify the expression and regulation of these genes.

Gene *yciB* also clusters conservatively between upstream gene, *yciC* and down upstream one, *yciA*. DNA fragments containing this region were cloned into pJL30 as indicated in Fig. 30 and the expression of *lacZ* measured. The results showed *yciA* was mostly expressed from the promoter located upstream of itself, and *yciB* was transcribed from a weaker promoter located upstream of itself (Table 6.) as predicted by Huerta *et al.* (2003). A promoter sequence was predicted upstream of *yciC*, another function unknown gene, but its activity remains to be examined. Therefore, they

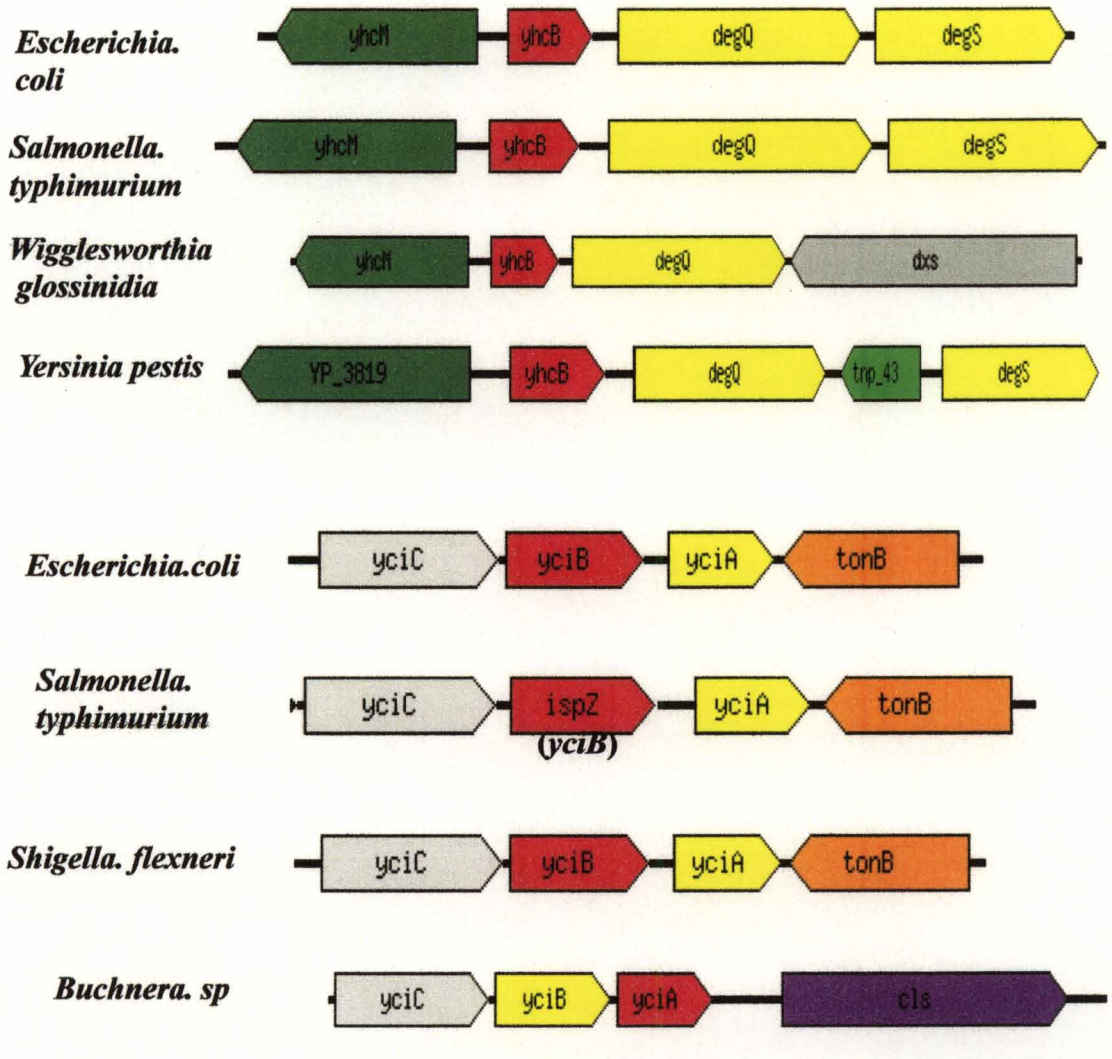


**Fig. 28 Genetic context of *yhcB* and *yciB***
Neighboring genes of *yhcB* and *yciB* were searched by Gene Context Toll II (http://bioinfo.ibt.unam.mx/gecont/index.cgi).

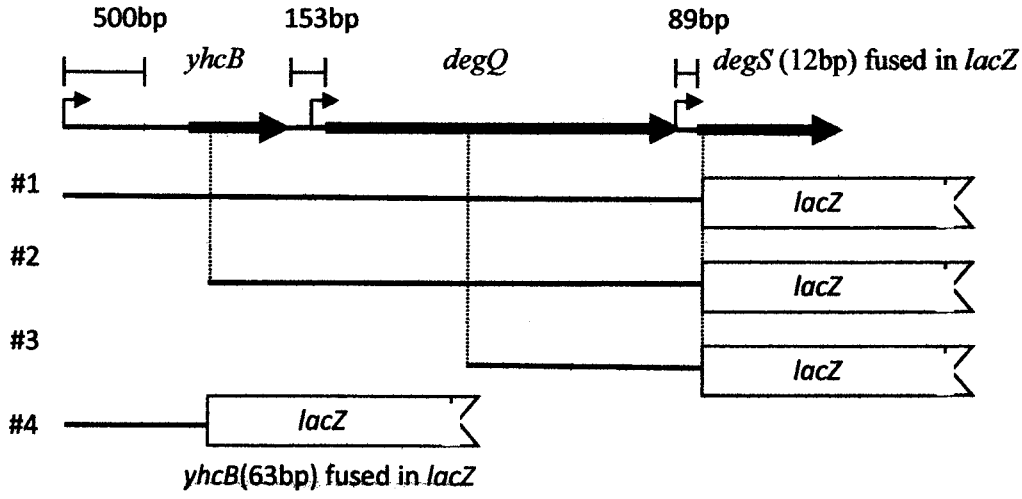


**Fig. 29 Construction of *lacZ* fusion for expression of *yhcB* gene**
Genetic organization of *yhcB, degQ* and *degS* genes and predicted promoters are depicted. The regions fused to *lacZ* gene on pJL30 plasmid are depicted (thick bar).

**Table 5. β-gal activities of the regions fused on *lacZ* for *yhcB* gene expression**

| sample | β-gal activity (Miller units) |
|---|---|
| control | 2 ± 1.7 |
| #1 | 13 ± 0.9 |
| #2 | 6 ± 0.4 |
| #3 | 10 ± 1.5 |
| #4 | 92 ± 16.0 |

Cells of strain KR0401 carrying individual plasmids were grown in LB medium containing ampicillin (100 μg/ml) at 37 °C to an $OD_{600}$ of around 0.5, their β-galactosidase activities (Miller units) were measured, and average values with standard deviation of three or more independent experiments are shown.

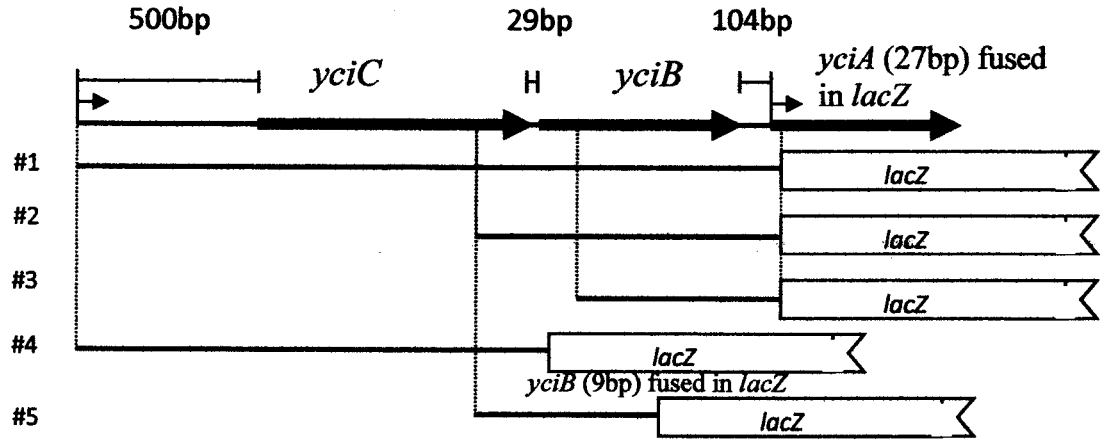


**Fig. 30 Construction of *lacZ* fusion for expression of *yciB* gene**
Genetic organization of *yciC*, *yciB* and *yciA* genes and predicted promoters are depicted. The regions fused to *lacZ* gene on pJL30 plasmid are depicted (thick bar).

**Table 6. β-gal activities of the regions fused on *lacZ* for *yciB* gene expression**

| sample | β-gal activity (Miller units) |
|---|---|
| control | 9 ± 3.6 |
| #1 | 237 ± 197.4 |
| #2 | 580±52.8 |
| #3 | 553±66.8 |
| #4 | 51±11.0 |
| #5 | 46±3.8 |

Cells of strain KR0401 carrying individual plasmids were grown in LB medium containing ampicillin (100 μg/ml) at 37 °C to an $OD_{600}$ of around 0.5, their β-galactosidase activities (Miller units) were measured, and average values with standard deviation of three or more independent experiments are shown.

seem to be transcribed separately. Nevertheless, the analyses of genetic and functional interaction between *yciB* and *yciC* might give hints to elucidate their function because of the conserved genetic organization.

## DISCUSSION

### I. Role of YhcB

Proteomic studies on the *E. coli* membrane proteins using a blue-native polyacrylamide gel electrophoresis (PAGE), postulated YhcB as a putative third subunit of the cytochrome *bd* ubiquinol oxidase, together with the other two subunits CydA and CydB (Stenberg *et al.*, 2005). However, in a later study on YhcB by Mogi *et al*, no YhcB like protein (15kDa) was detected in the cytochrome *bd* complex isolated from wild-type strains. In addition, they found no difference in the kinetic parameters for the quinol oxidation between wild-type and Δ*yhcB* strains. My results of BACTH strongly supported the idea of Mogi *et al.* Furthermore, cytochrome *bd* is widely distributed among bacteria and archaebacteria, and is assumed to be a hetero-dimeric oxidase (CydAB). On the other hand, *yhcB* is found only in γ-proteobacteria and the gene is located on the chromosome at 72.82' well separated from *cydAB* (16.6') in *E. coli*, which seems to indicate that YhcB does not participate in the activity of oxidase, even if it were associated with the complex.

In this study, I also examined the expression of *yhcB* together with its chromosomal neighbors, *degQ* and *degS*, and found that *yhcB* was expressed separately from *degQS*. However, it is still conceivable that YhcB and DegQS are functionally somehow related because DegQS are periplasmic proteases and involved in the protein quality control in the cell envelope (Sawa *et al.*, 2011).

### II. Why is the Δ*yhcB*Δ*rodZ* double mutant synthetically lethal?

*rodZ* (*yfgA*) and *yhcB* were identified as novel genes involved in biofilm formation by screening the Keio collection of gene deletion mutants (Niba *et al.*, 2007). The *rodZ* was later reported that it was required to maintain the proper cell shape (shiomi *et al.*, 2008; Bendezu′ *et al.*, 2008; Alyahya SA *et al.*, 2009). Cells lacking the *rodZ* were round or otherwise misshapen, and exhibited a highly reduced growth rate although *rodZ* is not essential for cell survival. The gene *yhcB* is also non-essential, deletion mutation of which exhibited no effect on the cell growth. However the cells with double deletion mutations of *rodZ* and *yhcB* seemed to be lethal and this lethality could be rescued by the introduction of $rodZ^{+}$ (Niba *et al.*, 2007).

In this study, I have given more evidence to support the synthetic lethality of Δ*yhcB*Δ*rodZ* mutant, and showed that *yhcB*$^{+}$ could rescue the lethality. This suggested that the physical interaction between YhcB and RodZ might be required for the cell survival and cell shape maintenance as well. Indeed, I have found that YhcB interacted with RodZ using BACTH system. Since *rodZ* was shown to be a crucial factor for the rod type cell morphogenesis and my examination confirmed that the amount of peptidoglycan in Δ*rodZ* mutant was significantly reduced (Results I-1, Niba *et al.*, 2010), it is conceivable that YhcB helps the function of RodZ in the synthesis of PG. I also confirmed the interaction of YhcB with MurG, a cytoplasmic enzyme for the final step in peptidoglycan precursor synthesis. Therefore, I speculate that YhcB might be required in transporting the precursor of peptidoglycan from cytoplasm to periplasm, which could also be a function of RodZ. It is said that a defect in any one of authentic cell-shape proteins such as MreBCD causes spheric cell morphology and eventually the cell dies but if the amount of FtsZ is slightly more than normal, the cell can survive. FtsZ, a tubulin-like protein with GTPase activity, is required for the cell division and growth. It assembles and forms the septal ring in the initiation of septation. On the other hand the Δ*rodZ* mutant also shows sphere phenotype but it continues to divide and grow, though the growth rate is significantly reduced. I therefore suspect that in Δ*rodZ* mutant the PG synthesis is very low but the cell can still manage to produce the septum and divide. However, if YhcB were also absent, the PG synthesis would be below the threshold of sustaining the septum formation and cause the lethality.

**III. The interaction domain of YhcB**

YhcB is multi-domains protein; it has a single trans-membrane domain at its N-terminal end that divides the protein into a periplasmic and a large cytoplasmic part. The cytoplasmic part was predicted to form coiled-coil structures by COILS (Lupas, A *et al.*, 1991; Lupas, 1996). Here I have shown that both the N-terminal TM domain and C-terminal coiled-coil structure domains are required for the YhcB interaction with RodZ and/or the protein stability. YhcB lacking the N-terminal TM domain (YhcBΔN) or the first C-terminal coiled-coil structure domain (YhcBΔC1) could not be detected by Western blotting analysis. Many recombinant proteins produced in *E. coli* are unable to obtain their native conformation and tend to be degraded rapidly by cell proteases. Cell proteases are an important arm of the quality control system, in which they act in

cooperation with folding assistant proteins to survey conformational quality (Fig. 31). I suppose that the protein stability of truncated YhcB was poor due to its misfolding. The YhcB lacking the TM domain probably has lost the intrinsic ability to be inserted into its original target, and remained in the cytoplasm, which could be harmful to the cell. So these abnormal proteins will be degraded by cell proteases. Similarly, YhcBΔC proteins would have lost its secondary structures required to maintain its overall architecture and/or its properties, although YhcBΔC with the TM domain probably retained its original localization in the membrane. Thus, proteases would degrade these misfolded YhcB variants into various lengths of fragments as observed in case of YhcBΔC2 (Fig. 18D). In addition or alternatively, the truncated proteins that have lost the ability to interact with their interaction partner and left separated could become susceptible to the degradation by proteases (Robichon C, 2011), and hence the truncated YhcB derivatives were unstable and could not be detected.

**IV. The property of interaction between YhcB and cell shape proteins**

In this study, I have examined the interaction of YhcB with cell shape proteins using the BACTH assay, and found positive interactions with MreC, MreD, RodA, and MurG, a biosynthetic enzyme for peptidoglycan precursor. However, no interaction with the cytoskeleton protein MreB was detected. MreB, MreC and MreD are encoded by the *mre* operon (Felipe *et al.*, 2007) and required by many rod-shaped bacteria in their elongation mode of peptidoglycan synthesis. MreB is the sole known bacterial actin in *E. coli*, and localizes just underneath the cytoplasmic membrane in a spiral-like pattern along the length of the cell. MreC is a bitopic inner membrane protein and MreD is a polytopic one. RodA is encoded by the *mrdB* (*rodA*) gene residing in the *mrd* (mureinD) operon, with its predicted 10 transmembrane segments and may somehow take part in the translocation of murein precursors (Holtje, 1998). Biochemical assays have shown that RodA along with PBP2 is required for proper peptidoglycan synthesis by transglycosylation, though it is unclear as to the mechanism of its contribution (Ishino, 1986). Thus, the fact that YhcB interacts with these proteins might indicate that YhcB, MreC and MreD together with RodZ form a kind of complex (Fig. 32) functioning in a mechanism of peptidoglycan synthesis such as, flipping the peptidoglycan precursor across the inner membrane. However, I also found that YhcB interacted with MreC, MreD and MurG clearly in the absence of RodZ, which might

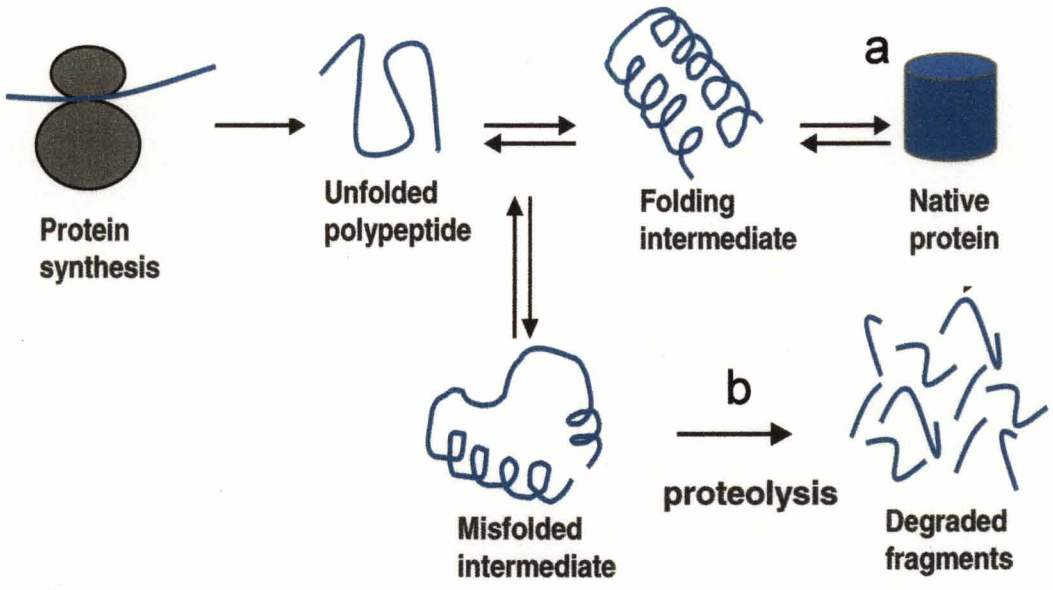


[Adapted from Elena et al. (2009)]

**Fig. 31 Conventional model of protein folding and proteolysis**
A chain newly synthesized on a ribosome may fold to a native state or can be proteolysed.

(a) Chaperon assist protein intermediates and folded proteins to reach their native state.

(b) Protease proteolyse misfold proteins that have failed to reach a native conformation. (Elena et al., 2009)

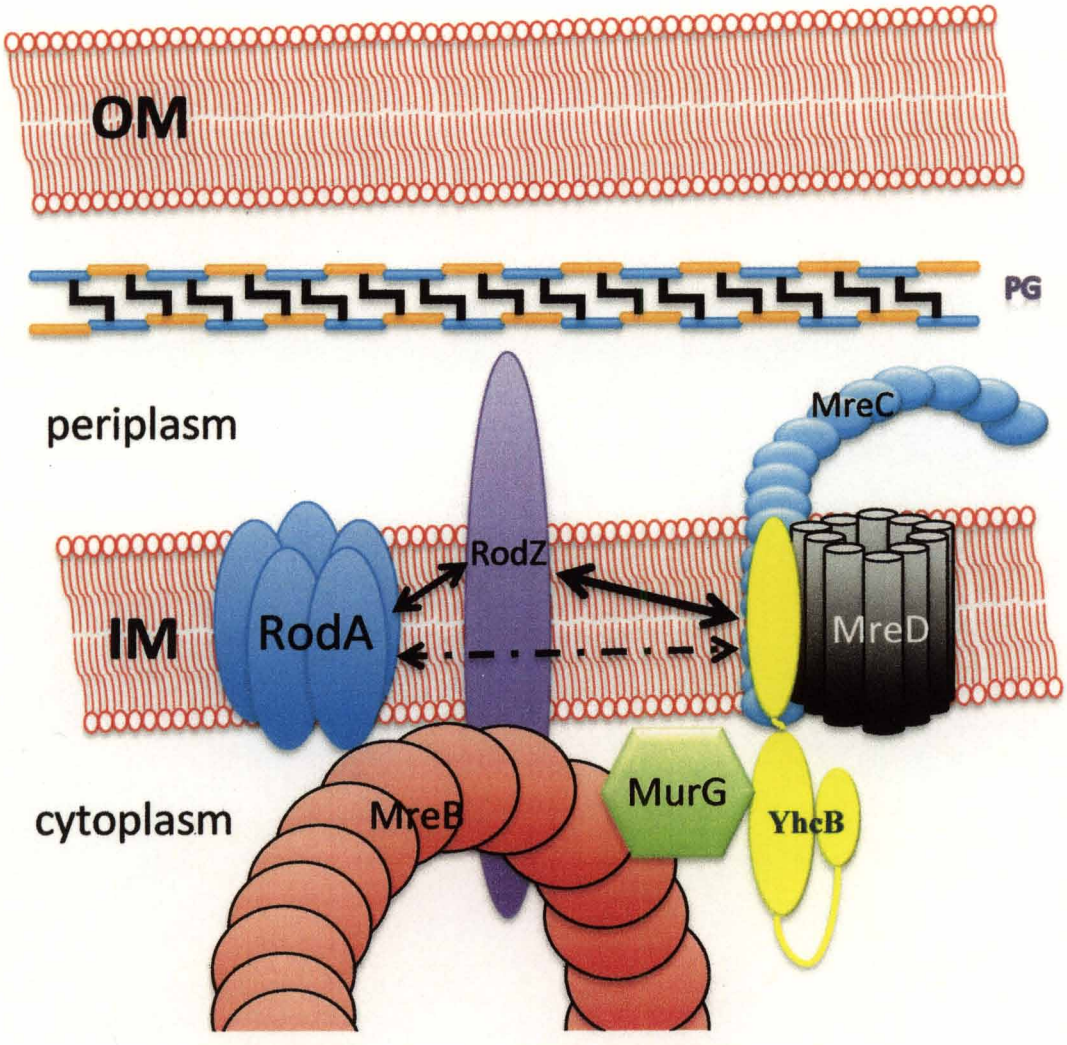


**Fig. 32 Model depicting the interaction of YhcB with bacterial morphogenetic protein and cell wall synthesizing protein**

YhcB directly interacts with MreC, MreD, RodZ and MurG. Broken line shows indirect interaction.

MreB is shown as a red helix beneath the inside of the inner membrane (IM) that interacts with RodZ. RodA is a five-pass inner membrane protein. MreD is a ten-pass inner membrane protein. OM, outer membrane. IM, inner membrane. PG, peptidoglycan.

indicate that these proteins are located nearby in IM but not forming a rigid complex, or RodZ could be the last component of the complex assembly. In case of RodA, only 20% of the transformants co-producing YhcB and RodA were positive in the assay of interaction, which could be due to the toxic effect of RodA overproduction in the absence of RodZ, however.

**V. YhcB interacts with itself**

The systematic analysis of membrane protein complexes in the cell envelope of *E. coli* found the molecular mass of YhcB in BN (Blue Native) PAGE to be 5~12 times larger than the one in SDS-PAGE, suggesting that YhcB existed in a homo-oligomeric complex (Maddalo, 2011). Using BACTH analysis, I proved that YhcB indeed interacts with itself, but it is not clear how many YhcB monomers interact and form a complex. The functional significance of oligomerization also remains to be examined.

**VI. Characterization of *yciB***

YciB is a predicted multi-pass inner membrane protein with five trans-membrane domains. It was speculated to function as an intracellular septation protein, because the mutant of its homologue in *Shigella flexneri*, *ispA*, was found defective in cell division leading to the formation of long filamentous shape lacking septa (Mac *et al*, 1996). In *E. coli*, Δ*yciB* mutation reduced the growth rate but *yciB* is not essential for the cell growth. Some of Δ*yciB* cells exhibited enlarged or misshapen morphology against normal rod shape, and dead cells or hollow sacculus were also observed. This observation seems to be consistent with the report about the *ispA* mutant of *Shigella flexneri*, suggesting that *yciB* in *E. coli* is also involved in cell division. Overexpression of *yciB* is harmful to the cell, and superfluous YciB seems to form abnormally large or irregular shape cells. Overproduced YciB could not be tolerated and was either degraded or led to the cell death. Due to this phenotype, characterization of YciB protein such as sub-cellular localization is so far unsuccessful and biochemical analyses remained to be performed. In Gram-negative bacteria, *yciB* gene is located conservatively on the chromosome between the genes *yciC* and *yciA*, however, it seem to be transcribed at a very low level and separately from the other ones, which might indicate a regulatory role of YciB. In this study, however, I could find that YciB

interacted with RodZ, which might be suggesting that YciB plays a new role between the cell elongation and cell division.

## VII. Perspective and Future experiments

In this study, I investigated the functional relation of *rodZ* and *yhcB* as well as *yciB* in *E. coli*, mainly by the technique of molecular genetics, and indicated that YhcB could be a new component of the cell morphology process in *E. coli*. Also, YciB which was predicted to be an intracellular septation protein, was found to interact with RodZ, suggesting that YciB might be another player participating in the cell morphologenesis and peptidoglycan synthesis. However, I have no firm, especially biochemical evidence to support this idea, and the molecular mechanisms in which these proteins function in the cell morphology remain to be investigated. Further investigation of YhcB as well as YciB would give more insights into the elaborated mechanisms of cell envelope biosynthesis and its regulation.

Apart from the basic research in molecular biology, the knowledge of cell envelope and division of *E. coli* is very important in clinical research, public health and food safety, because they are closely related to the pathogenesis of bacteria. Laboratory strains of *E. coli* are harmless and useful, but some *E. coli* is not friendly and cause urinary tract infections or diarrheal diseases and contributes to infant mortality. For example, a novel strain of *E. coli* O104:H4 caused a serious outbreak of foodborne illness in northern Germany in 2011 resulting in 810 cases of serious complications and 39 deaths (Bielaszewska M *et al.*, 2011). Thus, understanding how the cell envelope of *E. coli* is developed and the cell division is regulated under different conditions will help to solve public health and hygienic problems, as well as to develop new medicines.

## REFERENCE

**Allocati N, Federici L, Masulli M, Dillio C** (2009). Glutathione transferases in bacteria. *FEBS J.* 276 (1): 58-75.

**Alyahya SA, Alexander R, Costa T, Henriques AO, Emonet T, Jacobs-Wagner C.** (2009) RodZ, a component of the bacterial core morphogenic apparatus. *Proc Natl Acad Sci* 106(4):1239-44.

**Arifuzzaman M, Maeda M, Itoh A *et al.*** (2006) Large-scale identification of protein-protein interaction of *Escherichia coli* K-12. *Genome Res* 16(5):686-91

**Bendezú FO, Hale CA, Bernhardt TG, de Boer PA.** (2009) RodZ (YfgA) is required for proper assembly of the MreB actin cytoskeleton and cell shape in *E. coli. EMBO J.* 28(3):193-204.

**Bernhardt TG, de Boer PA.** (2004) Screening for synthetic lethal mutants in *Escherichia coli* and identification of EnvC (YibP) as a periplasmic septal ring factor with murein hydrolase activity. *Mol Microbiol.* 52(5):1255-69.

**Blattner, F. R., G. Plunkett, 3rd, C. A. Bloch, N. T. Perna, V. Burland, M. Riley, J. Collado-Vides, J. D. Glasner, C. K. Rode, G. F. Mayhew, J. Gregor, N. W. Davis, H. A. Kirkpatrick, M. A. Goeden, D. J. Rose, B. Mau, and Y. Shao.** (1997) The complete genome sequence of *Escherichia coli* K-12. *Science* 277(5331):1453-62.

**Britton RA, Grossman AD.** (1999) Synthetic lethal phenotypes caused by mutations affecting chromosome partitioning in *Bacillus subtilis. J Bacteriol.* 181(18):5860-4.

**Butland G, Peregrin-Alvarez JM, Li J *et al.*** (2005) Interaction network containing conserved and essential protein complexes in *Escherichia coli. Nature* 433(7025):531-7.

**Carine Robichon, Gouzel Karimova, Jon Beckwith, and Daniel Ladant** (2011) Role of Leucine Zipper Motifs in Association of the *Escherichia coli* Cell Division Proteins

FtsL and FtsB. *J Bacteriol.* 93(18):4988-92.

**Dai K, Xu Y, Lutkenhaus J.** (1996) Topological characterization of the essential *Escherichia coli* cell division protein FtsN. *J Bacteriol.* 178(5):1328-34.

**Datsenko KA,Wanner BL** (2000) One-step inactivation of chromosomal genes in *Escherichia coli* K-12 using PCR products. *Proc Natl Acad Sci USA* 97(12):6640-5

**Diao J.** (2010) Crystal structure of a super leucine zipper, an extended two-stranded super long coiled coil. *Protein Sci.* 19(2):319-26.

**D Sheehan, G Meade, V M Foley, and C A Dowd** (2001) Structure, function and evolution of glutathione transferases: implications for classification of non-mammalian members of an ancient enzyme superfamily. *Biochemical Journal* 360(1): 1-16.

**E. Hochuli, W. Bannwarth, H. Döbeli, R. Gentz & D. Stüber.** (1988) Genetic Approach to Facilitate Purification of Recombinant Proteins with a Novel Metal Chelate Adsorbent. *Nature Biotechnology* 6, 1321-1325

**Gerdes K.**(2009) RodZ, a new player in bacterial cell morphogenesis. *EMBO J.* 28(3):171-2.

**Gerken H, Misra R.** (2010) MzrA-EnvZ interactions in the periplasm influence the EnvZ/OmpR two-component regulon. *J Bacteriol.* 192(23):6271-8

**Giaever G, Chu AM, Ni L, Connelly C, Riles L, Véronneau S, Dow S, Lucau-Danila A, Anderson K, André B, Arkin AP, Astromoff A, El-Bakkoury M, Bangham R, Benito R, Brachat S, Campanaro S, Curtiss M, Davis K, Deutschbauer A, Entian KD *et al.*** (2002) Functional profiling of the *Saccharomyces cerevisiae* genome. *Nature.* 2002 Jul 25;418(6896):387-91.

**Handford JI, Ize B, Buchanan G, Butland GP, Greenblatt J, Emili A, Palmer T.** (2009) Conserved network of proteins essential for bacterial viability. *J Bacteriol.* 191(15):4732-49.

**Hochuli, E.; Bannwarth, W.; Döbeli, H.; Gentz, R.; Stüber, D.** (1988). Genetic Approach to Facilitate Purification of Recombinant Proteins with a Novel Metal Chelate Adsorbent. *Bio/Technology* 6 (11): 1321-5.

**Joong-Chul Lee, Jeong-Heon Cha, Dennis B. Zerbv, George C. Stewart** (2003) Heterospecific Expression of the *Bacillus subtilis* Cell Shape Determination Genes *mreBCD* in *Escherichia coli. CURRENT MICROBIOLOGY* 47(2):146-52.

**Joseleau-Petit D, Liebart JC, Ayala JA, D'Ari R.** (2007) Unstable *Escherichia coli* L forms revisited: Growth requires peptidoglycan synthesis. *J Bacteriol* 189: 6512–6520.

**Karimova G, Dautin N, Ladant D.** (2005) Interaction network among *Escherichia coli* membrane proteins involved in cell division as revealed by bacterial two-hybrid analysis. *J Bacteriol.* 187(7):2233-43.

**Karimova G, Pidoux J, Ullmann A, Ladant D.** (1998) A bacterial two-hybrid system based on a reconstituted signal transduction pathway. *Proc Natl Acad Sci USA.* 95(10):5752-6.

**Karimova G, Robichon C, Ladant D.** (2009) Characterization of YmgF, a 72-residue inner membrane protein that associates with the *Escherichia coli* cell division machinery. *J Bacteriol.* 191: 333-46.

**Karp PD, Keseler IM, Shearer A, Latendresse M, Krummenacker M, Paley SM, Paulsen I, Collado-Vides J, Gama-Castro S, Peralta-Gil M, Santos-Zavaleta A, Peñaloza-Spínola MI, Bonavides-Martinez C, Ingraham J.** (2007) Multidimensional annotation of the *Escherichia coli* K-12 genome. *Nucleic Acids Res.* 35(22):7577-90.

**Kitagawa M, Ara T, Arifuzzaman M, Ioka-Nakamichi T, Inamoto E, Toyonaga H,**

**Mori H.** (2005) Complete set of ORF clones of *Escherichia coli* ASKA library (a complete set of *E. coli* K-12 ORF archive): unique resources for biological research. *DNA Res.* 2005;12(5):291-9.

**Kobayashi K, Ehrlich SD *et al.*** (2003) Essential *Bacillus subtilis* genes. *Proc Natl Acad Sci USA* 100(8):4678–83

**Mac Síomóin RA, Nakata N, Murai T, Yoshikawa M, Tsuji H, Sasakawa C.** (1996) Identification and characterization of ispA, a *Shigella flexneri* chromosomal gene essential for normal in vivo cell division and intracellular spreading. *Mol Microbiol.* 19(3):599-609.

**Lupas,** (1996) Predicting Coiled Coils from Protein Sequences Science 252:1162-1164.

**Maddalo G, Stenberg-Bruzell F, Götzke H, Toddo S, Björkholm P, Eriksson H, Chovanec P, Genevaux P, Lehtiö J, Ilag LL, Daley DO** (2011) Systematic analysis of native membrane protein complexes in *Escherichia coli. J Proteome Res* 10:1848-59

**Mogi T, Mizuochi-Asai E, Endou S, Akimoto S, Nakamura H.** (2006) Role of a putative third subunit YhcB on the assembly and function of cytochrome bd-type ubiquinol oxidase from *Escherichia coli. Biochim Biophys Acta.* 1757(7):860-4.

**Mori H, Isono K, Horiuchi T, Miki T.** (2000) Functional genomics of *Escherichia coli* in Japan. *Res Microbiol*; 151: 121-8.

**Nerino Allocati, Luca Federici, Michele Masulli, Carmine Di Ilio** (2009) Glutathione transferases in bacteria *FEBS* 276(1):58-75.

**Niba ET, Naka Y, Nagase M, Mori H, Kitakawa M. (2007)** A genome-wide approach to identify the genes involved in biofilm formation in *E. coli. DNA Res.* 14(6):237-46

**Niba ET, Li G, Aoki K, Kitakawa M.** (2010) Characterization of *rodZ* mutants: RodZ

is not absolutely required for the cell shape and motility. *FEMS Microbiol Lett.* 309(1):35-42.

**Papp B, Pal C, Hurst LD** (2004) Metabolic network analysis of the causes and evolution of enzyme dispensability in yeast. *Nature* 429(6992):661-4

**Raetz CR, Dowhan W.** (1990) Biosynthesis and function of phospholipids in *Escherichia coli. J Biol Chem* 265: 1235-8.

**Reed JL, Palsson BO** (2004) Genome-scale *in silico* models of *E. coli* have multiple equivalent phenotypic states: assessment of correlated reaction subsets that comprise network states. *Genome Res* 14(9):1797-805

**Riley, M., Abe, T., Arnaud, M.B., Berlyn, M.K., Blattner, F.R., Chaudhuri, R.R., Glasner, J.D., Horiuchi, T., Keseler, I.M., Kosuge, T., Mori, H., Perna, N.T., Plunkett, G. 3rd, Rudd, K.E., Serres, M.H., Thomas, G.H., Thomson, N.R.,Wishart, D. andWanner, B.L.** (2006). *Escherichia coli* K-12: a cooperatively developed annotation snapshot -- 2005. *Nucleic Acids Res.* 34, 1-9.

**Robichon C, Karimova G, Beckwith J, Ladant D.** (2011) Role of leucine zipper motifs in association of the *Escherichia coli* cell division proteins FtsL and FtsB. *J Bacteriol.*193(18):4988-92.

**Rost B, Yachdav G, Liu J.** (2004) The PredictProtein Server. *Nucleic Acids Res.* 32(Web Server issue): W321-26.

**Rungrutai Udomsinprasert, Saengtong Pongjaroenkit, Jantana Wongsantichon, Aaron J. Oakley, La-aied Prapanthadara, Matthew C. J. Wilce, and Albert J. Ketterman** (2005) Identification, characterization and structure of a new Delta class glutathione transferase isoenzyme. *Biochemical Journal* 388(3): 763-71.

**Sheehan D, Meade G, Foley VM, Dowd CA** (2001). Structure, function and evolution of glutathione transferases: implications for classification of non-mammalian members

of an ancient enzyme superfamily. *Biochem. J.* 360 (Pt 1): 1-16.

**Shiomi D, Mori H, Niki H.** (2009) Genetic mechanism regulating bacterial cell shape and metabolism. *Commun Integr Biol.* 2(3):219-20.

**Shiomi D, Sakai M, Niki H.** (2008) Determination of bacterial rod shape by a novel cytoskeletal membrane protein. *EMBO J.* 27(23):3081-91.

**Stenberg F, Chovanec P, Maslen SL, Robinson CV, Ilag LL, von Heijne G, Daley DO.** (2005) Protein complexes of the *Escherichia coli* cell envelope. *J Biol Chem.* 280(41):34409-19.

**Thomas P. Hopp, Kathryn S. Prickett, Virginia L. Price, Randell T. Libby, Carl J. March, Douglas Pat Cerretti, David L. Urdal & Paul J. Conlon** (1988) A short polypeptide marker sequence useful for recombinant protein identification and purification *Nature Biotechnology* 6, 1204-10

**Tsuchiya M, Asahi N, Suzuoki F, Ashida M and Matsuura S.** (1996) Detection of peptidoglycan and b-glucan with silkworm larvae plasma test. *FEMS Immunol Med Microbiol.* 15(2-3),129-34.

**Typas A, Banzhaf M, Gross CA, Vollmer W.** (2012) From the regulation of peptidoglycan synthesis to bacterial growth and morphology. *Nat Rev Microbiol.* 10(2):123-36.

**van Langevelde P, Ravensbergen E, Grashoff P, Beekhuizen H, Groeneveld P van Dissel JT.** (1999) Antibiotic-induced cell wall fragments of Staphylococcus aureus increase endothelial chemokine secretion and adhesiveness for granulocytes. *Antimicrob Agents Chemother.* 43(12): 2984-9.

**Vollmer W.** (2008) Structural variation in the glycan strands of bacterial peptidoglycan. FEMS Microbial Rev 32: 287-306.

**Samuel Wagner, Louise Baars, A. Jimmy Ytterberg, Anja Klussmeier, Claudia S. Wagner, Olof Nord, Per-Åke Nygren, Klaas J. van Wijk and Jan-Willem de Gier** (2007) Consequences of Membrane Protein Overexpression in *Escherichia coli*. *Molecular & Cellular Proteomics*, 6; 1527-50.

**White CL, Kitich A, Gober JW.** (2010) Positioning cell wall synthetic complexes by the bacterial morphogenetic proteins MreB and MreD. *Mol Microbiol.* 76(3):616-33.

**Yasuda M, Iguchi-Yokoyama A, Matsuyama S, Tokuda H, Narita S.** (2009) Membrane topology and functional importance of the periplasmic region of ABC transporter LolCDE. *Biosci Biotechnol Biochem.* 73(10):2310-6.